THESIS

MODELING THE DISTRIBUTION OF MAJOR SALT IONS IN REGIONAL AGRICULTURAL GROUNDWATER AND SURFACE WATER SYSTEMS: MODEL CALIBRATION AND APPLICATION

Submitted by

Abdullah B. Javed

Department of Civil and Environmental Engineering

In partial fulfillment of the requirements

For the Degree of Master of Science

Colorado State University

Fort Collins, Colorado

Spring 2020

Master's Committee:

Advisor: Timothy K. Gates
Co Advisor: Ryan T. Bailey

Michael J. Ronayn

Copyright by Abdullah B. Javed 2020

All Rights Reserved

ABSTRACT

MODELING THE DISTRIBUTION OF MAJOR SALT IONS IN AGRICULTURAL GROUNDWATER AND SURFACE WATER SYSTEMS:
MODEL DEVELOPMENT AND APPLICATION

Irrigated lands in Colorado's Lower Arkansas River Valley (LARV), like many irrigated agricultural areas worldwide, suffer from salinization of soil, groundwater, and adjacent river systems. Waterlogging and salinization are prevalent throughout the LARV, which have diminished the crop yields and threatened the long-term sustainability of irrigated agriculture. Increased salinity concentrations are primarily due to the presence of salt minerals and high rates of evapotranspiration in the LARV, coupled with inefficient irrigation practices. Shallow groundwater in the LARV drives saline groundwater back to the stream network, thereby degrading the surface water quality, which affects the downstream areas where it evapo-concentrates when saline water is diverted for additional use.

The goal of the current study is to develop, calibrate and test a physically-based, spatially distributed numerical model to assess soil, groundwater and surface water salinity at a regional scale to better understand the baseline nature of the problem. Several salinity models have been developed in recent decades; however, no attempts thus far have been made at simulating the fate, storage, and transport of salt ions at a regional scale in both groundwater and streams within an irrigated stream-aquifer system. The model used in this thesis links MODFLOW-SFR2, which simulates the groundwater heads and stream flows, with RT3D/SEC-OTIS which addresses reactive solute transport in variably- saturated soil and stream-aquifer systems.

Sources and sinks within an agricultural system such as canal seepage, infiltrated water from flood and sprinkler irrigation, groundwater pumping, evapotranspiration from both the unsaturated and shallow saturated zones; root zone processes such as cycling of salt ions, crop uptake, and leaching to the water table; addition of salt mass via fertilizer and irrigation water; chemical kinetics affecting salt ions such as influence of dissolved oxygen and nitrate; equilibrium chemistry processes such as precipitation-dissolution, complexation and cation exchange; and 1D transport of salt ions in the streams due to advection, dispersion and sorption are addressed.

The coupled flow and reactive transport model is applied to an approximately 552 km^2 salinity-affected irrigated stream-aquifer system of the LARV between Lamar, Colorado and the Colorado-Kansas border. The model is tested against an extensive set of field data (soil salinity data from field salinity surveys, groundwater salinity collected from a network of groundwater monitoring wells, salt loading from the aquifer to the Arkansas River, and salt concentrations measured from in-stream sampling). Model calibration and parameter estimation include manual and automated calibration using PEST. Runs were conducted to describe the current levels of root zone salinity which markedly exceeds threshold levels for crop yield reduction. Spatiotemporal distribution of groundwater levels and concentrations, mass and return flow rates to streams, and stream concentrations are also simulated for current baseline conditions. The calibrated and tested regional scale salinity model is in need of further refinement but shows promise for future implementation to explore potential solution strategies for the irrigated valley of the LARV, and similar salt-afflicted areas of the world, by applying different best management practices.

ACKNOWLEDGMENTS

As with any thesis, this research was not conducted in a vacuum. I must thank my entire committee and would like to express my sincere gratitude to all the people who helped me to complete this research. My special gratitude goes to my advisor Dr. Timothy K. Gates; thanks to him for giving me the opportunity and for picking up a stray graduate student and seeing it through to the end. My co-advisor Dr. Ryan T. Bailey also deserves thanks. His door was always open, allowing me to enter and question. As well, I wish to acknowledge and thank Dr. Michael J. Ronayne for always being supportive of this work and Dr. Saman Tavakoli Kivi for his guidance and nudging me in the direction I needed to go.

Additionally, I want to express my gratitude to the US Agency for International Development through the US Pakistan Centers for Advance Studies in Water for funding this project. I am also indebted to my friends and fellow graduate students for their company, friendship, and support.

Last but not least, special and generous thanks go to my father, my mother, and all of my family members for their continuous support and encouragement. Without their backing, this research would not have been accomplished.

DEDICATION

For my parents, grandparents, phopo, and family for their steady encouragement, unconditional love, and tremendous support.

TABLE OF CONTENTS

LIST OF TABLES

LIST OF FIGURES

CHAPTER 1

INTRODUCTION

1.1 Challenges in Irrigated Agriculture

Water development is critical for food security. In order to provide food for the growing world's population, which is expected to reach 9.7 billion people by 2050 (Rosegrant et al., 2002), the pressure to produce more with less water is intensifying. Around 70% of global water use is for irrigation and agriculture (UNESCO-WWAP., 2003); and, it is essential to maintain irrigated agricultural lands which are by far the most productive worldwide. To meet the food demand of the growing population, natural ecosystems have been altered to increase cultivated areas and make more water available for crop production, yet a number of water quality and water quantity problems have been created which threaten the long-term sustainability of irrigated agriculture. Such tradeoffs have increased short-term food production but adversely affected long-term ecosystem services. Tilman et al. (2002) estimated that nitrogen and phosphorus fertilizer application would need to increase 1.9 – 3.9-fold and 2.4-fold respectively by 2050 to meet the food demand of the growing population. Irrigation water usage would need to increase by 1.9-fold by 2050 (Tilman et al., 2002). The author pointed out that these increases will have a significant impact on the environment, including the salinization of soils and degradation of the surface water and groundwater natural resources.

Salinization and waterlogging pose a major challenge to sustaining crop yield (Scanlon et al., 2007; Gates et al.,2002; Morway et al., 2012; Wichelns et al., 2015) while accompanying non-beneficial consumptive use wastes water on vegetation with little economic value. It is estimated

that 20% of total cultivated lands and 33% of irrigated lands are affected by high salinity (Ghassemi et al., 1995, Shirvastava et al., 2014) and that salt-affected areas are a growing challenge all over the world. High salinity is exacerbated by waterlogging from shallow saline groundwater with associated evaporative upflux (Morway and Gates, 2012), along with the dissolution of salt minerals such as gypsum, halite, and calcite (Harrington et al., 2014). High groundwater loading to the nearby surface water bodies also affects the downstream-irrigated lands that divert the water from these polluted surface water bodies.

Salinization in the root zone is a major impediment to the sustainability of irrigated lands and reduces crop yield in many areas of the world including Pakistan (Mahmood et al., 2001; Qureshi et al., 2008; Latif et al., 2009). Out of 16.2 Mha of irrigated land in Pakistan, approximately 40,000 ha of land is lost to crop yield each year in Pakistan (Yasin et al., 1998). In the United States, more than 27% of the irrigated land is impacted by salinization (Schoups et al., 2006, Ghassemi et al., 1995). Irrigated areas in China (Pereira et al. 2007; Chen et al, 2010; Wang et al. 2018) and Australia (Herczeg et al., 2001; Tweed et al., 2007) also suffer from crop yield reduction due to salinity. Figure 1.1 illustrates the global extent of total salt-affected land, both irrigated and non-irrigated, amounting to about 1128 Mha (Wicke et al., 2011). The map shows that salt-affected land is widespread but the severity of the salt-affected areas varies considerably among different regions. The largest salt-affected areas are located in the Middle East (189 Mha), Australia (169 Mha) and North Africa (144 Mha).

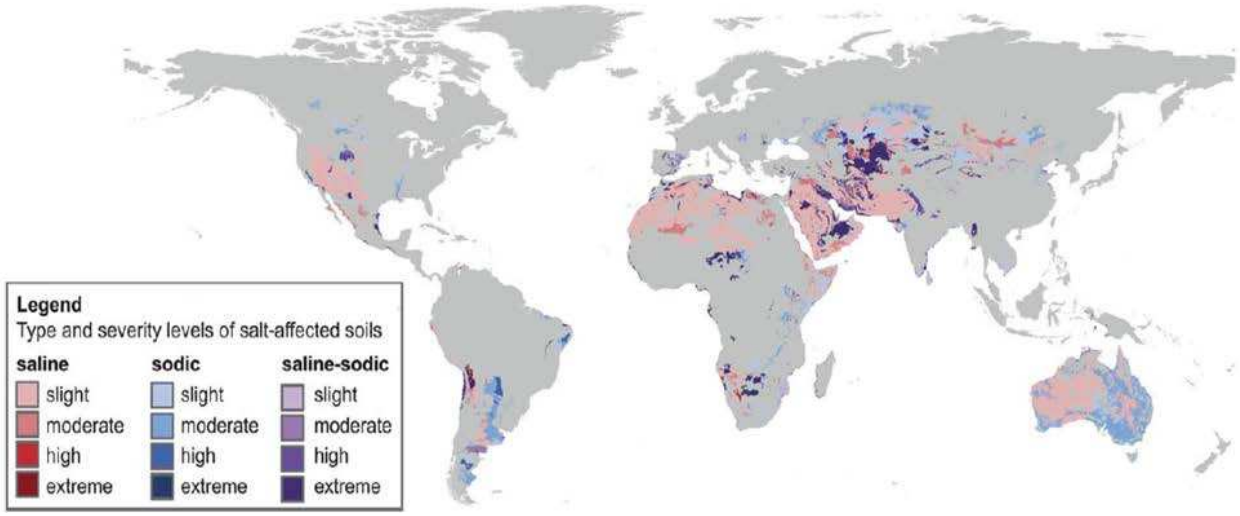

Figure 1. 1. Global salt-affected soils by type and severity (Wicke et al., 2011).

In the United States, the Colorado River Basin, the Rio Grande Basin of New Mexico and Texas, the Central Valley of California, the Snake River Basin in Idaho, the Yakima River Basin in Washington, the Arkansas and South Platte River Basins in Colorado, Kansas, Nebraska, and Oklahoma are suffering from salinity problems. Irrigation-induced salinity and waterlogging have affected the semi-arid region of Colorado due to insufficient drainage and inefficient irrigation practices. In addition to major salt ions, other naturally occurring chemical pollutants such as selenium (Se), uranium (U), and arsenic, along with nutrient pollutants like nitrate (NO_3) are also important in Colorado because they often exceed total maximum daily loading (TMDL) standards (Gates, 2008; Bailey, 2012). Salts and naturally occurring pollutants not only degrade river quality by entering the river with return flows but also affect downstream irrigated areas where salts continue to evapo-concentrate (Wallender and Tanji.,2012) and affect crop productivity of the crop (Silva et al., 2008).

Salinization and waterlogging accompany each other in arid and semiarid regions. Waterlogging refers to the process by which the oxygen in the soil pores of the crop root zone is displaced by water, usually due to a shallow groundwater table, and salinization refers to the

built-up of salts in root zone due to evaporative concentration and dissolution. As the salinity in the root zone increases, crops that are sensitive to the salinity will transpire less water and their yield will drop (Fullen and Catt, 2004). The Lower Arkansas River Valley (LARV) is an example located in Colorado where crop yields have been degraded due to the salt built up in the root zone and waterlogging, greatly affecting the rural economy of the area. (Houk et al., 2006, Gates et al., 2012).

1.2 Description of Study Area

The Lower Arkansas River Valley (LARV) is located in southeastern Colorado between the city of Pueblo and the Colorado Kansas state line. It is a semi-arid region that contains a large extent of the productive irrigated land in the state, irrigated by canals and shallow groundwater pumping wells. The annual precipitation in the area is 300 mm and monthly temperatures vary from -1^{o}C in winter months to 25^{o}C in summer months. The alluvial aquifer LARV is 4 to 34 m thick and is underlain by Cretaceous shale of late Cambrian to Tertiary age and Dakota Sandstone (Darton., 1906). The layers above the Dakota Sandstone are divided into three groups: 1- Benton Group, 2- the Niobrara formation and 3- the Pierre Shale. Benton is overlain by the Niobrara formation that underlies the aquifer between Manzanola and Swink, CO. Pierre shale overlies the Niobrara formation and spreads under the alluvial aquifer between Pueblo and Manzanola, CO. Between Lamar and Holly the Dakota sandstone is overlain by Carlisle shale of Turonian age. The cross-section of the geology below the alluvial aquifer of LARV is synthesized by Darton (1906) and is shown in Figure 1.2.

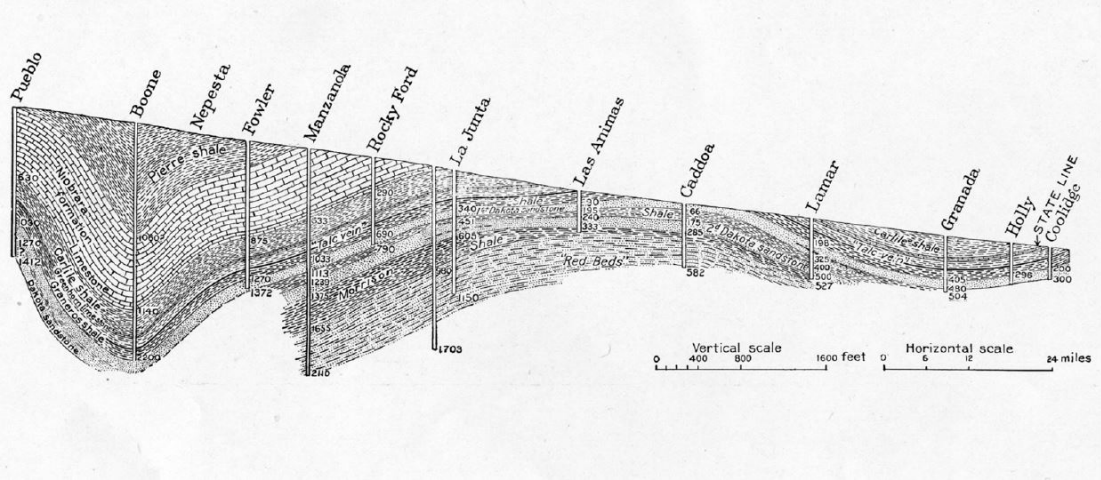

Figure 1. 2. Geology of the Lower Arkansas River Valley (Darton, 1906).

Soils in the LARV include clay loam, silty clay loam, loam, and sandy loam (Sweet and Inman,1930; Wittler., 2005; Gates et al., 2008; USDA NRCS database). The LARV has been divided into two study regions by Colorado State University (CSU) i.e. the Upstream Steady Region (USR) that represents the irrigated valley area upstream of John Martin Reservoir and the Downstream Study Region (DSR) that represents the irrigated valley area downstream of John Martin Reservoir as shown in Figure 1.3.

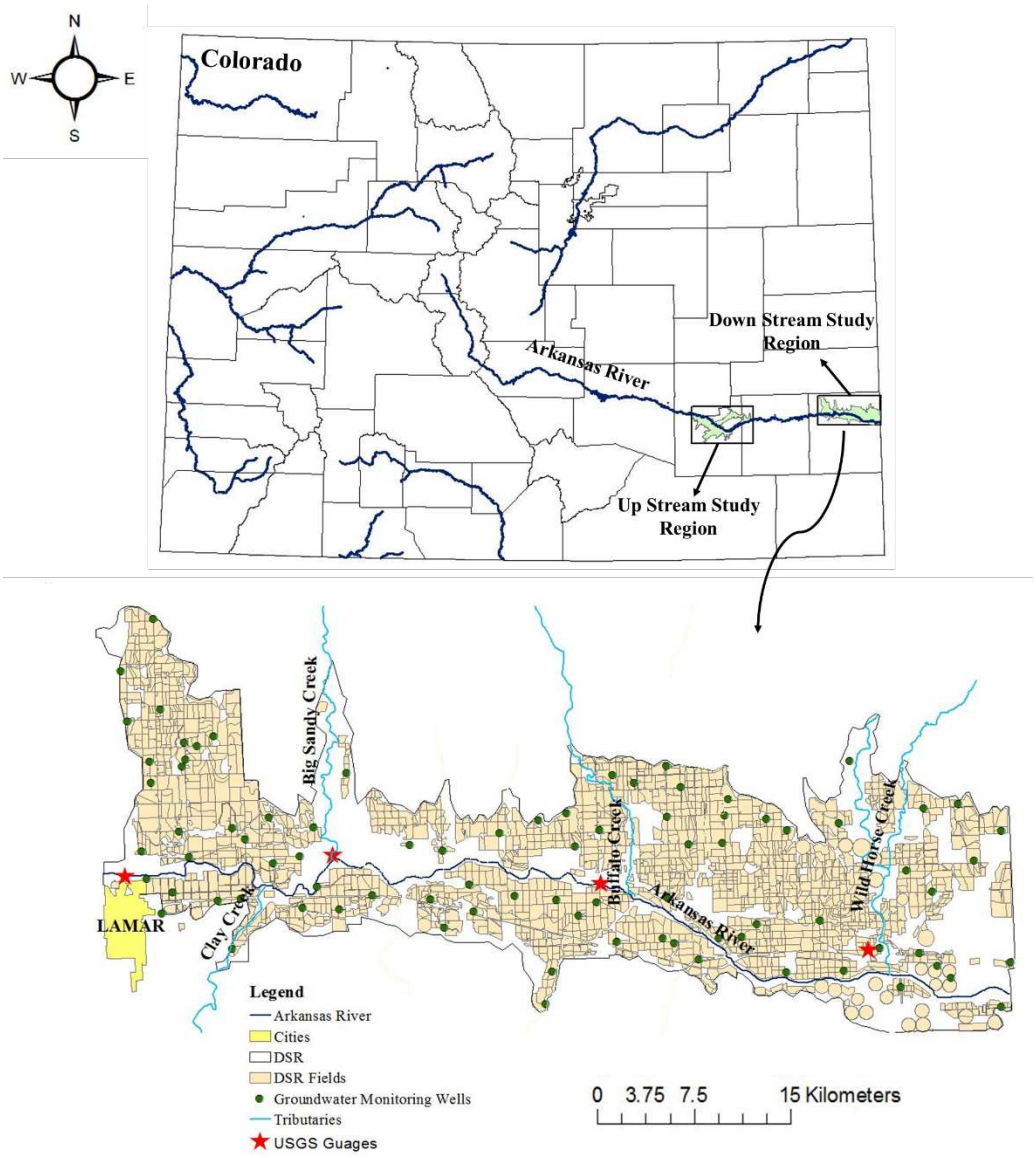

Figure 1. 3. Upstream study region (USR) and downstream study region (DSR) in the Lower Arkansas River Valley, Colorado USA, with detail of the DSR.

The introduction of agriculture in LARV occurred in the 1870s, and has benefited both the local farmers and the state of Colorado (Sherow, 1990). Approximately 109,000 ha (270,000 acres) are irrigated across about 14,000 fields in the LARV using 25 main canals that divert water from the river as per Colorado water law and with about 2400 wells that pump from alluvial groundwater (Morway et al., 2013). Most of the fields in the region are irrigated using surface irrigation systems, but sprinkler irrigation has grown to about 20% in the DSR over the

last ten to fifteen years (Gates et al., 2012, Osborn et al 2017). The irrigation season goes between the 15th of March to the 15th of November each year.

The major crops that are cultivated in the DSR are alfalfa, corn, grass, wheat, and sorghum. The major tributaries that are included in the DSR are Clay Creek, Big Sandy Creek, Buffalo Creek, and Wild Horse Creek, these tributaries are fed by irrigation return flows from the irrigated fields and by occasional runoff from rainfall in the valley and in the arid lands outside. The Arkansas River and its tributaries typically are gaining streams (Longenbaugh., 1967; Goff et al., 1998; Shultz et al., 2018) which mean usually water flows from groundwater into the tributaries and to the Arkansas River. There are many outcrops of shale which along with the bedrock shale releases SO_4 (sulfate) and SeO_4 (selenate) into the alluvial aquifer in the presence of dissolved oxygen and nitrate (Gates et al., 2009). Other major salt ions and trace elements also enter the groundwater system due to different chemical and microbially-mediated geochemical processes. Reduced U (IV) minerals are oxidized to dissolved U (VI) when it is exposed to groundwater, resulting in high solute concentrations. Polluted groundwater along with the surface return flows enter the river and tributaries and degrade the quality.

Colorado State University has been collecting data in the LARV since 1998. In USR, the data have been gathered from 1999 to the present, while in DSR the data have been gathered from 2002 to the present. Canal samples were collected using the peristaltic pump and sent to the laboratory to analyze the concentration of $C_{SO_4\text{-}S}$, C_{Na}, C_K, C_{Ca}, C_{Mg},C_{CO_3}, C_{HCO_3} , $C_{SeO_4\text{-}Se}$ and C_{O_2}. The concentrations of C_{NH_4} and C_{NO_3}in the irrigation water were analyzed by using a continuous flow analyzer QuickChem. The river water quality has been degraded due to inefficient irrigation practices (Gates et al., 2009; Bailey, 2012). Total Dissolved Solids (TDS) in

the river increases from 500 mg/L to 4000 mg/L moving downstream from Pueblo to the Colorado-Kansas state line (Odell et al., 1964). Geonics EM-38 electromagnetic induction sensor surveys were conducted in many fields over a number of years to measure the electrical conductivity of the soil paste extract (EC_e) as an indicator of soil salinity. Approximately 54,000 sites were measured in USR and 34,000 sites were measured in DSR for EC_e values.

In LARV, water quality data samples were collected from groundwater monitoring well from 1998 to the present. The present study uses water quality data gathered from 82 groundwater monitoring wells from 2003 to 2007 located in DSR and analyzed for dissolved oxygen (*DO*), sodium (C_{Na}), calcium (C_{Ca}), potassium (C_K), magnesium (C_{Mg}), carbonate (C_{CO_3}), bicarbonate (C_{HCO_3}) and sulfate ($C_{SO_4\text{-}S}$) concentrations. The location of the monitoring wells is shown in Figure 1.3. Soil salinity data collected at more than 122,000 locations in the LARV reveals that average electrical conductivity exceeds the crops salt tolerance. Plots of average $C_{SO_4\text{-}S}$ and TDS measured in groundwater monitoring wells within 15 subregions of the DSR, described Section 3.3 below, are summarized in Figure 1.4 with respective overall average values of 730 mg/L and 2470 mg/L. According to the US Environmental Protection Agency's (USEPA) drinking water quality standards, the secondary maximum contaminant levels (SMCL) for $C_{SO_4\text{-}S}$ and TDS are 250 mg/L and 500mg/L and the average $C_{SO_4\text{-}S}$ and TDS in the groundwater of DSR is higher than U.S Environmental Protection Agency standards.

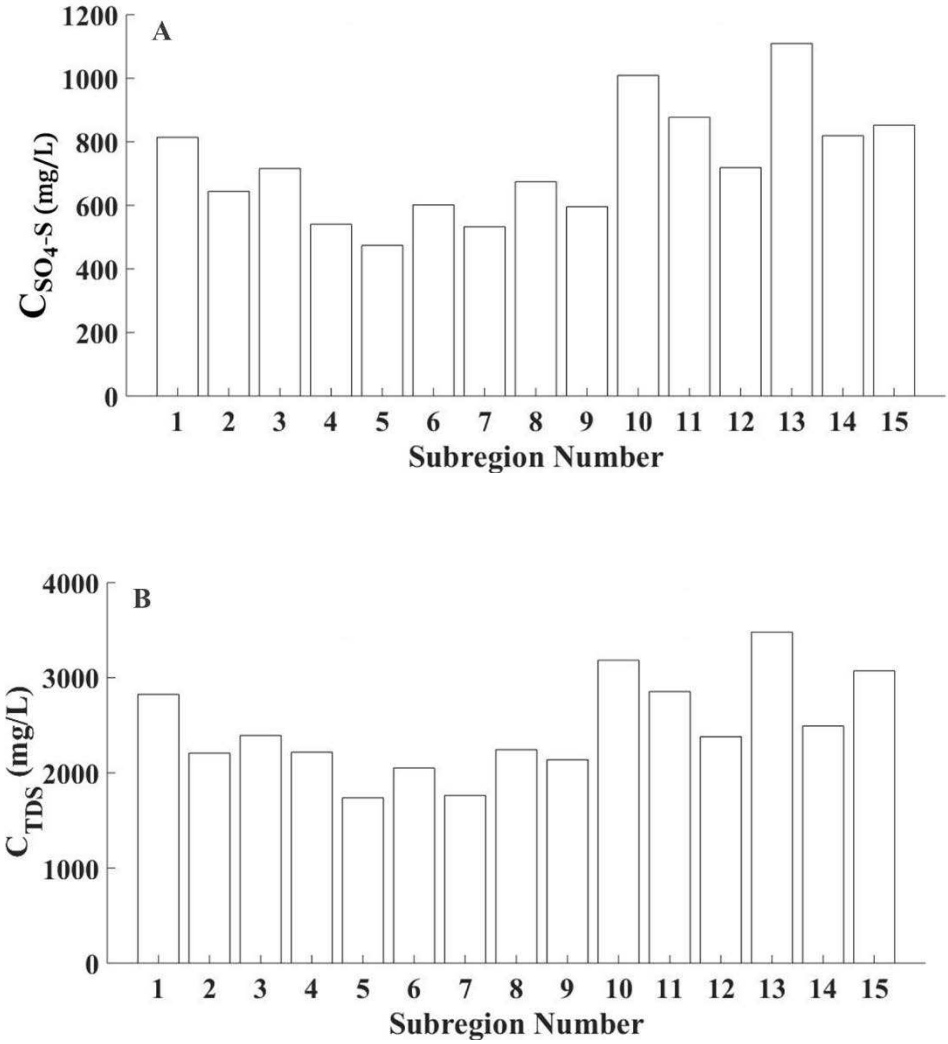

Figure 1. 4. (A) $C_{SO_4\text{-}S}$ (mg/L) in Groundwater (B) TDS (mg/L) in Groundwater measured in the different subregions of the DSR.

Waterlogging, salinity and non-beneficial consumptive use threaten the long-term sustainability of irrigated agriculture around the world (Wicke et al., 2011). In the 1990s, 68% of producers in the LARV stated that high salinity levels are a significant concern (Frasier et al., 1999). About 70 % of the area in the LARV has salinity levels that exceed the threshold tolerance levels of crops with crop yield reduction from salinity and waterlogging estimated to range from 11% to 19% (Gates et al., 2002; Morway et al., 2012; Tavakoli Kivi et al., 2019).

1.3 Research Objectives

The goal of this research is to calibrate, test and apply a numerical model for simulating the fate and transport of major salt ions in irrigated stream-aquifer systems over the regional scale. The particular aim is to apply the already developed model for characterizing the nature and extent of irrigation-induced salinity problems in Colorado's LARV and to study the baseline nature of the problem. The aim of this study is to be achieved through the following objectives:

1. Refine the existing UZF-RT3D/SEC numerical modeling code in the application to the irrigated stream-aquifer system of the DSR in the LARV to simulate subsurface multispecies reactive transport of major salt ions through the system;
2. Couple UZF-RT3D/SEC with the OTIS stream water quality model to simulate the transport of dissolved salts in streams in connection with groundwater within the irrigated stream-aquifer system;
3. Calibrate the coupled model using both manual and automated procedures to achieve a satisfactory match between simulated and observed data of the DSR in the LARV; and
4. Apply the model to provide a preliminary assessment of the baseline salinity problem in the soil, groundwater, and streams of the DSR, and to recommend next steps in refining and applying the coupled model to predict how alternative BMP's could reduce salinity and waterlogging in the LARV and other similar areas of the world suffering from irrigation induced salinity problems.

1.4 Thesis Organization

The remainder of the thesis includes four chapters. Chapter 2 contains a literature review of salinity problems in irrigated regions and their computational modeling, with a focus on past monitoring and modeling studies in Colorado's LARV. Chapter 3 focuses on the first three objectives, which involve the calibration and application of a coupled reactive transport capable of simulating the reactive transport of major salt ions in the stream-aquifer system. Chapter 4 details the method and results of applying the regional scale reactive transport model to characterize baseline salinity conditions in the DSR of the LARV. Chapter 5 provides conclusions and recommendations for future work.

CHAPTER 2

LITERATURE REVIEW

2.1 Effects of Salinization

Waterlogging and salinization are age-old nemeses of irrigated agriculture and continue to threaten the agricultural productivity of semi-arid regions of the world. Waterlogging and salinity problems usually occur in intensively irrigated alluvial valleys, which have been irrigated for a few decades and have high evapotranspiration rates. Protection of these irrigated lands from waterlogging and salinity is vital in order to meet the feeding demand of the growing population, since irrigated agriculture produces approximately one-third of the available food supply while making up only about 18% of the available cropland (Acquaah, 2005).

Salinization of the stream-aquifer system is an inevitable problem in irrigation lands, which adversely affects the crop yield (Hutmacher et al., 1996; Sparks, 2003; Vaze et al., 2003; Gates et al., 2002; Lin and Garcia, 2008; Morway and Gates, 2012; Wichelns and Qadir, 2015; Tavakoli Kivi et al., 2019). The challenge to maintain crop yield is becoming increasingly difficult as approximately 20% to 25% of the irrigated land in more than 100 countries of the world is affected by salinization (Wicke et al., 2011). Wild (2003) estimated about 15% of the total land area of the world has been degraded by soil erosion, physical and chemical degradation including soil salinization. Specifically, in the United States, 27% of the irrigated land is affected by salinization (Ghassemi et al., 1995; Postel, 1999; Tanji and Kielen, 2002).

Due to limited rainfall and water scarcity, agriculture in semi-arid regions is dependent on irrigation. During the last century, the irrigation canal system in southeastern Colorado has diverted and distributed water from the Arkansas River to the LARV. Although the irrigation

system in Colorado has greatly strengthened the agricultural economy of the rural area (Burkhalter et al., 2005), depth to the water table in the irrigated alluvial valley has decreased due to the extensive irrigation. Salts accumulation occurred in the topsoil because of the salt minerals presence in the soil and high evaporative concentrations. In addition, the groundwater and surface water sources became more saline because of the irrigation inefficiencies, seepage from the earthen canals, groundwater pumping, inadequate drainage and return flows to the Arkansas River and its tributaries (Miles et al., 1977; Gates et al., 2002; Shultz et al., 2018). Irrigation of the alluvial soils also results in the dissolution of salts and metals (selenium and iron) from the underlying and outcropped marine shale. Elevated salinity in return flow and tailwater flow not only pollutes the river but also affects the quality of water at downstream diversions. High solute concentrations in the surface water bodies i.e. river and its tributaries affect the crop yield of the irrigated land and the ecological health of the river.

High ionic concentrations not only have detrimental effect on the surface water quality but also affect soil and aquifer system. The irrigation water of high ionic concentrations than a crop can tolerate results in yield loss. The high concentration of sodium in irrigation water can induce potassium deficiency, calcium deficiency, and waterlogging due to degradation of well-structured soils (Prince, 2016). Exalted levels of chloride ions in the irrigation water lead to accumulation of chloride ions in the leaves, which may cause leaves burning (Jennings, 1976). Elevated levels of sodium in the drinking water contribute to the elevation of blood pressure in humans (Calabrese and Tuthill, 1980; Foster, 2000). Gypsum ($CaSO_4.2H_2O$) is one of the sulfate minerals present in the soils of Colorado (Cooper, 2006). Gypsum is slightly dissolvable in water, which can percolate to groundwater via irrigation, or rainwater. The amount of calcium present in the water can form an insoluble solid and cause hardness when interferes with soap, if

used for domestic consumption. Also, sulfate minerals could have severe effects on human health: ingestion of small amounts of sodium sulfate ($NaSO_4$) and magnesium sulfate ($MgSO_4$) with drinking water causes catharsis in adult males (Cocchetto & Levy, 1981; Morris & Levy, 1983). The high concentration of solutes can impair surface water as well. For instance, high concentrations of sulfate in the tailwater runoff from the agriculture area of Florida Everglades discharge to the wetlands. It has impaired the Florida Everglades by stimulating the production of methyl mercury (Corrales et al., 2011). In order to sustain the ecological health of the rivers and irrigated agriculture regions, long-term water quality degradation must be resolved.

2.2 Solute Transport Modelling Efforts in Variably Saturated Subsurface Systems

Annually $11 billion is lost due to the decrease in crop yield associated with waterlogging and salinization in the world (Ghassemi et al., 1995). Properly constructed regional stream-aquifer model is one of the solutions to the agro-environmental and economic problem of salinization. These models have become increasingly popular, as they are capable of representing the complex hydrologic systems to capture the flows and 3-D reactive transport of solute due to the different chemical reactions in stream-aquifer systems.

Several geochemical models have been developed during the past three decades based on the difference of approach with which a model determines the species distribution at equilibrium, dimensions in which model will simulate the reactive transport and spatial scale at which the model is applied. PHREEQE (Parkhurst et al., 1980; Parkhurst & Appelo, 1999) is a reactive transport model for saturated groundwater flow system which is a combination of flow and 3D solute transport model HST3D (Kipp, 1987 and 1997) and aqueous geochemical reaction model PHREEQC (Parkhurst and Appelo, 1999). GMIN (Felmy, 1990) is a chemical equilibrium model which calculates the chemical composition of systems composed of pure solid phases, solid-

solution phases, gas phases, adsorbed phases, and the aqueous phases. MINTEQ (Felmy et al., 1995) was developed by USEPA in which geochemical equilibria is solved for dissolved, adsorbed, solid and gas phases by using a set of mass balance equations. UNSATCHEM-2D (Simunek and Suarez, 1994) is a 2D finite element modeling code used to analyze water and solute movement in unsaturated and partially saturated or fully saturated porous media. SAHYSMOD (Oosternbaan, 2005; Singh and Panda, 2012) coupled agro hydro salinity model SaltMod (Oster, 1989) and groundwater model SGMP (Boonstra and Ridder, 1990) for simulation and prediction of soil and groundwater salinity. Surface hydrology model CATSALT (Tuteja and Vaze, 2003) predicts the effects of land use change on landscape salinization and stream salinity. To model stream-aquifer flow and reactive transport of tetrachloroethylene (PCE) and trichloroethylene (TCE), Hussien and Schwartz (2010) used FTSTREAM and FTWORK (Faust et al., 1993). In other studies, soil and water assessment tool SWAT (Arnold et al., 1996) is coupled with a finite difference model MODFLOW (McDonald and Harbaugh, 1988) and contaminant transport model MT3D (Zheng, 1990) to simulate the reactive transport of solute in stream-aquifer systems (Narula and Gosain, 2013). Schoups et al. (2005) developed a hydro-salinity model by linking MODHMS (HydroGeoLogic Inc., 2006, Panday and Huyakorn, 2004) with UNSATCHEM (Saurez and Šimůnek,1997) to simulate subsurface salt transport and storage due to irrigated agriculture for the past 60 years in a 1400 km^2 region of the San Joaquin Valley California. Goff et al (1998) used a 2D distributed parameter flow and transport digital computer model developed by Konikow and Bredehoeft (1974) to examine the changes to alluvial aquifer quantity and quality. Bailey et al (2016) used coupled SWAT (Arnold et al., 1996) and MODFLOW (McDonald and Harbaugh, 1988) to study the spatiotemporal patterns of

groundwater discharge to the river system in a semi-arid region of Sprague River Watershed in Oregon USA.

WATEQ (Truesdell & Jones, 1974) is a FORTRAN computer program to model the thermodynamic specification of inorganic ions and complex species in the solution for any given water analysis. The Geochemist's Workbench (Bethke, 1994, 1996) is a reactive transport model which simulates chemical reactions with hydrological transport. MINTEQA2 (Allison et al., 1991) is used to calculate the equilibrium composition in natural aqueous systems. UNSATCHEM (Simunek and Suarez, 1997) is a 1D unsaturated water flow and solute transport for predicting major ions and plant water in the root zone. LEACHM (Wagenet and Hutson, 1987) simulates the transport of solute in unsaturated or partially saturated soils to a depth of about two meters. WATSUIT (Oster and Rhoades, 1975) is used to predict the solute concentration in the root zone and evaluate the effects of salinity on the crop yield. HYDRUS-1D (Simunek et al., 2005), which is used to simulate the movement of water and multi solutes in variably saturated porous media was coupled with UNSATCHEM (Simunek and Suarez, 1994) for simulating water, heat, carbon dioxide and solute movement in one-dimensional variably saturated media.

All of these models are applied and used at different spatial scales; ranging from 1D soil profile to river basins and employ varying degrees of complexity from simple advection transport to multispecies reactive transport in a stream-aquifer system as a whole.

2.3 Modeling Efforts in the Lower Arkansas River Valley

Modeling efforts in the LARV started with the work of Moore and Wood (1967) in which an analog model was used to study the effects of the pumping on the Arkansas River. Longenbaugh (1967) developed a transient model for LARV and concluded that the river is depleting during the irrigation season and being recharged from the return flows during winter months. Konikow and Bredehoeft (1974) developed the first flow and transport model in the LARV over a 5-year simulation period by repeatedly using the field data of 1-year period in an 11-kilometer reach of the valley between La Junta and the Bent-Otero county line. Person and Konikow (1986) revised the model developed by Konikow and Bredehoef using 11-year dataset to represent the field conditions more accurately. Goff et al. (1988) studied the groundwater salinity and return flows to the Arkansas River by applying the groundwater model developed by Konikow and Bredehoeft (1974) under different best management practices over a 24-year study period from 1971 to 1995. Results demonstrated that the aquifer salinity can be reduced moderately but the reduction in the stream salinity is limited. Cole et al. (1994) developed a MODFLOW model spanning from Pueblo to Colorado Kansas state line to study the groundwater flows, sources, and sinks.

At the beginning of the 21st century, Dai and Labadie (2001) coupled MODSIMQ and QUAL2E to model flows and water quality in the LARV between Pueblo and Colorado Kansas state line. In 2002, High water table was reported in the Pueblo County under the Bessemer Canal. Brendle (2002) developed a transient groundwater model for this area of Pueblo County and studied the effects of reduced recharge from over-irrigation, lining various lengths of the Bessemer Canal, installing subsurface drainage, and increasing groundwater extraction through pumping. Model results predicted that each management scenario was effective to lower the

water table, though to a varying amount. The sealing of the Bessemer Canal demonstrated the most significant increase in the groundwater table depth of 5.0 ft over the entire area. Colorado State University has been collecting data in the LARV since 1998. Gates et al. (2002) published results from a steady state model discussing that agriculture in the area is affected by irrigation-induced salinity. Steady state model also looked at the impacts of different best management practices to reduce salinity levels. Results demonstrated shallow groundwater with an average salinity of 3100 mg/L and an average depth of 2.1m to the water table. Burkhalter and Gates (2005) used the GIS-compatible interface known as the Groundwater Modeling System (GMS) Version 3.1 (BYU, 1999) to alter the steady state model developed in 2002 to transient state model. Computational finite difference grid was developed to use in U.S. Geological Survey's solute transport model MT3DMS (Zheng and Wang, 1999) and flow model MODFLOW (McDonald and Harbaugh 1988) to study the irrigation-induced salinity in the LARV. The results indicated that salinization has damaged the rural economy and reduced the crop yield in the fields across LARV by 0 to 89%. Cooper (2006) used Hydrus-1D (H1D) to study the soil salinity in the LARV and concluded that potentially costly management practices are required to decrease the soil salinity. Lin and Gracia (2008) designed a computer program using WETSUIT (Oster and Rhoades, 1975) to compute the quantity and quality of the return flows to the Arkansas River and simulate the soil-water composition. The results showed that the river salinity was lower during the irrigation season and higher during the off-season.

The salinity levels at downstream reaches were also high in comparison to the upstream reaches due to the salts brought to the downstream reaches by return flows. The average observed concentrations of TDS in USR and DSR soil root zones are 4180 mg/L and 5240mg/L, respectively. In some recent studies, Shultz et al. (2018) developed a regional scale stream-

aquifer modeling framework by coupling UZF-RT3D with OTIS-QUAL2E. The model, which is capable of simulating the reactive transport of selenium and nitrate was applied at upstream study region (USR) of the LARV. On the same route, Qurban (2018) developed, calibrated and tested a model which simulates the reactive transport of selenium and nitrate in the stream-aquifer system of the downstream study region (DSR) in the LARV.

All of these modeling efforts prove that with the use of properly constructed and calibrated models, engineers are able to help decision makers identify the best land and water management practices, which in return restore the quantity and quality of the river systems.

2.4 Flow, Salinity and Fate Transport Modelling Efforts in the LARV

The simulation of groundwater table and flow conditions is a prerequisite for solute transport modeling in the stream aquifer system. To address irrigation-induced waterlogging and water quantity issues in the LARV in southeastern Colorado, Morway et al. (2013) developed a finite-difference flow model MODFLOW-NWT (Niswonger et al., 2011) to study the current baseline conditions and examine the impact of different BMPs. An objective of the research was to find ways to increase the depth to the shallow saline water table in both the USR and DSR. The model is used to describe the shallow water table levels, non-beneficial groundwater consumptive use, the rate and timing of groundwater return flows to the streams.

The developed model is based on six years of observed data, i.e. from 2002 to 2007, in the DSR. Over 7200 depth to water table measurements were taken in the DSR from 118 monitoring wells. The average observed water table depths generally increased over the dry period of 2002 to 2003 then began to decrease in wetter years from 2004 to 2007 (Gates et al., 2016).

Unsaturated zone flow processes were simulated by incorporating the unsaturated zone flow (UZF1) package (Niswonger et al., 2006) with MODFLOW-NWT. The UZF1 module employs a kinematic wave approximation to Richards' equation and uses the method of characteristics for solving the one-dimensional downward vertical flow in the unsaturated zone. Hydraulic properties in the unsaturated zone are assumed to be uniform for each vertical column of model cells in the UZF1 package. The unsaturated-zone flow equation solved by the UZF1 package is given below:

$$\frac{\partial \theta}{\partial t} + \frac{\partial K(\theta)}{\partial z} + q_{ET} = 0 \qquad \text{EQ.1}$$

where

θ = Volumetric water content in the unsaturated zone [L^3L^{-3}],

$K(\theta)$ = Vertical hydraulic conductivity of the unsaturated zone as a function of θ [LT^{-1}], and

q_{ET} = The rate of evapotranspiration removal from the unsaturated zone per unit depth [$LT^{-1}L^{-1}$].

The kinematic-wave equation is employed to simulate the unsaturated-zone flow, ET and recharge over regional scales. When ET potential is not satisfied by unsaturated zone water then MODFLOW-NWT simulates ET derived from groundwater up flux on the basis of a linear function of water table depth (Harbaugh, 2005).

Colorado Division of Water Resources (CDWR) diversion record was used by Morway et al (2013) to designate surface water diversions to the canals in the MODFLOW-UZF application to the DSR. An algorithm was written to correctly represent the spatiotemporal irrigation pattern and the timing of seepage losses from canals. Farmers and extension agents were interviewed for a better understanding of irrigation schedules. A priority ranking code along with irrigation

frequency codes were used to distribute the available irrigation water among fields served by each canal. Raster maps were created for precipitation estimates on each cultivated field by using the rainfall data gathered from National Oceanic and Atmospheric Administration (NOAA). Well pumping data were also obtained from the Colorado Division of Water Resources (CDWR) historical records and the model was constructed to account for the monthly pumping volume. Groundwater measurements were taken from 118 groundwater monitoring wells in the DSR and return flows to the Arkansas River were simulated by water balance using the USGS stream gauges located on the Arkansas River as shown in Figure 2.1.

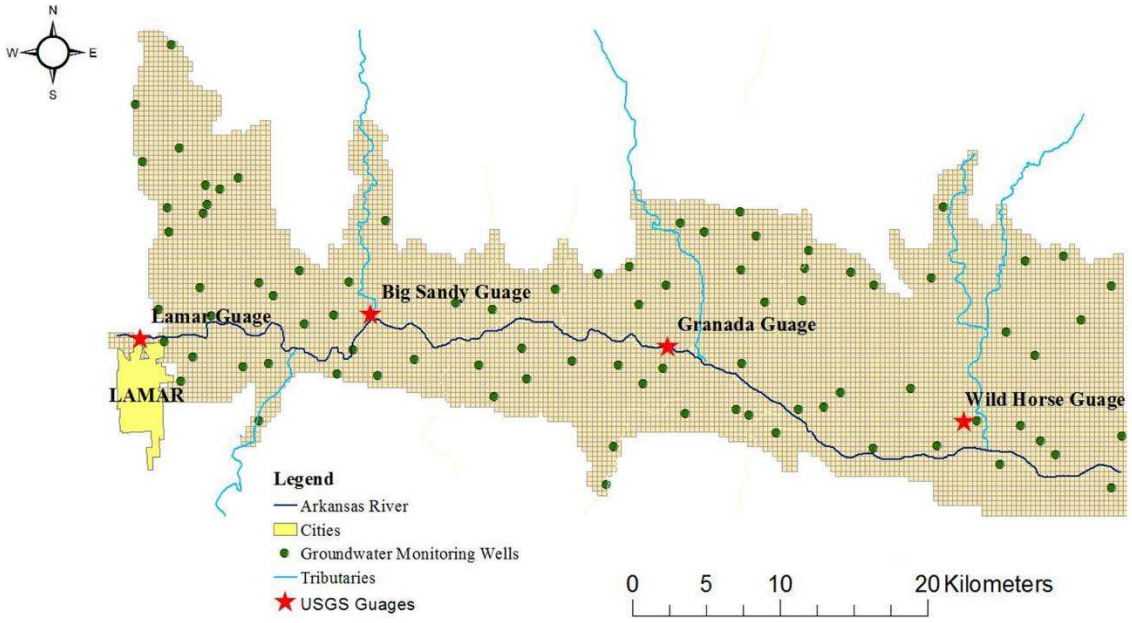

Figure 2. 1. DSR finite-difference grid showing the location of pumping wells and USGS stream gauges in the region.

Spatially varying values of potential evapotranspiration and reference evapotranspiration rates were used in the model. Potential evapotranspiration is the amount of evapotranspiration in a given time by a large vegetation of short green crop, completely shading the ground of uniform height and with adequate moisture at all the times in the soil and the reference evapotranspiration

is the amount of evapotranspiration from an extensive surface of green grass of uniform height, actively growing, completely shading the ground, and with adequate moisture at all the times in the soil. There are two approaches to measure the potential ET values for the whole study region: 1) Zonation/Parameterization framework (Hsieh et al., 2007); 2) Kriging (Kitanidis and Vomvoris, 1983). The second approach was selected to estimate the potential evapotranspiration rate. The reference evapotranspiration (ET_r) was measured at CoAgMet weather stations (Colorado Climate Center, 2007) and interpolated using ordinary kriging to obtain the values of ET_r over the entire model region. Reduced value of potential ET was applied to those lands that do not receive irrigation water and are considered as a fallow or natural cultivated land.

Actual evapotranspiration is the actual amount of water that is removed from the surface was calculated by the model and checked against ET rates estimated by processing satellite image with the RESET model (Elhaddad and Garcia, 2008) for both cultivated and naturally-vegetated land and field estimates of groundwater ET (Niemann et al., 2011).

Morway et al (2013) used the river package (RIV) in MODFLOW to represent the groundwater and surface water interaction such as canal seepage to groundwater and return flows from groundwater to streams. In the MODFLOW RIV package, water levels along the canals and streams were specified using data measured or estimated from the field. Surface water inflow to tributaries at the boundaries of the modeled region was assumed negligible.

The Morway et al (2013) flow model of the DSR is vertically-discretized into two layers. The first layer is approximately 5m thick and it encompasses the maximum extent of deeply-rooted crops (i.e. alfalfa). The second layer extends from the bottom of the first layer down to the impervious shale. The dimension of the grid cells is 250 m x 250 m in the horizontal direction and is comparable to the dimensions of the cultivated fields. Groundwater inputs include

precipitation, irrigation water from both canals and shallow groundwater pumping wells, canal seepage and seepage from tributaries and Arkansas River. Model outputs include evapotranspiration and groundwater pumping that either discharges water to the Arkansas River or its tributaries (Morway et al., 2013). When the water table is either within the root zone of plants or when the water from the groundwater rises into the root zone of plants through capillary action, it contributes to non-beneficial ET. This non-beneficial ET has been estimated to be approximately 18555 acre-feet of water per year under fallow and naturally vegetated land in the LARV (Morway et al., 2013).

The groundwater flow equation was solved for the hydraulic head for each computational grid cell and the volumetric flow rate between grid cells. The model was calibrated both manually and automatically. The automated parameter estimation software codes UCODE (Poeter et al., 2005) and PEST (Doherty, 2002) are used to calibrate hydraulic conductivity values to find a good match between observed and simulated data. The aquifer parameters like saturated zone horizontal hydraulic conductivity (K_H), saturated zone vertical hydraulic conductivity (K_v), unsaturated zone vertical hydraulic conductivity (K_s), the ratio of (K_s/K_H) in layer 1, the ratio of (K_v/K_H) in layer 2, specific yield for layer 1 and layer 2, saturated water content θ_s in the unsaturated zone, Brooks-Corey exponent (ε), canal conductance, and extension depth of soil were used in the flow model and are listed in Table 2.1.

Table 2. 1. Aquifer Properties of the Downstream Study Region (From Morway et al., 2013)

Number	Model Parameter	Range Value
1	Layer 1 K_H	0.3-160 m/d
2	Layer 1 K_S/K_H	$7x10^{-5}$ - $2.9x10^{-2}$
3	Layer 2 K_H	1.4 - 75 m/d
4	Layer 2 K_V/ K_H	0.1
5	Layer 1 *Sy*	0.01-0.33
6	Layer 2 *Sy*	0.01-0.34
7	Layer 1and 2 *Ss*	$1.7x10^{-5}$
8	Canal conductance	$1.7x10^{-3}$-8.6 m^2/d/m
9	Saturated *K* in UZF1	$1.1x10^{-2}$-0.26 m/d
10	ε (Brooks-Corey exponent)	3.5
11	θ_s (UZF1)	0.18-0.39
12	Extinction depth	1.3-4.5 m

2.5 Field Studies for Fate and Transport of S Species

Salinity is one of the most significant problems in the LARV (Miles et al., 1977; Goff et al., 1998; Ward and Waskom., 2002). There are multiple sources of salinity in the LARV such as geology of the area (craterous shale), agriculture return flows to the Arkansas River and its tributaries, waterlogging due to the extensive irrigation and rise in groundwater levels (Miles, 1977; Konikow and Person, 1985; Hukkinen,1993; Goff et al., 1998; Gates et al., 2002; Shultz et al., 2018).

Colorado State University has collected data from more than 200 groundwater monitoring wells located all over the LARV. The electrical conductivity of the soil was measured using the EM-38 probe in dozens of different fields in the LARV over a period of 8 years between 1999

and 2006. To monitor the solute concentration in the stream water, samples were collected from the Arkansas River, its tributaries and canals that are diverted from the river to irrigate the fields in the valley. The location of the groundwater monitoring wells and ECe surveyed fields are shown in Figure 2.1. Research work in the LARV by Colorado State University has addressed salinity, *Se, NO_3* and *U* pollution problems in both USR and DSR while extending the model to simulate *Se* and NO_3 concentration in surface water as well.

Most of the irrigation in the study region is done by flood irrigation that provides more than required water to the irrigated land. Hence, an excess amount of water infiltrates to the alluvial aquifer which further increases the water table (Morway et al., 2013). Water also seeps into the alluvial aquifer due to the canal seepage from the earthen canals, which in return reduces the depth to the water table (Gates et al., 2006). Moreover, the salts that are present in the irrigation water stay in the soil while water infiltrates the aquifer that has increased the soil salinity. These salts in the surface soil are detrimental for plant growth, makes it difficult for plants to uptake water from the soil and hence, decreases the crop yield (Gates et al., 2006).

In arid and semi-arid regions, calcite and gypsum are believed to be the dominant salt minerals (Bresler et al., 1982; Hillel .,2000; Saurez., 2005). Calcite (calcium carbonate) solubility is controlled by pH and carbonate (CO_3^{-2}) concentrations (Olsen and Watanabe, 1959; Lindsay, 1979). In freshwater, the solubility of gypsum is controlled by solubility product (ksp) (Glas et al., 1979) but in irrigation water, the solubility of gypsum is primarily controlled by the composition of the irrigation water (Kemper et al., 1975). Gypsum can precipitate and dissolve within the soil profile due to its solubility properties (Skarie et al., 1987a; Skarie et al., 1987b). At a pH of approximately 7.8 gypsum and calcite can precipitate and coexist in soils. (Lindsay, 1979). USDA NRCS database shows that in the DSR, calcite is present in the soil approximately

0 to 11% of the dry weight while gypsum is present in the DSR approximately 0 to 1.5% of the dry weight.

Tavakoli Kivi et al. (2017) simulated the fate and transport of *S* species using UZF-RT3D at field scale in two corn test fields at Arkansas Valley Research Center (ARVC). Collected observed data i.e. fertilizer application, the quantity of applied irrigation water, tailwater runoff, quality of the irrigation water, and the solute concertation in the soil for the year 2009 growing season. In order to compare the simulated results with the observed data UZF-RT3D (S module) finite difference model's grid was discretized coomparing to the depth at which the soil samples were taken. Flows were calculated by using the MODFLOW-UZF, which is a prerequisite of UZF-RT3D. Two hundred UZF-RT3D simulations were run to determine the influence of model parameters for the unsaturated zone. During the growing season, The mineralization of *S* to SO_4-*S* decreases during the growing season but increases sharply after the Harvest (October 10th) and Plowing (November 7th) days. The concentration of SO_4-*S* also increases abruptly near the planting day due to the application of *S* fertilizers. It has been concluded that the chemical reduction rate of sulfate (λSO_4) is the parameter that has strongly affected the sulfate concentrations in the soil.

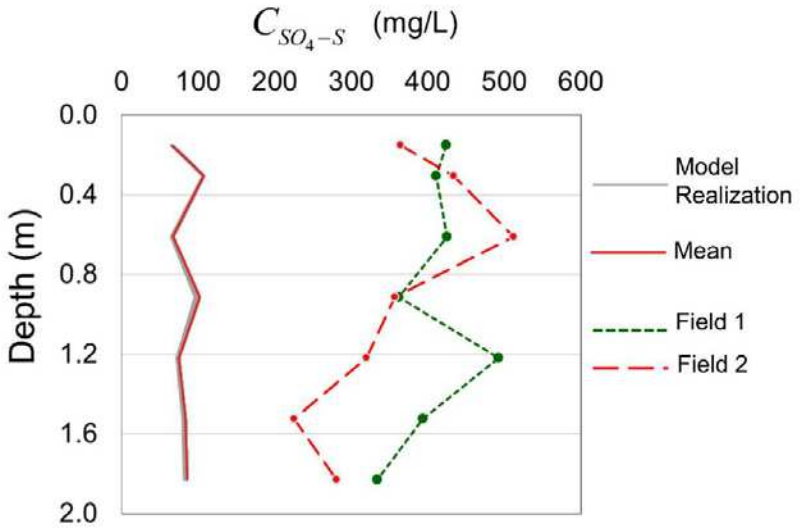

Figure 2. 2. Observed and simulated concentrations of *SO_4-S* with depth for the test field at the Arkansas Valley Research Center. (Tavakoli Kivi et al., 2017).

In Figure 2.2, the observed concentrations are represented with the dashed lines for field 1 and field 2, the simulated model concentrations are represented with gray lines and the mean of the ensemble is represented with a red line. The results show that the model is underpredicting during the daily simulation period of the year 2009 pointing to the deficiency in the model itself. The reason for this discrepancy in the model results was due to the absence of Salinity Equilibrium Chemistry (SEC) module in the model which accounts for the precipitation/dissolution of salt ions. Salt minerals (gypsum and calcite) are prevalent in the soils throughout the LARV as studied by Cooper (2006) and observed in the USDA NRCS database.

2.6 Models Used in this Study

This section provides a description of the models used in the present study. The detail description of model coupling and integration is given in Chapter 3 of this thesis.

USGS groundwater flow model (MODFLOW) is used to simulate the 3-Dimensional saturated groundwater flows. Unsaturated Zone Flow package UZF1 and streamflow routing

package SFR2 (Niswonger and Prudic, 2005) is used with the MODFLOW to model the unsaturated zone and stream-aquifer interaction respectively. Stream-aquifer interaction in SFR2 package is computed by using Darcy's Law, streambed thickness and streambed hydraulic conductivity (Niswonger and Prudic et al., 2004). Previous studies (Morway et al., 2013) done in the LARV to model the saturated groundwater flows used RIV (Harbaugh, 2005) package to simulate the stream-aquifer interaction. RIV package is not adequate to be used in BMP's analysis as it requires a predefined stream stage and changes in flow rates. Due to this difference, BMPs cannot be modeled correctly. MODFLOW simulates the flows in the stream-aquifer systems and feed head values as an input to the RT3D/SEC-OTIS.

The numerical model (RT3D/SEC-OTIS) is based on UZF-RT3D (Bailey et al., 2013a) and UZF-RT3D/SEC (Tavakoli Kivi et al., 2019). UZF-RT3D (Bailey et al., 2013a) combines unsaturated zone flow (UZF1), 3D reactive transport model RT3D (Clement, 1997) and flow model MODFLOW to simulate the reactive transport of multiple interacting chemical species in variably saturated groundwater flow systems. UZF-RT3D/SEC model (Tavakoli Kivi et al., 2019) links Salinity Equilibrium Chemistry (SEC) module with UZF-RT3D (Bailey et al., 2013a) to simulate the movement and transformation of major salt ions (magnesium, sodium, potassium, sulfate, chloride, bicarbonate, and carbonate) in soil aquifer system. The source code of RT3D/SEC-OTIS is developed by linking UZF-RT3D/SEC code with OTIS (Runkel, 1998) model. OTIS is a mathematical simulation model that computes advection, dispersion, transient storage, lateral inflow/outflow, first-order decay and sorption of fate and water born solutes in streams and rivers. The RT3D/SEC-OTIS simulates the fate and transport of major salt ions in a regional scale stream-aquifer system and accounts for salt inputs, equilibrium chemical reactions, oxidation-reduction reactions and the cycling of (*C*), nitrogen (*N*), and sulfur (*S*) in the plant-soil

system. Moreover, it has the capability to model in three dimensions, simulates the solute concentrations in the saturated zone, unsaturated zone and surface water at the same time, capable to be applied both at large scale watersheds and small scale field studies, has the ability to handle sources such as fertilizer and irrigation and of simulating multiple salt species. To the best of our knowledge, this is the first effort of developing a model that is capable of computing the salinity of fate and transport of major salt ions due to precipitation dissolution, complexation, cation exchange, first-order degradation and redox reactions in coupled stream-aquifer systems at a regional scale. The developed model can also be applied to other regions that are suffering from problems of high salinity and can be used to investigate the best management practices to reduce the levels of salinity in stream-aquifer systems.

CHAPTER 3

METHODS: COUPLED SALT TRANSPORT MODEL CALIBRATION AND APPLICATION

This chapter outlines the methods of the application of the finite-difference reactive transport model UZF-RT3D/SEC-OTIS, which simulates the movement of major salt ions in the stream-aquifer system, and its calibration for the DSR of Colorado's LARV. The groundwater flow model (MODFLOW-UZF) and subsurface reactive transport model (UZF-RT3D/SEC) are described with an emphasis on the coupling of MODFLOW-UZF with the SFR2 stream routing module and the joining of UZF-RT3D/SEC with the one-dimensional stream transport model OTIS in application to salinity modeling.

3.1 Groundwater Flow Model

3.1.1 Background of Groundwater Flow Modeling

Groundwater flow models are prerequisite to reactive transport models. This section focuses on water quantity issues and presents a finite-difference numerical model developed by Morway et al. (2013) to describe shallow water table levels, saturated and unsaturated flow, non-beneficial groundwater consumptive use, and return flows to the streams. Before 1984, there were several groundwater flow models used by USGS such as Trescott (1975), Trescott and Larson (1976). In 1984, McDonald and Harbaugh consolidated the capabilities of these flow models into a single code called USGS Modular Three-Dimensional Finite-Difference Ground-Water Flow Model later known as MODFLOW. Over the years, different packages were added to the MODFLOW to make it more accurate and thorough. Today, MODFLOW is used all over the world to study the groundwater flows.

The MODFLOW-2005 version of MODFLOW uses a modular structure wherein similar subroutines are grouped together and hydraulic options are independent of each other. New packages can be linked with the original MODFLOW code without making any changes to the existing code (Harbaugh, 2005). MODFLOW-2005 uses linear and non-linear numerical-solution methods to solve the groundwater flow equations. There are different methods to solve the system of non-linear equations i.e. Picard method and Newton method. The Newton method of solving the non-linear equations is very useful for problems which represent the unconfined aquifer and surface water/groundwater interaction. MODFLOW-NWT uses the Newton solution method and unstructured, asymmetric matrix solvers to calculate groundwater head, often referred to as a Newton-Krylov method (Knoll and Keyes, 2004).

The hydrologic process that occurs near the land surface such as infiltration and evapotranspiration are important to be incorporated in regional scale stream-aquifer flow models. Unsaturated Zone Flow (UZF1) (Niswonger et al., 2006) Package for MODFLOW-2005 is used to simulate these hydrologic processes in the unsaturated zone. UZF1 uses one-dimensional form for the Richard's equations, which is approximated by kinematic-wave equation and solved by the method of characteristics (Smith, 1983).

The groundwater flow model developed by Morway et al (2013) in application to the USR and DSR of Colorado's LARV uses the MODFLOW-NWT version of the groundwater flow model along with the UZF module for unsaturated flow. In the current study, UZF-MODFLOW was joined with the SFR2 module for routing flow within streams in exchange with groundwater return flows.

3.1.2 Modifications to MODFLOW-UZF for this Application

A modified form of the flow model developed by Morway et al. (2013), in whichthe RIV package was replaced with the SFR2 package, was used in this study. This modification was made by Shultz et al (2018) and implemented by Qurban (2018). The RIV package is used to simulate head-dependent flux boundaries to represent stream-aquifer interaction. It requires the user to provide stream stage data for each model stress period and does not simulate streamflow. On the other hand, the SFR2 package has the capability to model stream-aquifer flow interactions using Darcy's law, quantifies water exchange rates between each SFR2 cell and adjacent aquifer cell. Stream flow routing from upstream to downstream along the river and its tributaries in SFR2 is based on the continuity equation assuming uniform flow. The Arkansas River is discretized in this study into 488 cells along the river, with each cell being 250 m x 250 m in the horizontal plane. This stream-aquifer interaction and routing are required to simulate the solute concentration of major salt ions within the stream water.

The simulated results of the modified MODFLOW-UZF/SFR2 model are tested against observed data collected from four USGS gauges (Lamar Gauge: ARKLAMCO, Granada Gauge: ARKGRACO, Big Sandy Gauge: BIGLAMCO, and Wild Horse Gauge: WILDHOCO) along the river. The locations of these four USGS gauges are shown in Figure 2.1. MODFLOW simulates the flow for 261 weekly stress periods from May 2002 to August 2007. Observed data is collected at 15 minutes interval with flow aggregated to compare it with the weekly-simulated MODFLOW data. Observed groundwater levels in monitoring well are available for the year 2003 to 2007. Calibrated cell-by-cell hydraulic conductivity (m/day), hydraulic head (m) and depth to the water table (m) computed by flow model, are shown in Figure 3.1, 3.2 and 3.3

respectively. The UZF-RT3D/SEC-OTIS utilizes the flow patterns to simulate the reactive transport of major salt ions, which is explained in later sections.

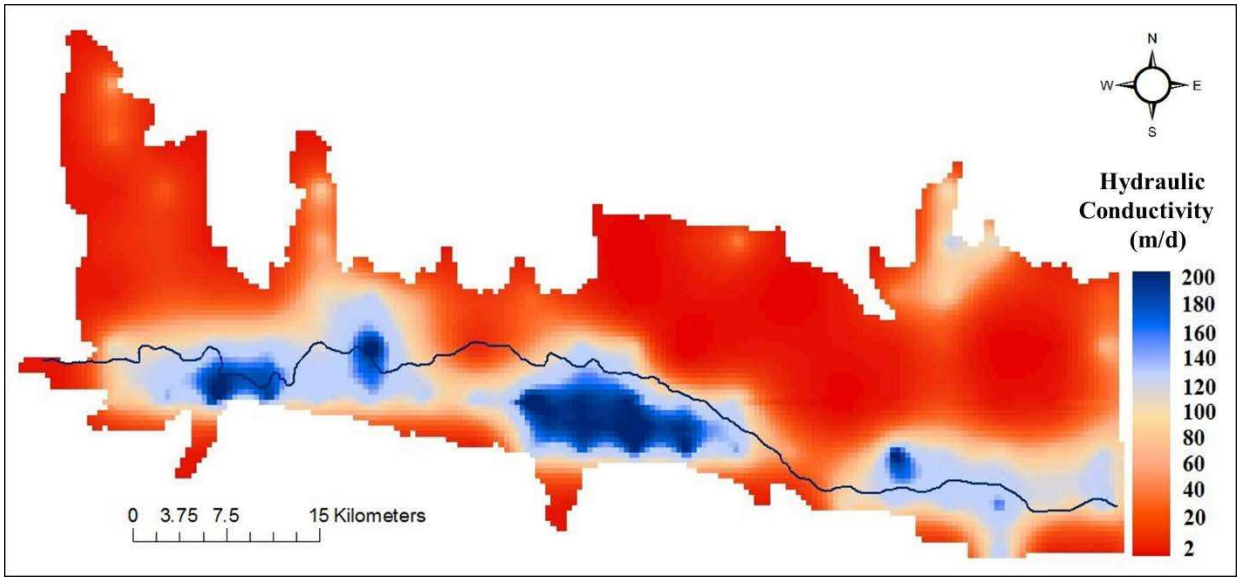

Figure 3. 1. Calibrated hydraulic conductivity (m/d) values in the DSR (Qurban, 2018).

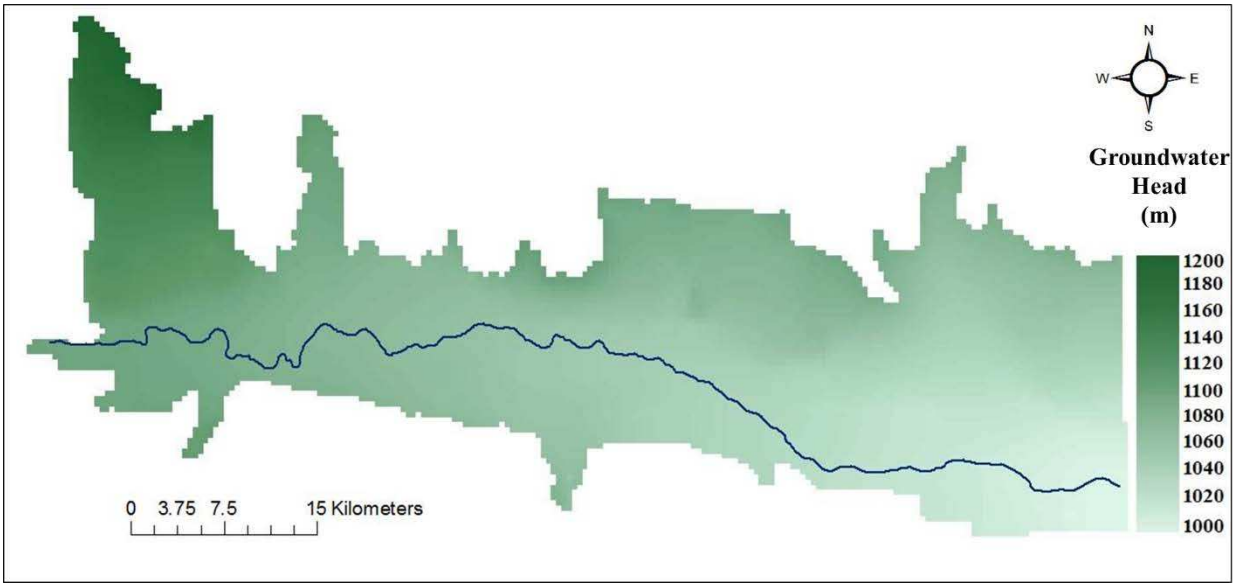

Figure 3. 2. Computed groundwater head values in the DSR averaged over the simulation period (Qurban, 2018).

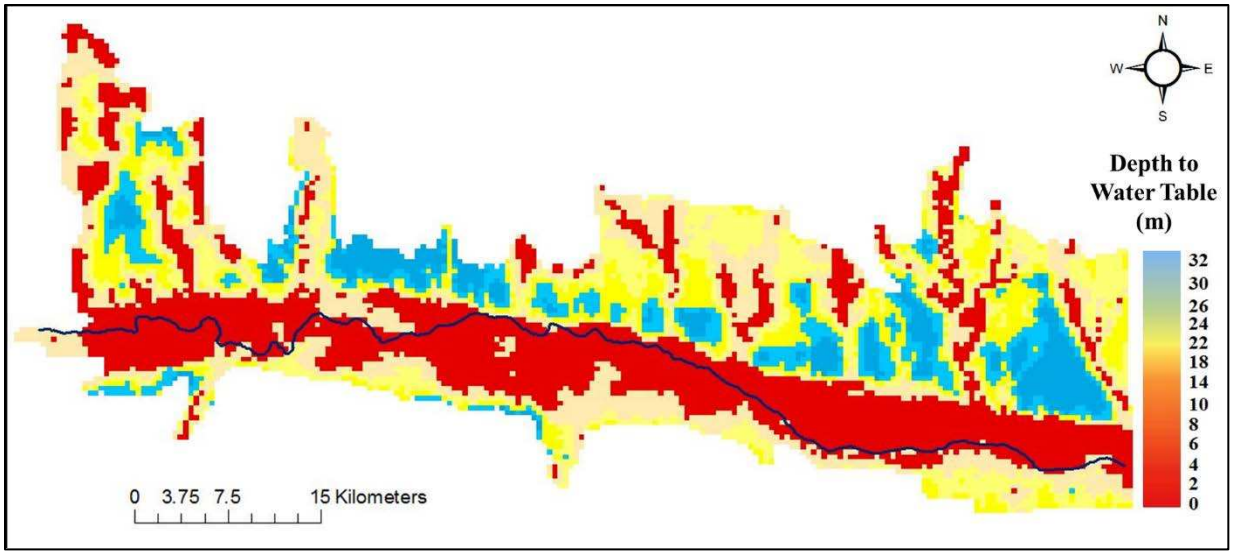

Figure 3. 3. Computed water table depth in the DSR averaged over the simulation period (Qurban, 2018).

3.2 Reactive Transport Model

3.2.1 Summary

The development of reactive transport models started two decades ago. The first few reactive transport models were limited to saturated zones only (e.g., Rubin, 1983; Clement et al., 1997a; Prommer et al., 2003; Parkhurst et al., 2004; Parkhurst et al., 2010).

UZF-RT3D can be used to model solute concentration in the aquifers at a regional scale. It has the capability to include site chemical species and reactions. The kinematic wave approximation was applied to the Richards' equation that decreases the computational burden of the model and made it more efficient. To neglect the diffusive terms in the Richards equation, the unsaturated Zone Flow (UZF1) package (Niswonger et al., 2006) assumes vertical homogeneity of the unsaturated zone and neglects the capillary pressure gradient. Therefore, there are tradeoffs that exists between the speed of UZF1 and the accuracy of the Richards equation, as solving the complete Richards equation will require longer computation period.

3.2.2 Development of UZF-RT3D (Bailey et al 2013a)

The UZF-RT3D consists of mass balance equations. UZF-RT3D uses the finite difference (FD) approximations method to solve a system of advection-dispersion reaction (ADR) equations with one equation for each chemical species for both dissolved phase and the solid phase in variably saturated groundwater systems (Clement, 1997; Clement et al., 1998). The ADR system of the equation solved by RT3D is:

$$\emptyset \frac{\partial C_k}{\partial t} = -\emptyset \frac{\partial}{\partial x_i}(\upsilon_i C_k) + \emptyset \frac{\partial}{\partial x_i}\left[D_{ij} \frac{\partial C_k}{\partial x_j}\right] + q_s C_{s_k} - \rho_b \frac{\partial \bar{C}_k}{\partial t} + \emptyset_r \qquad k=1,2,\ldots m \qquad \text{EQ.2}$$

where

m = The total number of dissolved phase species,

C_k = Solute concentration of the k^{th}species in the aqueous phase [$M_f L_f^{-3}$],

f = Represents the fluid phase,

D_{ij} = The hydrodynamic dispersion coefficient [L^2T^{-1}],

v = Average seepage velocity [L_bT^{-1}],

b = Denotes the bulk phase,

$\emptyset$ = Soil porosity [$L_f^{-3}L_b^{-3}$],

q_s = Volumetric flux of water representing sources and sinks of the species [$L_f^3T^{-1}L_b^{-3}$],

C_{s_k} = Concentration of the solute in source or sink [$M_f L_f^{-3}$],

r = Rate of all reactions that occur in the aqueous phase [$M_f L_f^{-3}T^{-1}$],

ρ_b = Bulk density of the porous media [$M_bL_b^{-3}$], and

$\bar{C}_k$ = The concentration of kth species sorbed on the solids [$M_f M_b^{-1}$].

The retardation factor R_k [-] is equal to $1+(\rho_b K_{d_k})/\emptyset$ for linear sorption where K_{d_k} is the partitioning coefficient [$L_f^{-3}M_b$] for the k^{th} species and is equal to $\frac{\bar{C}_k}{C_k}$. Incorporating these values in equation 2 yields:

$$\frac{\partial C_k}{\partial t} R_k = -\frac{\partial}{\partial x_i}(\upsilon_i C_k) + \frac{\partial}{\partial x_i}\left[D_{ij}\frac{\partial C_k}{\partial x_j}\right] + \frac{q_s C_{s_k}}{\emptyset} + r \qquad k=1,2,\ldots m \qquad \text{EQ.3}$$

Where *r* represents the decay or production of species according to simple, Monod or dual Monod kinetics and in relation to the concentration of other simulated species. Saturated thickness, groundwater flow velocities and volumetric flux of water into and out of the model domain are applied by 3D groundwater flow model MODFLOW through a transport link file. Operator-split (OS) numerical scheme (Clement, 1997; Yeh and Tripathi, 1989) is used to solve ADR equations to simulate the changes in solute concentrations. Variably-Saturated Transport (VST) package is used to simulate the reactive transport of solute in the unsaturated zone. Variably-Saturate Transport (VST) package can be turned off in the in input files to revert UZF-RT3D to original RT3D functionality.

The UZF-RT3D model was tested for 1D and 2D simulations against the UZF-MT3DMS code developed by Morway et al (2012). The results of UZF-RT3D were also tested against the analytical model published by van Genuchten (1981) and the coefficient of determination R^2 values were compared. The simulated mass balance error for the 2D and 3D systems is found to be less than 0.005%.

3.2.3 Sulfur Cycling and Reaction Module for UZF-RT3D (Tavakoli Kivi et al., 2017)

The cycling of sulfur mass occurs in the soil organic matter, which is composed of litter and Humus. During the plowing sulfur mass mineralized to sulfate and during the growing seasons the crops take up this sulfate. The sulfate present in soils dissolves with the applied irrigation

water and enter the streams as return flows, which increases the concentration of sulfate in the streams. Moreover, when irrigation water with a high concentration of sulfate is applied to the fields or seeps from the canal bed, it reaches the subsurface system and adds sulfate to the subsurface water. Another source of sulfate contamination for the subsurface system is the fertilizer application.

Marine sedimentary rock forms the bedrock beneath 8,050,000 km^2 of the Western United States. Existence of these pyrite (FeS_2) bearing sedimentary rocks (shale) and application of N fertilizer along with irrigation water can also release sulfate via autotrophic reduction of O_2 and NO_3, hence leading to the mobilization of SO_4 and contamination of groundwater and surface water bodies (Frind et al., 1990; Postma et al., 1991; Pauwels et al., 1989).

$$2FeS_2 + 7O_2 + 2H_2O \longrightarrow 2Fe^{2+} + 4SO_4^{2-} + 4H^+ \quad \text{EQ.4}$$

$$5FeS_2 + 14NO_3^- + 4H^+ \longrightarrow 5Fe^{2+} + 10SO_4^{2-} + 7N_2 + 2H_2O \quad \text{EQ.5}$$

Field measurements done by Frind et al in 1990 also proves that sulfate reacts with solid organic carbon present in the aquifer material when the nitrate concentrations fall below a threshold level of 1 mg/l. The organic carbon serves as the electron donor for the microbial desulfurization. The reaction takes place in a nitrate free groundwater zones.

$$SO_4^{2-} + 2C_{org} + 2H_2O \longrightarrow 2HCO_3^- + H_2S \quad \text{EQ.6}$$

The processes that govern the sulfur cycling in the soil aquifer systems in an agricultural area is shown in Figure 3.4.

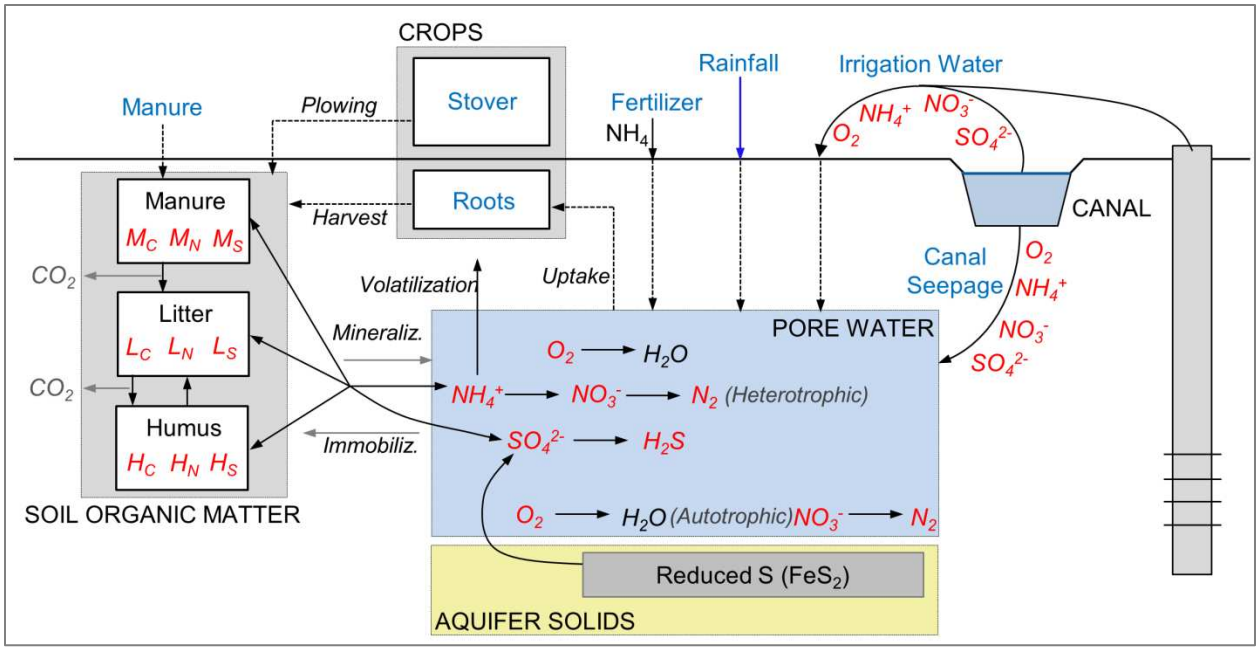

Figure 3. 4. Cycling of sulfur in agricultural root zones and groundwater water systems including plat mass input/outputs, organic matter decomposition, mineralization/immobilization, and oxidation-reduction reactions (Tavakoli Kivi et al., 2017).

The sulfur reaction module for UZF-RT3D consists of mass balance equations, chemical reactions, rate laws, and source and sinks of *S* mass. The *S* module of UZF-RT3D solves a system of advection-dispersion-reaction (ADR) equations for both dissolved-phase and solid-phase species using a finite difference approach (Tavakoli Kivi et al., 2017).

$$\frac{\partial(C_k\theta)}{\partial t}R_k = -\frac{\partial}{\partial x_i}(\theta v_i C_k) + \frac{\partial}{\partial x_i}\left[\theta D_{ij}\frac{\partial C_k}{\partial x_i}\right] + q_f C_{fk} + \theta r_f \qquad k=1,2,\ldots m \qquad \text{EQ.7}$$

$$\frac{\partial(C_l\,\varepsilon)}{\partial t} = \alpha_l P_s + \varepsilon r_s \quad l=1,2,\ldots n \qquad \text{EQ.8}$$

where

m and n = The total number of dissolved and solid phase species,

C_k= Solute concentration of the kth species in the aqueous phase [$M_f L_f^{-3}$],

C_l = Solute concentration of lth species in the solid phase [$M_f L_f^{-3}$],

f = Represents the fluid phase,

D_{ij} = The hydrodynamic dispersion coefficient [L^2T^{-1}],

υ = Pore velocity [$L_b T^{-1}$],

b = Represents the bulk phase,

θ = Volumetric water content [$L_f{}^3 L_b{}^{-3}$],

ε = Volumetric solid content [$L_f{}^3 L_b{}^{-3}$] where s denotes the solid phase and is equal to $1 - \emptyset$ with $\emptyset$ representing the porosity,

q_f = Volumetric flux of water representing sources and sinks such as irrigation water, canal seepage, pumped groundwater, groundwater discharge to the river [$L_f{}^3 T^{-1} L_b{}^{-3}$],

C_f = Concentration of the solute in source or sink [$M_f L_f{}^{-3}$],

P_s = Mass application rate for the L^{th} solid phase sources ($M_s L_b{}^{-3}$),

α_l = Fraction of P_s attributed to species l,

r_f = Rate of all reactions that occur in the dissolved phase [$M_f L_f{}^3 T^{-1}$],

r_s = Rate of all reactions that occur in the solid phase [$M_s L_s{}^3 T^{-1}$],

R_k = Retardation factor for species k and is equal to $1 + (\rho_b + K_{dk})/\theta$ for linear sorption,

ρ_b = Bulk density of the porous media [$M_b L_b{}^{-3}$], and

K_{dk} = Partitioning coefficient for the kth species [$M_b L_f{}^{-3}$].

Saturated thickness, groundwater flow velocities and volumetric flux of water into and out of the model domain are applied by three-dimensional groundwater flow model MODFLOW which uses the Unsaturated Zone Flow package (UZF1) (Niwsonger et al., 2006) for pore velocity (υ) and volumetric flux of water representing sources and sinks (q_f). These outputs from the MODFLOW are used in UZF-RT3D/SEC to simulate the solute reactive transport of major salt ions.

The equation 7 is divided into four distinct equations to solve for the changes in SO_4-S in dissolved phase, S in the litter pool (Ls) , S in humus pool (Hs), and S in the manure pool (Ms), with later three solid-phase species which are explained in Tavakoli Kivi et al., (2017).

Sulfate reaction module of UZF-RT3D also solves the mass balance equation for NH_4, NO_3, and O_2 and includes carbon and nitrogen cycling as O_2 and NO_3 have an influence on the fate and transport of SO_4-S. S and Se are from the same group of elements i.e. Chalcogen. Being the element of the same group, the parameters responsible for the release of SO_4-S from the marine shale formations must be constrained by their associated influence on the release of selenate (SeO_4-Se). Therefore, the reactive transport of Se species including selenate (SeO_4) is also included in the source code of UZF-RT3D/SEC. The Se reaction module for UZF-RT3D is described in Bailey et al., (2013b), Shultz et al., (2018) and Qurban (2018). Furthermore, nitrogen fertilizer loading, crop uptake of NH_4, NO_3 and SeO_4-Se are also included in the source code along with the chemical reactions associated with these species i.e. nitrification, NH_4 volatilization, heterotrophic denitrification, and chemical reduction of SeO_4.

The reaction rates of S are analogous to the Se reaction rates in the solid phase (Tavakoli Kivi et al., 2019). The rate expressions for microbial-mediated chemical reduction of SO_4 (r^{het}_{f,SO_4}) and for the decomposition of Ls, Hs, Ms, and inter-pool mass transfer are given in Tavakoli Kivi et al., (2017).

3.2.4 Salinity Equilibrium Chemistry Module

The presence of salt minerals in the soils of LARV (Cooper, 2006) and the difference between the simulated and observed concentration of C_{SO_4-S} (Tavakoli Kivi et al., 2017) lead to the introduction of a new equilibrium chemistry module (SEC). The SEC module simulates the

movement and transformation of major salt ions (calcium, magnesium, sodium, potassium, sulfate, chloride, bicarbonate and carbonate) due to advection, dispersion, source/sink mixing, redox reactions, precipitation-dissolution of salt minerals, complexation, cation exchange, crop uptake, soil organic matter decomposition, and mineralization/immobilization of carbon, nitrogen, and sulfur species. The SEC module coupled with UZF-RT3D by Tavakoli Kivi et al (2019).

Geology of the irrigation regions around the world is different from one place to another, which determines the presence of different salt minerals. In order to make the model feasible for application in other areas of the world, the source code has been written in such a way that it can be altered for additional salt minerals that may be present in other irrigated areas. *C* and *N* cycling, and the release of SO_4 from pyrite (FeS_2) in the presence of O_2 and NO_3 are also included. The fate and transport of major salt ions in an irrigated region are presented in Figure 3.5.

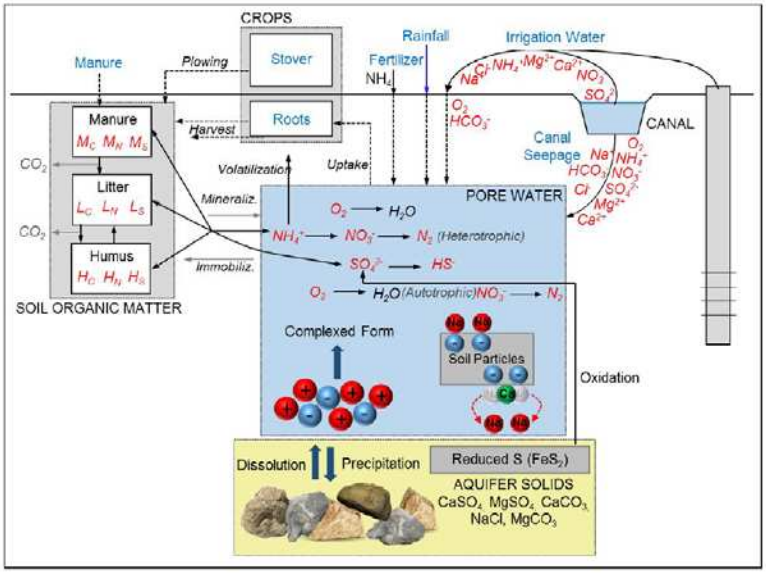

Figure 3. 5. Nutrient cycling in soil and groundwater system in an agricultural area, including plant mass inputs/output, organic matter decomposition, mineralization/immobilization, oxidation-reduction reactions, precipitation-dissolution, complexation, and cation exchange. (Tavakoli Kivi et al., 2019).

The cycling of *S* mass occurs as an organic *S*, which is incorporated into the soil organic matter. SO_4 can also be released from FeS_2 via autotrophic reduction of O_2 and NO_3 (Frind et al., 1990; Postma et al., 1991; Pauwels et al., 1998). These SO_4 mass can be added to the groundwater via irrigation water or seepage from the canals and can be added to surface water bodies (Arkansas River and its tributaries) with return flows. Salt ion concentrations can also be increased or decreased in the stream-aquifer systems due to the precipitation/dissolution of salt minerals ($CaSO_4$, $CaCO_3$, $MgCO_3$, $MgSO_4$, and $NaCl$).

The Salinity Equilibrium Chemistry (SEC) module is developed and linked with the UZF-RT3D to add the major physical-chemical process of salt ions i.e. precipitation/dissolution of salt solids, complexation and cation exchange to predict major ion solute chemistry in the soil aquifer system. The SEC module have eight aqueous species, ten complexed species, five solid species, and four exchange species, which are listed in table 3.1.

Table 3. 1. Species included in the SEC module of UZF-RT3D (Tavakoli Kivi et al., 2019)

Group Name	Species
Solid Species	*CaSO4,CaCO3,MgCO3,NaCl, MgSO4*
Complexed Species	$CaSO_4^0$, $MgSO_4^0$, $CaCO_3^0$, $CaHCO_3^+$, $MgCO_3^0$, $MgHCO_3^+$, $NaSO_4^-$, KSO_4^-, $NaHCO_3^0$, $NaCO_3^0$
Exchanged Species	*Ca, Mg, Na, K*
Aqueous Species	Ca^{2+}, Mg^{2+}, Na^+, K^+, SO_4^{-2}, CO_3^{-2}, $HCO3^-$, Cl^-

Law of mass action is used in the SEC module to determine the concentration of each ion within the system along with mass balance equations. The mass balance equation of the SO_4 aqueous components is given below which states that the total concentration of species in the

solution is the sum of free ions and complex form of those ions. The mass balance equations for other major salt ions are given in Tavakoli Kivi et al., (2019).

$$SO_{4_T}=\left[SO_4^{2-}\right]+\left[CaSO_4^0\right]+\left[MgSO_4^0\right]+[NaSO_4^-]+[KSO_4^-] \quad \text{EQ.9}$$

where

Subscript T = The total concentration of the aqueous component and

Brackets = Indicates the molality of the species within the solution.

The presence of complexes increases the solubility of minerals because complexation lowers the activity of free ions (Appelo and Postma, 2005). The law of mass actions is used to define the equilibrium constants for the complex species and the values of the equilibrium constant are taken from the literature (From Truesdell and Jones, 1974) which are listed in Tavakoli Kivi et al., (2019).

The SEC module also calculates the cation exchange replaceability by using the electrostatic forces, which determines the adsorbed ions to the soil particles and released ions from the soil particles to the solution. The order of the replaceability is determined by Coulomb's law and found to be $Na>K>Mg>Ca$. The Gapon equation is used to simulate the cation exchange reactions.

SEC module also includes dissolution or precipitation reactions for each salt. The stoichiometric reaction for a salt mineral AB_s and the free ions A_{aq}^+ and B_{aq}^- is:

$$AB_s \leftrightarrow A_{aq}^+ + B_{aq}^- \quad \text{EQ.10}$$

The values of precipitation and dissolution are dependent on the saturation level of the solution. Five major salt solids are included in the SEC module for this study i.e. $CaSO_4$, $CaCO_3$, $MgCO_3$, $MgSO_4$, and $NaCl$. The precipitation-dissolution reactions of these salts are explained in Tavakoli Kivi et al., (2019). The solubility product values for salt minerals are taken from the

appendix 2 of Handbook of Chemistry and Physics, Hyanes et al., 2016). More salt minerals can be added to the SEC module depending on the region under study and their precipitation/dissolution reactions can be simulated without making any changing into the applied method.

Table 3. 2. Solubility product values (Hyanes et al., 2016).

Salt Mineral	Solubility Product	Value
$\mathbf{CaSO_4}$	K_{sp1}	3.0702×10^{-9}
$\mathbf{CaCO_3}$	K_{sp2}	4.7937×10^{-6}
$\mathbf{MgCO_3}$	K_{sp3}	7.888×10^{-5}
$\mathbf{MgSO_4}$	K_{sp4}	0.007244
NaCl	K_{sp5}	37.3

The SEC module is further subdivided into three submodules i.e. precipitation- dissolution submodule, complexation submodule, and cation exchange submodule. The summary and sequence for the calculation done in the SEC module are shown in Figure 3.6. The SEC module runs repeated calculations until the ionic strength criteria is met. The saturation index (Q_{sp}) and the solubility product (K_{sp}) is employed to specify the direction of the reaction in the precipitation dissolution submodule.

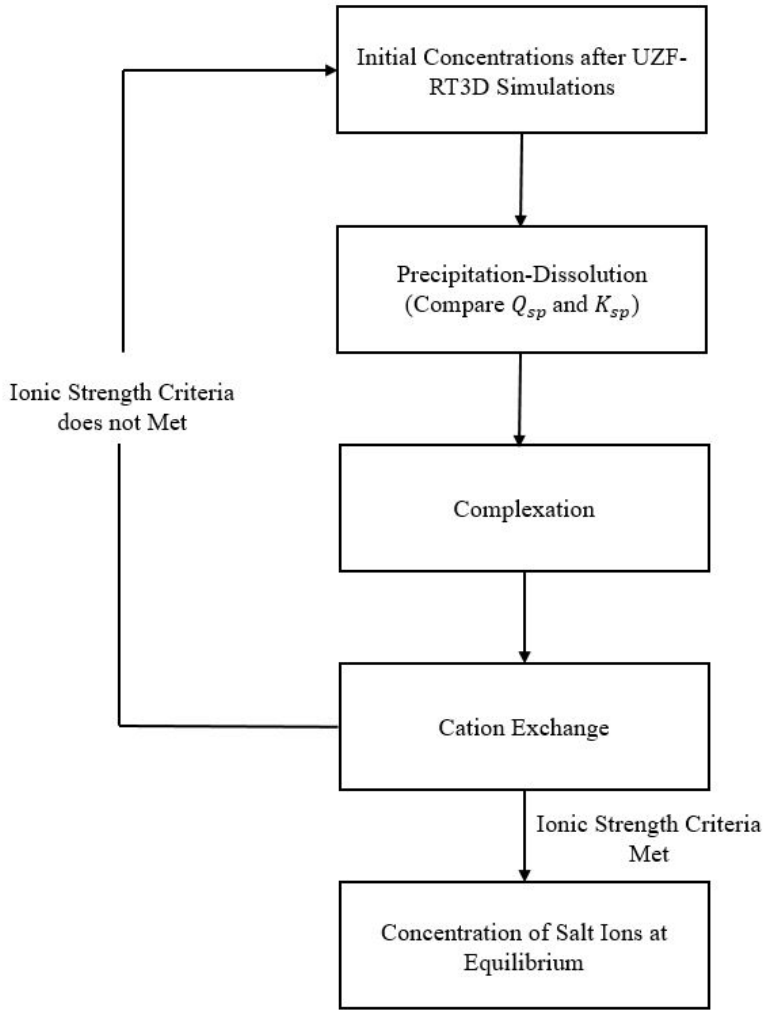

Figure 3. 6. SEC Module Flow Chart.

UZF-RT3D and SEC module were coupled by Tavakoli Kivi et al., (2019) by using the sequential non-iterative approach (Barry et al., 2000; Carrayrou et al.,2018) in which the transport and chemical kinetic equations of UZF-RT3D are followed by internal iterations for equilibrium chemical reactions as shown in the Figure 3.10.

3.2.5 UZF-RT3D/SEC-OTIS Coupled Model for Major Salt Ions Fate and Transport

Reactive transport of major salt ions in an irrigated stream-aquifer system is developed in this thesis by linking the UZF-RT3D/SEC model (Tavakoli Kivi et., al. 2019) with OTIS (Runkel,

1998), in conjunction with UZF-MODFLOW-SFR for flow modeling. Steps taken to achieve this model coupling are explained in the current section. The equations for reactive transport in the soil aquifer system are presented in Chapter 2. Here, the equations for reactive transport in a network of stream channels are discussed and the method for exchanging water and solute mass between the two systems in a coupled modeling framework of stream aquifer system is presented. A schematic of the stream-aquifer modeling framework flow chart is shown in Figure 3.7.

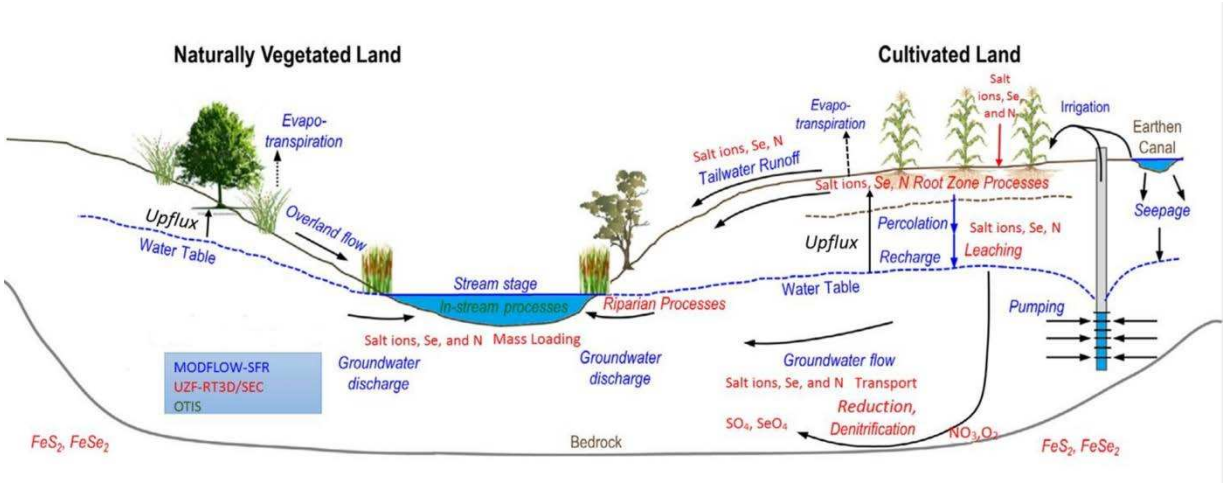

Figure 3. 7. Conceptualization of couple stream-aquifer reactive transport model, MODFLOW-SFR and RT3D/SEC-OTIS (Shultz et al., 2018a).

RT3D/SEC-OTIS is a single FORTRAN code developed by linking UZF-RT3D/SEC with OTIS. MODFLOW-UZF simulates flows for the coupled transport models by taking into account irrigation from both the canals and groundwater wells, evapotranspiration (ET), tailwater runoff from fields, percolation from the vadose zone, canal seepage, 3D-groundwater flow in a saturated zone, 1-D flow in the unsaturated zone, including upflux from a shallow water table, and water exchange with the streams. In order to simulate the flows in the streams in relation to observations at stream stages, the stream flow routing package (SFR2) is used in MODFLOW-SFR. For the unsaturated zone, MODFLOW simulates the volumetric water content for the

saturated zone, groundwater hydraulic head, and groundwater flow at each computational location (finite-difference cell). Processes which are simulated by MODFLOW-SFR are represented in blue text within Figure 3.7. UZF-RT3D is used to simulate the reactive transport of solute in the variably saturated groundwater system, which is shown in red text. It includes salt ions cycling in the root zone, salt ions leaching in the vadose zone, salt ions transport in the saturated zone via advection, dispersion, and chemical reactions and the release of the salt from the shale bedrock. OTIS, a 1D-stream transport with inflow and storage model (Runkel, 1998) is used to simulate the chemical transport of solute in the streams, which is represented by green text in Figure 3.7. OTIS solves the 1D partial differential equation that represents advection, dispersion, lateral outflow, lateral inflow, and sorption. The equation that represents the solute in the stream channel is solved by using a Crank-Nicolson finite-difference solution (Runkel, 1998). The stream network is divided into a set of smaller stream segments and each segment is further divided into a set of grid cells as shown in Figure 3.8. Mass balance mixing is calculated at stream junctions, with the length and other physical parameters like dispersion, storage area and transfer coefficient are defined for each stream segment. The concentration of major salt ions collected from field sampling data is specified at the upstream end of the Arkansas River and any originating tributaries within the DSR. The upstream end where the initial solute concentrations are defined is referred as an input location and is shown in Figure 3.8.

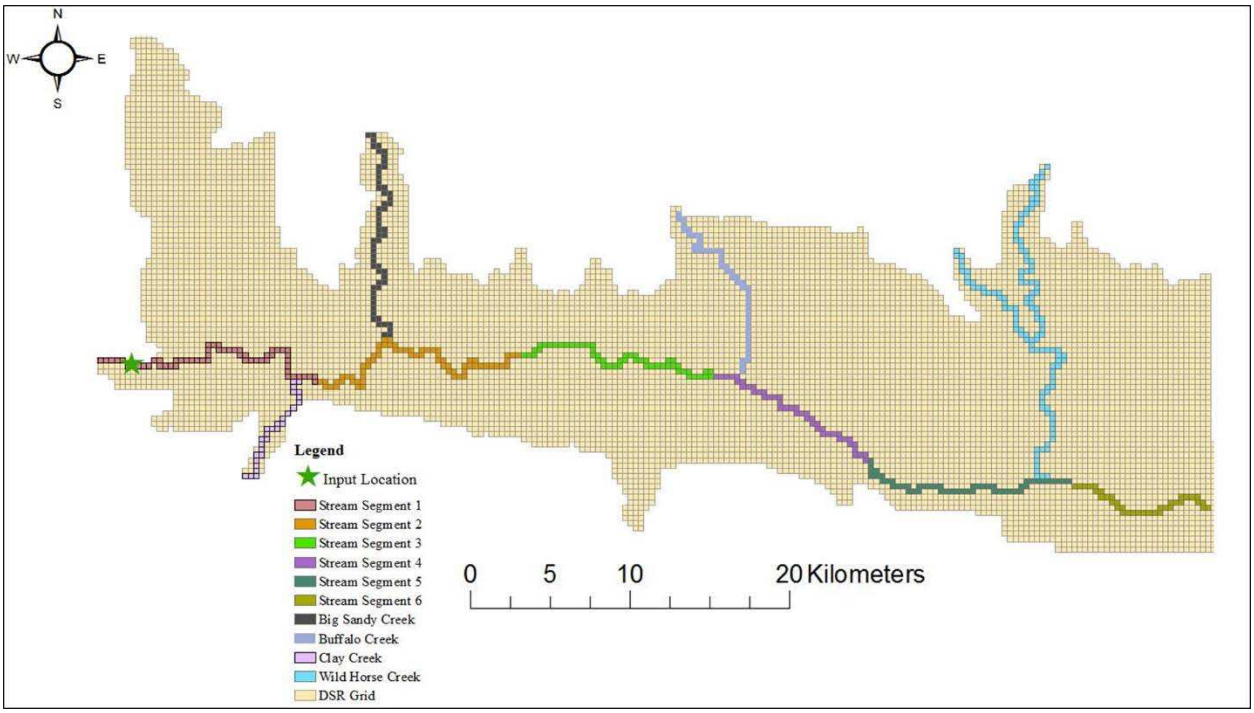

Figure 3. 8. DSR grid, stream segments and the location of input point where the initial solute concentrations were specified in the Arkansas River.

The cross-sectional area and flow rates in the stream segments are computed by the stream flow routing package (SFR2) of MODFLOW. As the water travels downstream, OTIS simulates the 1D reactive transport of solute in stream segments and adjoining tributaries. Solutes are transported downstream by advection and dispersion, which are the dominant transport mechanisms in the OTIS (Runkel, 1998). OTIS performs by solving mass balance equations for the two conceptual areas as shown in Figure 3.9: the main channel and the storage zone. The main channel is that portion of the stream where advection and dispersion occur and the storage zone is defined as that portion of the stream where transient storage occurs e.g. small pockets of slow-moving water.

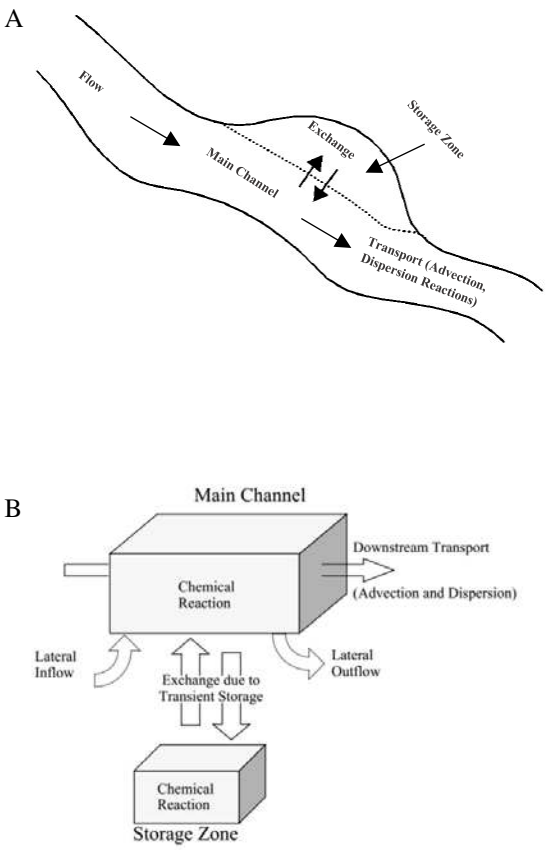

Figure 3. 9. (A) Transient storage mechanism in the OTIS model (B) OTIS conceptual model that includes the main channel and the storage zone (Runkel, 1998).

OTIS solves the partial differential equation for advection, dispersion, lateral inflow, lateral outflow, and sorption, along with other equations to solve sorption on the streambed and solid phase species on the streambed (Runkel and Broshears, 1991; Runkel 1998; Bencala, 1983). The equation for the solute in the stream channel is:

$$\frac{\partial C_j}{\partial t} = -\frac{Q}{A}\frac{\partial C_j}{\partial x} + \frac{1}{A}\frac{\partial}{\partial x}\left(AD\frac{\partial C_j}{\partial x}\right) + \frac{q_L}{A}\left(C_{L_j} - C_j\right) + S_j + r_j \qquad j=1,\ldots,\ n \qquad \text{EQ.11}$$

$$S_j = \bar{\rho}\,\lambda_{S_j}(C_j^* - K_{d_j}\,C_j) \qquad \text{EQ.12}$$

Sorbate on the streambed:

$$\frac{\partial C_j^*}{\partial t} = -\frac{S_j}{\bar{\rho}} \qquad \text{EQ.13}$$

Solid-phase species on the streambed:

$$\frac{\partial C_k^{sol}}{\partial t} = r_k^{sol} \qquad k=1, \ldots, w \qquad \text{EQ.14}$$

where

n = The number of dissolved phase species,

w = The number of solid phase species in the streambed,

C_j = The main channel concentration of the jth dissolved phase species [ML^{-3}],

C_k^{sol} = The main channel concentration of the jth solid phase species [MM^{-1}],

T = Time [T],

Q = The volumetric flow rate [L^3T^{-1}],

A = The channel cross-sectional area [L^2],

X = The distance along the channel axis [L],

D = The dispersion coefficient [L^2T^{-1}],

q_L = The lateral inflow rate [$L^3T^{-1}L^{-1}$],

C_{L_j} = The lateral inflow solute concentration of the jth species [ML^{-3}],

$\bar{\rho}$ = The mass of accessible sediment per volume of stream water [ML^{-3}],

λ_S = The first order sorption rate co-efficient [T^{-1}],

C^* = The solute concentration on streambed sediment [MM^{-1}],

K_d = The partition coefficient [L^3M^{-1}],

S = The rate of change in solute mass concentration on the streambed [$ML^{-3}T^{-1}$],and

r_k^{sol} = The rate of change of solid phase species concentration due to biochemical reaction [$ML^{-3}T^{-1}$].

Equation 11 simulates the fate and transport of liquid phase species. Solid phase species on the streambed with transformations is simulated by equation 14. The mass exchange of the solute between the water column and streambed due to the net sorption is calculated by equation 12 (Runkel, 1998). The equation 13 calculates the concentrations of the sorbed solute on the streambed.

The flow chart of the coupled stream-aquifer flow and transport model is shown in Figure 3.10. Groundwater head and flow, unsaturated zone water content and flow, along with the stream stage and discharge, are simulated by MODFLOW-SFR. In the next step, UZF-RT3D/SEC reads in the volumetric water content, hydraulic heads in the aquifer, and flow rates for every grid cell for every time step. The code then simulates the change in concentration of all the solute species in the groundwater system due to advection (ADV), dispersion (DSP), source-sink mixing (SSM), chemical reactions, precipitation-dissolution, complexation and cation exchange for every time step. Simulated UZF-RT3D/SEC saturated zone concentrations in cells adjacent to the streams are used as an input by OTIS to simulate the concentration of solute within each stream segment for every time step. OTIS maps solute concentration values to UZF-RT3D/SEC grid cells in preparation for the next groundwater transport time step. OTIS does its calculations in hourly time steps while UZF-RT3D/SEC does its calculations in daily time steps. The Surface Water Transport (SWT) package is the linkage between UZF-RT3D/SEC and OTIS, which can be turned off in the input files to revert to the original UZF-RT3D/SEC simulations.

Tailwater runoff volumes from irrigated fields are calculated by the stream flow routing package. To simulate and account for the solute concentrations in the tailwater runoff a new subroutine was added in the source code. The initial concentration of the solute in the tailwater runoff is assumed to be equal to the solute concentration in the irrigation water applied to each field. Unfortunately, this subroutine was commented out in the current version of the model and this deficiency must be addressed before publishing this work. Another subroutine was added to measure the concentration of solute in the irrigation water. If the canal is diverted from the river at a point which is not in the model domain, then the values for each mobile species that are specified in the UZF-RT3D/SEC input files are specified according to field-sampled values. On the other hand, if the canal is diverted from the river at a point within the model domain, then the values for each mobile species that are specified in the UZF-RT3D input files are assigned the values computed by OTIS in the stream grid cell at that point.

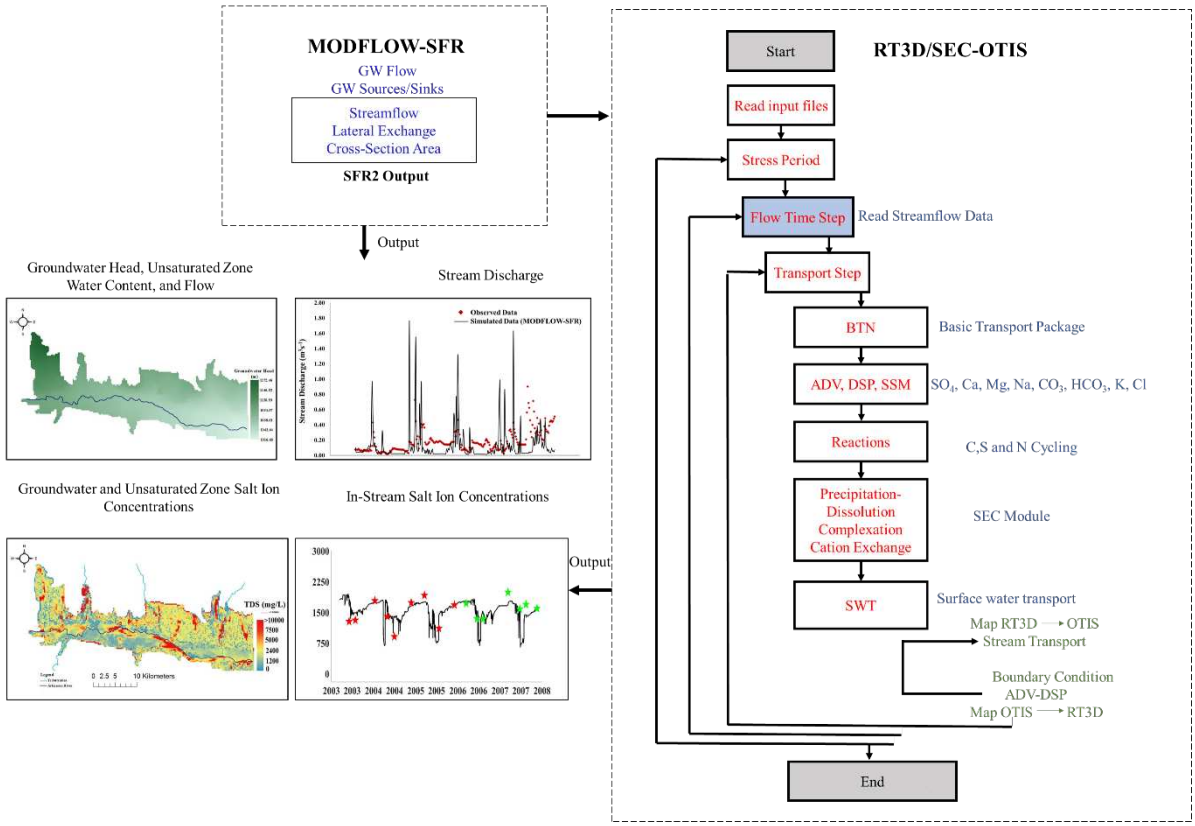

Figure 3. 10. Stream-aquifer flow and transport model flow chart.

3.3 RT3D/SEC-OTIS Application to the Lower Arkansas River Valley, Colorado

The entire DSR of the LARV is discretized into 22,134 finite difference grid cells of 250 m x 250 m for application of both MODFLOW-SFR and RT3D/SEC-OTIS. The aquifer is divided into two vertical layers for MODFLOW while for RT3D/SEC-OTIS the aquifer is divided into 6 vertical layers. The first two vertical layers in RT3D/SEC-OTIS are 0.5 m thick, the third layer has a thickness of 1.0 m, and the remaining depth of the aquifer to the shale bedrock is equally divided into three vertical layers. The stream network in DSR consists of nine stream segments, with five segments representing the Arkansas River and four segments representing the four different tributaries as shown in Figure 3.8.

The DSR is divided into 15 sub-regions in this study for a more accurate comparison between the field data and the simulated results. The division of the study region into 15 sub-regions is similar to that explained in Qurban (2018). The division criteria are based on: (1) the geology of the area; (2) fields irrigated by the different main irrigated canals (Amity, Buffalo, Fort Lyon, Fort Bent, and Lamar); (3) OTIS stream segments: the Arkansas River reaches and four main tributaries (Clay Creek, Big Sandy Creek, Buffalo Creek, and Wild Horse Creek); (4) location of the groundwater monitoring wells; and (5) location of each sub-basin based on the watershed delineation for routing surface runoff from irrigation and precipitation.

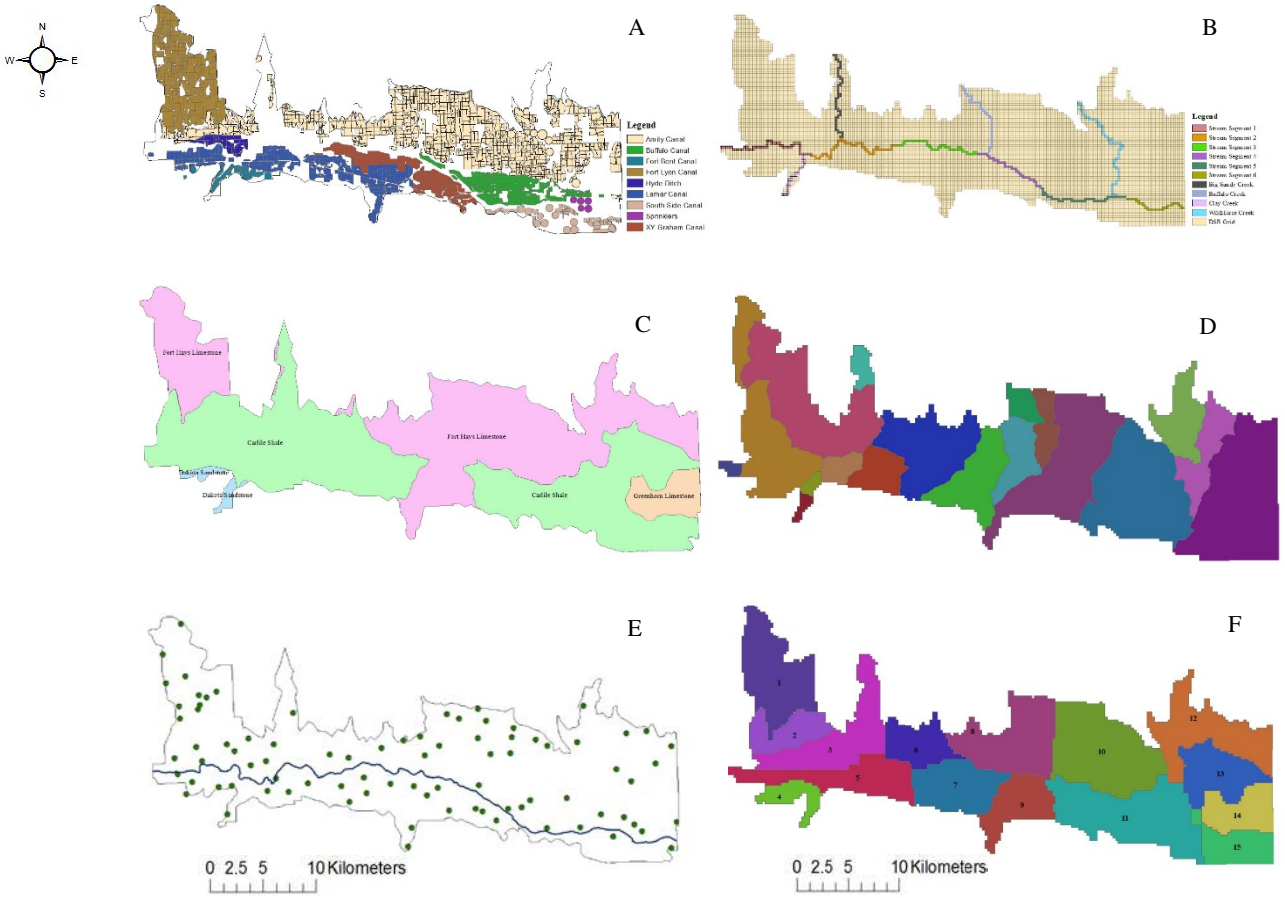

Figure 3. 11. Division criteria for diving the DSR into subregions; (A) Irrigated fields, (B) River stream segments and its tributaries, (C) Geological formations, (D) Subbasins, (E) Location of groundwater monitoring wells, and (F) the resulting 15 subregions of the DSR.

The MODFLOW-SFR model has weekly time steps, UZF-RT3D/SEC has daily time steps and OTIS has hourly time steps. The model is applied for the period of January 1, 2003, to December 31, 2007.

There are five RT3D/SEC-OTIS input packages in which changes have been made to specify the initial salt ion concentration for the salinity module simulations and are looped seven times for forty years spin up the simulation. In the basic transport package (BTN), in which boundary condition and initial solute concentrations are specified, the number of stress periods are increased from 252 to 2085 weeks and the number of days are increased from 1764 to 14,595 days to match with the spin-up simulation of 40 years. The source and sink-mixing package (SSM) reads, prepares, and solves the solute concentration change due to source or sink (loading in irrigation water and canal seepage, fertilizer loading, and crop uptake). The initial solute concentration and the water supply source index of active cells in the SSM package is specified from field data. The irrigation package (IRG) accounts for the concentrations of solutes that enter the system through surface water (pump, canal, or rainfall). The observed data of solute concentrations for 240 sampling events are taken from the DSR database for the years 2003 – 2007. The agriculture package (AGR) contains entered information about crop parameters for each crop and includes planting harvesting and plowing dates. It also contains fertilizer application and crop uptake information. In the surface water transport package (SWT), the initial solute concentrations at the upstream boundary of the Arkansas River (R1) were defined by using regression model results (Gates et al., 2018) based on flow and EC relationships for the year 2003 – 2007. The data in the input packages is looped seven times to match with the spin up simulation of seven years. Furthermore, the changes made for daily temperature, daylight hours, hourly solar radiations, and algae concentrations are discussed in detail in Qurban (2018). The

spatial distribution of salt minerals ($CaSO_4$ and $CaCO_3$) in DSR are based on the soil survey performed by USDA's Natural Resources Conservation Services (NRCS, 2017). Arc GIS environment was used to divide the whole study area into 15 sub regions. An average percent of $CaCO_3$ and $CaSO_4$ for every sub region is taken from USDA survey maps. The average percent values are taken at a depth of 72 inches, which is defined as a 3rd layer in RT3D-SEC/OTIS. Based on the USDA survey values, concentration of $CaCO_3$ and $CaSO_4$ are simulated for every cell in every stress period. The model parameters for chemical reactions that are used in this reactive transport model include organic matter decomposition, dissolved oxygen, nitrogen species, reduction rate of sulfate and concentration of salt minerals are listed in the Table 3.3.

Table 3. 3. Chemical reaction parameters for the model application to the DSR of the LARV.

Number	Model Parameter	Range Value
1	$\lambda_{O_2}^{auto}$	0.00012-3.0 mg/L
2	$\lambda_{O_2}^{het}$	2.0 mg/L
3	$\lambda_{NO_3}^{auto}$	0.0002-1.0 mg/L
4	I_{O_2}	1.0 mg/L
5	I_{NO_3}	0.50 mg/L
6	K_{CO_2}	0.75 mg/L
7	K_{O_2}	1.0 mg/L
8	$\lambda_{SO_4}^{het}$	0.0009 d^{-1}
9	ξ	30000
10	$CaCO_3$	0-11% by dry weight
11	$CaSO_4$	0-1.5% by dry weight

3.4. Model Calibration and Testing

In order to find a good match between the simulated and the observed values of the target variables (concentrations of salt ions and TDS in stream water and groundwater and relative frequency of TDS in the soil root zone) the parameter estimation methodology includes a recursive manual and automated calibration methods (Parameter Estimation Software Package)

guided by sensitivity analysis. A spin-up simulation (Bailey et al., 2014) of 10 years from 2003 to 2012 was included in this modeling effort due to the dependence of results on initial solute concentrations and the desire to achieve steady seasonal fluctuation of salt ion concentrations in the stream-aquifer system and a steady fluctuation of groundwater salt ion mass loading to the Arkansas River. The spin-up simulation was prepared by repeating the cropping and the flow pattern for the years 2003 to 2007 twice.

The calibration and testing were done in a manner advocated by Konikow (2011) and described in Tavakoli Kivi et al. (2019) with the aim that the model should be able to reproduce major trends and spatiotemporal statistics over the region rather than time series of solute concentrations at point locations of measurement (e.g. monitoring wells). The calibration period was defined as January 1st, 2003 to December 31st, 2005, and the testing period as January 1st, 2006 to December 31st, 2007. Both calibration and testing periods include dry and wet years.

A sensitivity analysis was conducted to explore the impact of different parameters on the model results. The most sensitive model input parameters, as defined in Tavakoli Kivi et al (2019), were adjusted within the physically-realistic range of values reported in the literature to find a reasonable match between simulated and observed average concentrations of salt ions in groundwater for each subregion, TDS concentration in soil root zone, salt loading to the Arkansas River, and the OTIS stream segment and tributary concentrations for major salt ions and TDS. Sensitivity analysis showed that simulated results are greatly dependent on the solubility product (K_{sp}) of salt ions in the model and the weighted percentage of salt minerals in the soil profile. The value of the solubility product is temperature dependent. For this reason, a separate value of K_{sp} is given to each of the saturated and unsaturated zones for each salt mineral since the temperature in the unsaturated and saturated zone varies in a different manner.

For groundwater concentrations, model results were compared using the average concentrations of each salt ion in each subregion. The observed relative frequency distribution of C_{TDS} (mg/L) for the unsaturated zone is taken from approximately 34,000 measurements of soil electrical conductivity from fields distributed throughout the DSR (Morway and Gates, 2012). The observed electrical conductivity of soil paste extract (EC_e)values (dS/m) are converted to C_{TDS} (mg/L) using the relationship $C_{TDS} = 883.3EC_e$, R^2=0.89 reported in Gates et al. (2016). To compare the simulated relative frequency distribution of C_{TDS} with the observed data, only those grid cells were included which have a near saturation water content i.e. above 95%. This is because the observed soil EC_e values were estimated in the laboratory setting using a saturated paste extract prepared from field soil samples. An adjusted Brier Score (BS) (Brier, 1950; Tavakoli Kivi et al., 2019) is used to compare the simulated and observed relative frequency distributions of C_{TDS}. The value of BS varies between 0 and 1, with zero indicating a perfect match, and is computed as

$$BS=\left(\frac{1}{n_b}\right)\sum_1^{n_b}(f_i-o_i)^2 \qquad \text{EQ.15}$$

where

n_b= The number of bins,

f_i= The relative frequency of simulated values in the i^{th} bin, and

o_i = The relative frequency of observed values in the i^{th} bin.

For the surface water, simulated spatiotemporal values of solute concentrations are compared with the observed values taken from different sampling events at a different location in the Arkansas River and its tributaries. River mass-balance calculations were done using a method similar to Mueller-Price and Gates (2008) to determine the approximate daily mass loadings of $C_{SO_4\text{-}S}$ and C_{TDS} to the Arkansas River.

The first step in the manual calibration was the adjustment of salt minerals in the soil according to the initial values from the NRCS soil survey data to find a reasonable match between the observed and simulated C_{TDS} values in the unsaturated and saturated zones. Following a reasonable match between the observed and the simulated target variables for the saturated and unsaturated zone by adjusting the salt minerals and the K_{sp} values, the match between the observed and simulated target variables in streams is achieved by adjusting the reduction rate of sulfate. Once the manual calibration is completed, the PEST (Parameter Estimation) software (Doherty, 2007) was used to further refine the K_{sp} values for each salt and the reaction rate of sulfate. PEST adjusts the values of the selected parameters to minimize the objective function, which is the sum of the squared weighted residuals between the observed and the simulated values:

$$O=\sum_{i}^{n_v} w_i\left(O_{v_i}-m_{v_i}\right)^2 \qquad \text{EQ.16}$$

where

O = The objective function,

n_v =The number of target variables,

w_i =The weight assigned to the ith target variable,

O_{v_i} = The observed value of the i^{th} target variable, and

m_{v_i} = The simulated value of the i^{th} target variable.

The overall procedure of automated calibration is similar to that explained in Tavakoli Kivi et al. (2019). The weight assigned to every target variable is calculated as the product of uncertainty weight and a unit discrepancy weight. The value of an uncertainty weight was calculated as the inverse of an estimated coefficient of variation reflective of the relative uncertainty in the observations of the target variable. The value of a unit discrepancy weight was

calculated by unifying the sum of the square of each observed variable value. Initial K_{sp} values for the SEC module were taken from the literature as listed in table 3.3. The automated calibration procedure is summarized as follows:

1- Initial conditions were established using 10 years of spin-up simulations for the years 2003 –2007.

2- To minimize the uncertainty between the observed data and simulated data, PEST was used to provide a revised set of K_{sp} values.

3- The spin-up was re-run with the new set of K_{sp} values to specify new initial conditions to achieve a dynamic equilibrium condition at the end of the model's simulation period for the final baseline run.

4- The observed and simulated concentration of TDS, major salt ions within the testing period for the soil root zone, groundwater, and stream water, as well as the groundwater salt mass loadings to the Arkansas River were compared for the further confirmation of the calibration model. Final K_{sp} values were computed using PEST.

The final parameter values resulting from the RT3D/SEC-OTIS calibration process are given in Table 3.3, all of these fall within the range of values reported in the literature.

Table 3. 4. Solubility product values using PEST

Salt Mineral	Solubility Product	Unsaturated Zone	Saturated Zone
$CaCO_3$	K_{sp1}	3.04×10^{-9}	1.73×10^{-9}
$MgCO_3$	K_{sp2}	1.74×10^{-6}	1.00×10^{-6}
$CaSO_4$	K_{sp3}	7.88×10^{-5}	7.88×10^{-5}
$MgSO_4$	K_{sp4}	0.007257	0.007170
$NaCl$	K_{sp5}	50	50

CHAPTER 4

RESULTS AND DISCUSSION

4.1 Flow Model Results

The performance of the MODFLOW-SFR model in computing groundwater hydraulic head data, groundwater return flow, and stream flow in the DSR is described and evaluated in Qurban (2018). The simulated groundwater and stream flow conditions were found reasonably similar to observed data. Thus, the flow model for the DSR was implemented in this study for use in simulating salt transport and distribution in the stream-aquifer system.

4.2 Baseline Stream-Aquifer Conditions

4.2.1 Reactive Transport Results in the Saturated Zone

The cell by cell concentrations of simulated groundwater C_{Ca}, $C_{SO_4\text{-}S}$, C_{HCO_3}, C_{Mg}, C_{Na},C_K, C_{Cl} and C_{TDS} within layer 4 of the model are averaged over the simulation period of 5 years (2003-2007) and plotted spatially across the DSR as shown in Figure 4.1 and Figure 4.2. Layer 4 values are used for comparison since groundwater monitoring wells in the DSR are typically screened at a depth corresponding to the elevation of this layer within the model. The overall temporal and spatial average values of groundwater C_{Ca}, $C_{SO_4\text{-}S}$, and C_{TDS} are 629 mg/L, 793 mg/L, and 4024 mg/L, respectively, which are markedly greater than the EPA drinking water standard and the irrigation water guideline (USEPA, 1994). The simulated spatiotemporal average values of C_{Ca}, $C_{SO_4\text{-}S}$, C_{HCO_3}, C_{Mg}, C_{Na},C_K, C_{Cl} and C_{TDS} over the region for the calibration period are 515 mg/L, 725 mg/L, 403 mg/L, 221 mg/L, 524 mg/L, 12.9 mg/L, 151 mg/L, and 3985 mg/L respectively. The observed spatiotemporal average values of C_{Ca}, $C_{SO_4\text{-}S}$,

C_{HCO_3}, C_{Mg}, C_{Na},C_K, C_{Cl} and C_{TDS} over the region during the calibration period are 385 mg/L, 760 mg/L, 401 mg/L, 193 mg/L, 623mg/L, 15.7 mg/L, 200 mg/L, and 3928 mg/L respectively. Similarly, simulated spatiotemporal average values of C_{Ca}, $C_{SO_4\text{-}S}$, C_{HCO_3}, C_{Mg}, C_{Na},C_K, C_{Cl} and C_{TDS} over the region for the testing period are 630 mg/L, 715 mg/L, 398 mg/L, 217 mg/L, 520mg/L, 12.9 mg/L, 150 mg/L, and 4060 mg/L, respectively, and the observed spatiotemporal average values of C_{Ca}, $C_{SO_4\text{-}S}$, C_{HCO_3}, C_{Mg}, C_{Na},C_K, C_{Cl} and C_{TDS} for the testing period are 378 mg/L, 740 mg/L, 430 mg/L, 207 mg/L, 647mg/L, 14.5 mg/L,185 mg/L, and 3900 mg/L respectively.

The values of groundwater salt ions are high in subregions 1, 10, 11, 12, and 15 (Figure 3.12). $C_{Ca}$is high in segments where the $C_{SO_4\text{-}S}$ is also high which could be an indication of the presence of gypsum. A reason for high concentrations in subregions 1, 3, 10, 11, and 15 is likely the presence of shale bedrock as shown in Figure 4.5.

There are 85 groundwater monitoring wells in the DSR, where observed values of solute concentrations determined from water samples are available during the period of 2003-2007. The observed values were averaged for each monitoring well and contoured over the DSR using the Kriging method of interpolation (Matheron,1963) in the ArcGIS environment. The general magnitude and trends of the observed data have been simulated reasonably well by the model, as shown in Figure 4.3 and Figure 4.4. This accords with an objective of this study to predict the major trends observed in the field data rather than producing exact same values at each grid cell. Regions of high concentration often are located near streams due to the presence of the near surface shale as shown in Figure 4.5.

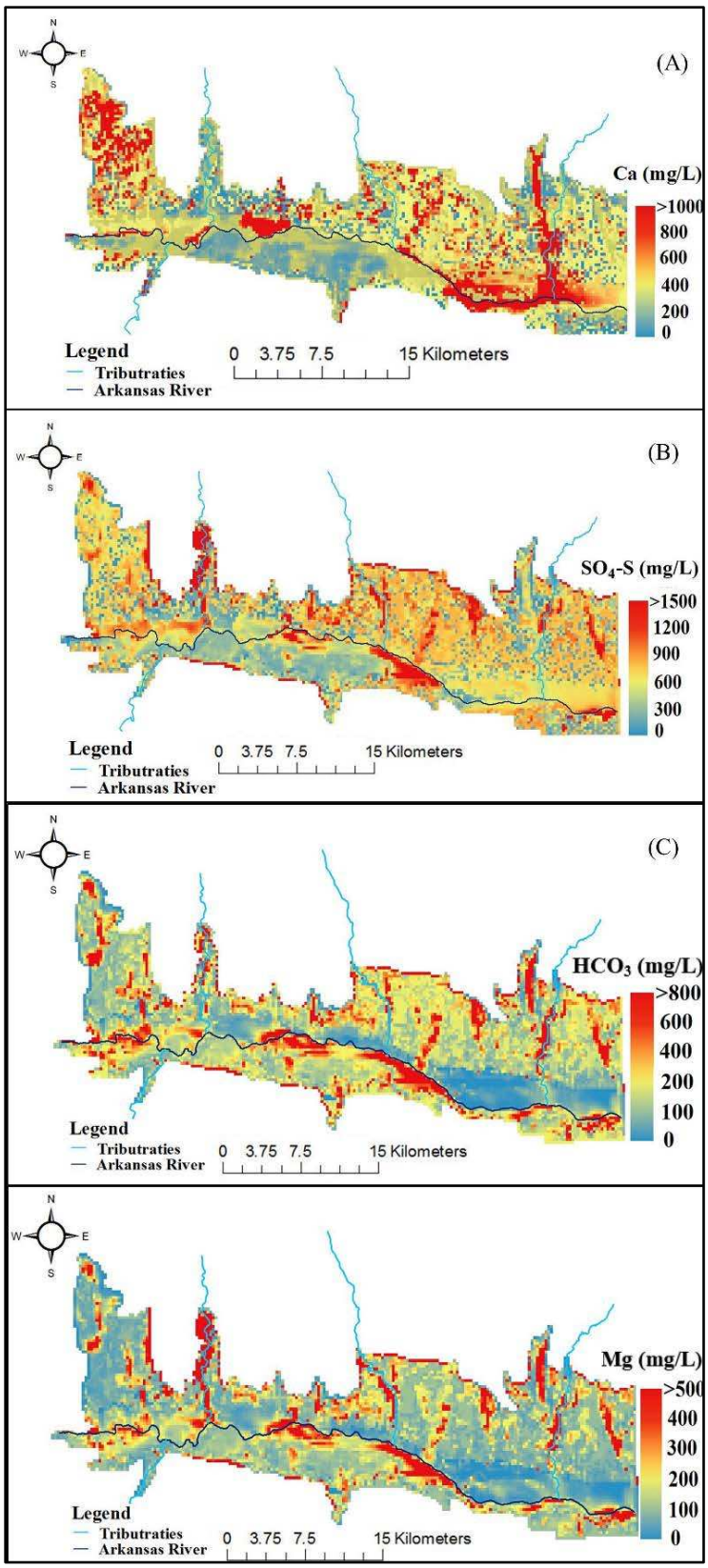

Figure 4. 1. Raster plots of average simulated (A) C_{Ca} (mg/L), (B) C_{SO_4-S}(mg/L), (C) C_{HCO_3}(mg/L) and (D) C_{Mg} (mg/L) in the middle alluvium (layer 4 of the model) of the DSR.

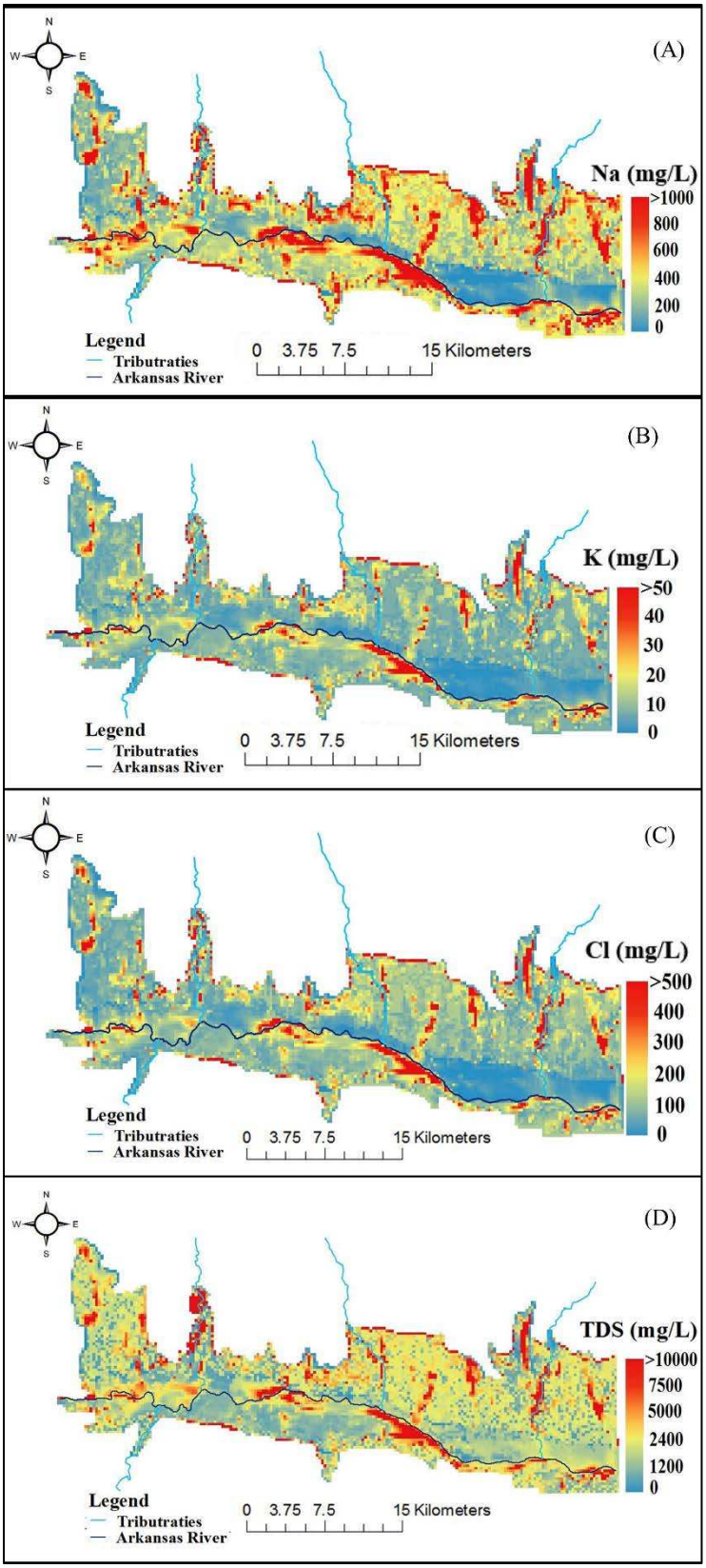

Figure 4. 2. Raster plots of average simulated (A) C_{Na} (mg/L), (B) C_K(mg/L), (C) C_{Cl} (mg/L) and (D) C_{TDS}(mg/L) in the middle alluvium (layer 4 of the model) of the DSR.

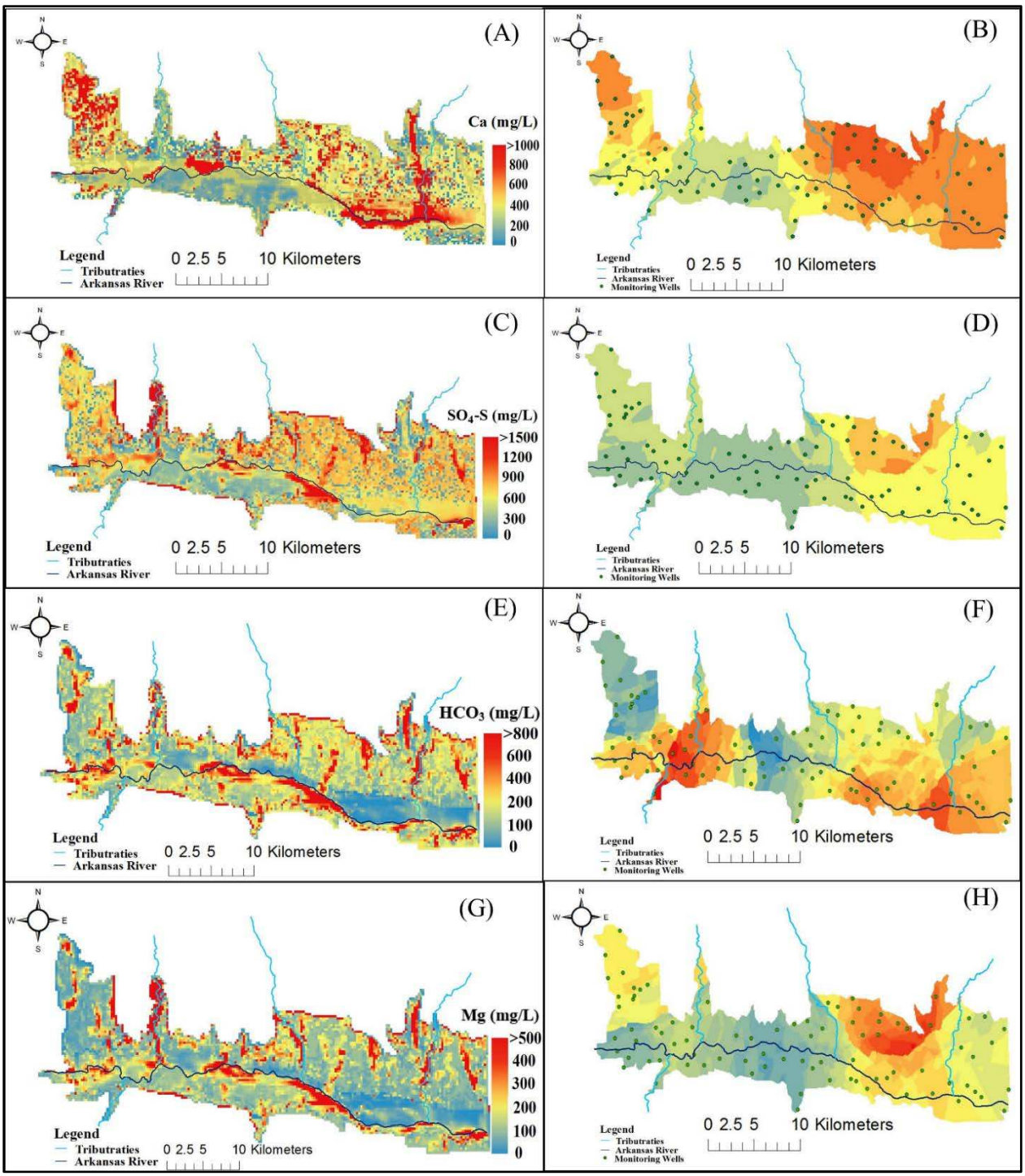

Figure 4. 3. Raster plots of (A) average simulated C_{Ca} (mg/L), (C) average simulated C_{SO_4-S} (mg/L) (E) average simulated C_{HCO_3}(mg/L), (G) average simulated C_{Mg} (mg/L), and contour plots (estimated by Kriging) of (B) average observed C_{Ca} (mg/L), (D) average observed C_{SO_4-S} (mg/L), (F) average observed C_{HCO_3} (mg/L), (H) average observed C_{Mg} (mg/L) in the middle alluvium (layer 4 of the model). The color bar is same for both the observed and the simulated data set.

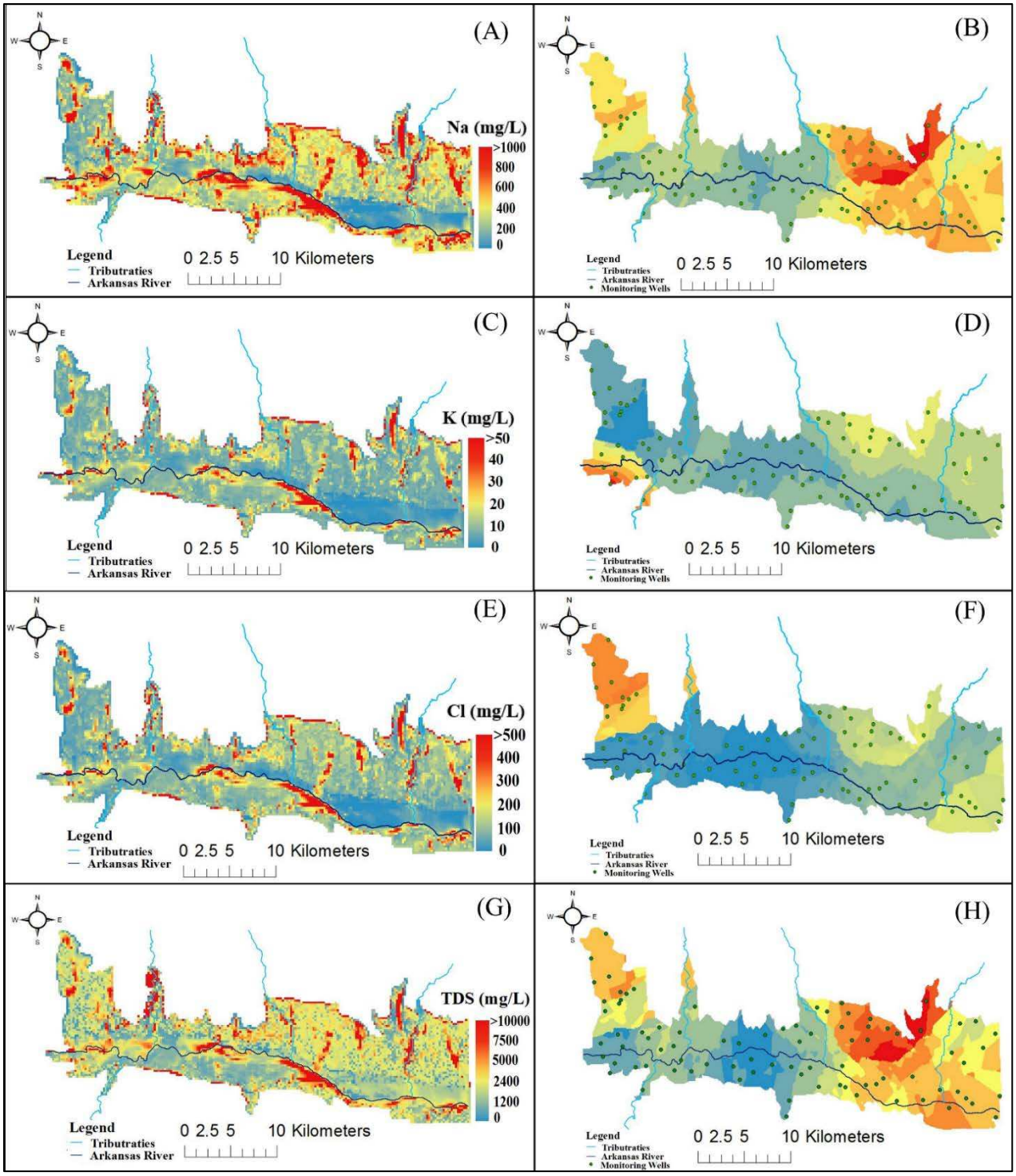

Figure 4. 4. Raster plots of (A) average simulated C_{Na} (mg/L), (C) average simulated C_K (E) average simulated C_{Cl} (mg/L), (G) average simulated C_{TDS} (mg/L), and contour plots (estimated by Kriging) of (B) average observed C_{Na} (mg/L), (D) average observed C_K (mg/L), (F) average observed C_{Cl} (mg/L), (H) average observed C_{TDS} (mg/L) in the middle alluvium (layer 4 of the model). The color bar is same for both the observed and the simulated data set.

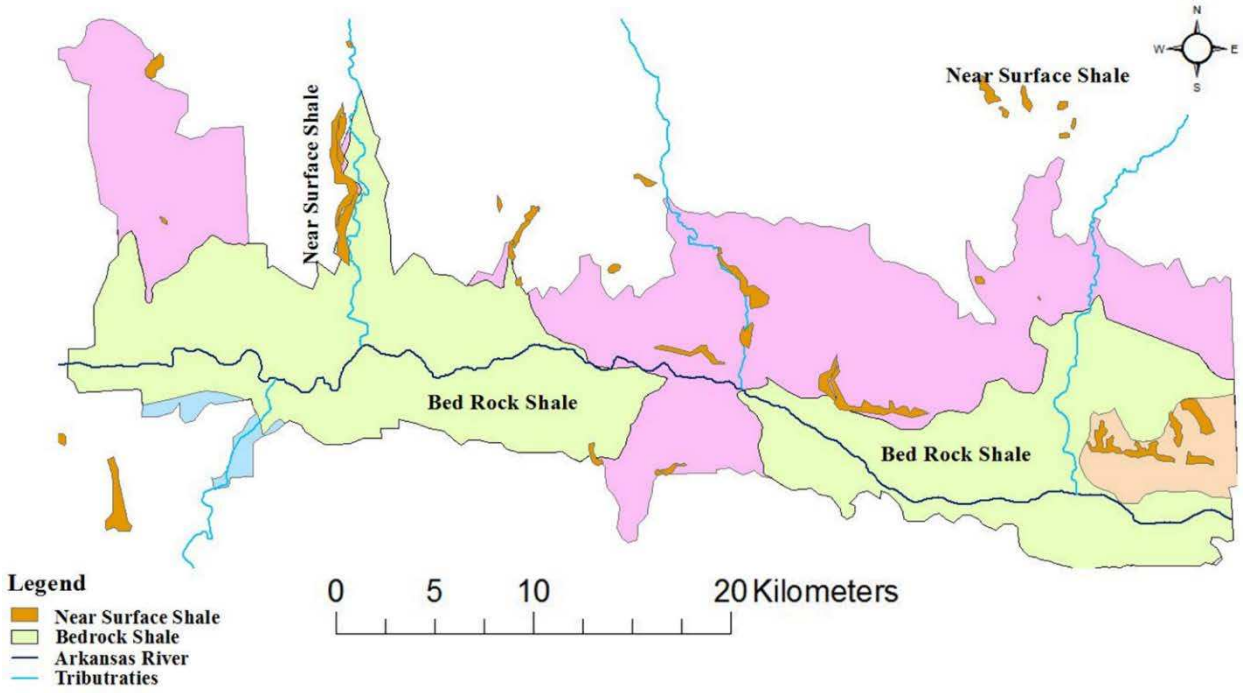

Figure 4. 5. Map of near-surface and bedrock shale (Qurban 2018).

The uncertainty in the observed data due to the measurement error and scale discrepancy is estimated using the methods presented in Bailey et al (2014). Whiskers representing ± one standard deviation of an assumed normal distribution with CV=0.25, are plotted in Figure 4.6 and Figure 4.7. on the histograms of observed data for C_{Ca}, C_{SO_4-S}, C_{HCO_3}, C_{Mg}, C_{Na}, C_K, C_{Cl} and C_{TDS} for each subregion of the DSR for both the calibration (2003-2005) and testing periods (2006-2007). Corresponding simulated results, also shown in Figure 4.6 and Figure 4.7, lie within the uncertainty range of the observed data. Calibration period histograms of simulated concentrations show a better match to the observed data compared to those for the testing period. The model is over-predicting C_{Ca} in most of the subregions for both the calibration and testing period. The over-prediction of this and other groundwater constituent concentrations may be due in part to the inadvertent omission (commenting out) from the current version of the model of the

subroutine for simulating mass transfer of solutes in up flux from the shallow water table into the unsaturated zone. The observed average C_{Na} and C_{Cl} concentrations are high in subregion 1 and 15 in both calibration and testing periods, which is due in part to the presence of possible outliers in the observed data.

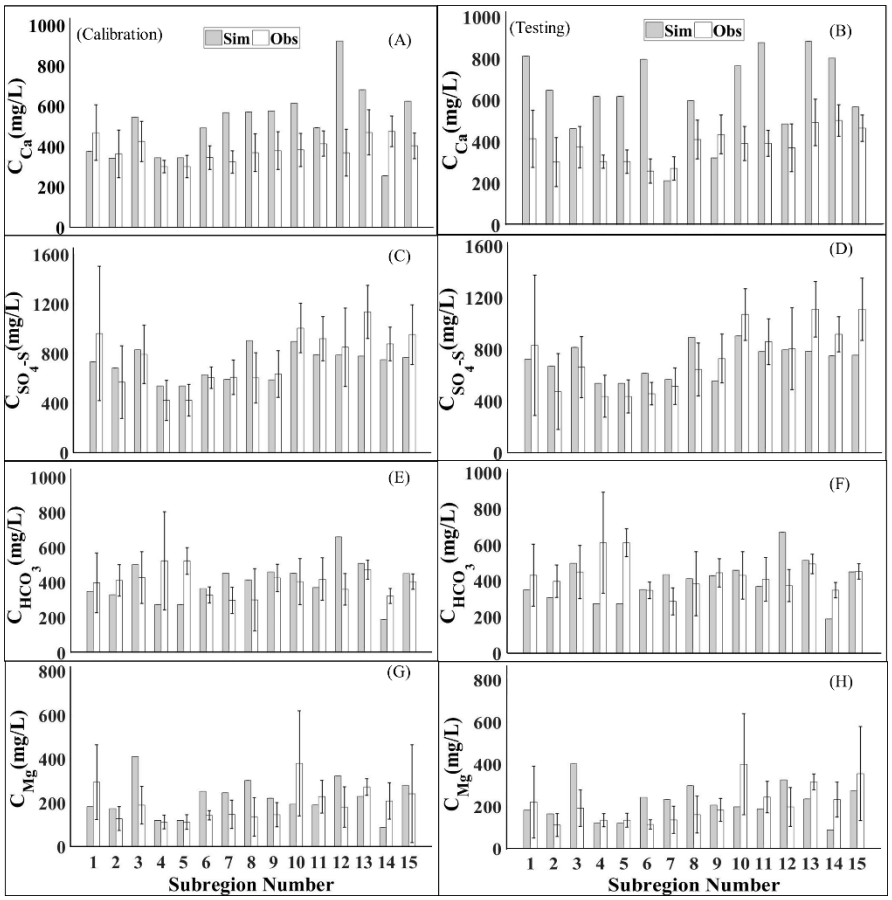

Figure 4. 6. Comparison between the simulated and observed average of C_{Ca}, C_{SO_4-S}, C_{HCO_3}, and C_{Mg} respectively for each subregion for the calibration period (A, C, E, G) and testing period (B, D, F, H).

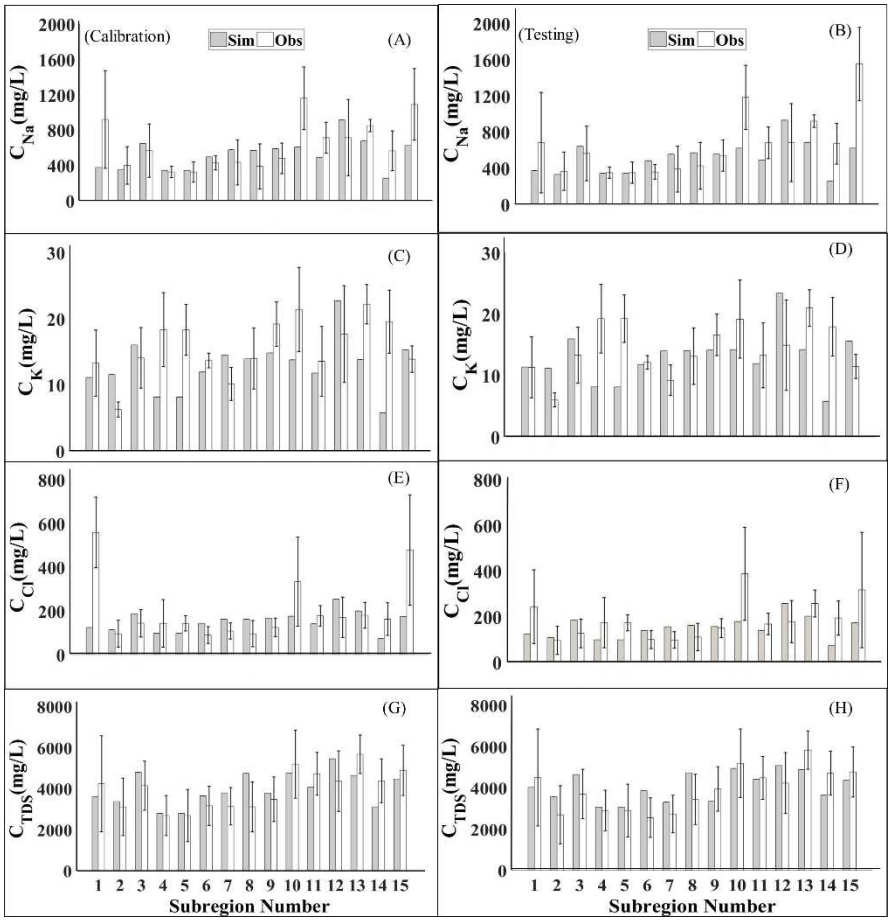

Figure 4. 7. Comparison between the simulated and observed average of C_{Na}, C_K, C_{Cl} and C_{TDS} respectively for each subregion for the calibration period (A, C, E, G) and testing period (B, D, F, H).

The histograms in Figure 4.6 and Figure 4.7 indicate the ability of the model to generally reproduce the distribution of solute concentrations across the study region within the model calibration and testing periods. The adjusted Brier score $(BS)^{1/2}$ is more easily understandable and interpretable as compared to Brier Score (BS) (Tavakoli Kivi et al., 2019). The $(BS)^{1/2}$ values for C_{Ca} , $C_{So_4\text{-}S}$ and C_{TDS} are calculated across both calibration and testing period as 0.13, 0.042, and 0.043 respectively, which indicates that the model is not only reproducing concentration averages fairly well but the distributions of the observed data as well. The adjusted Brier score values $(BS)^{1/2}$ for C_{Na}, C_{Mg}, C_{Cl}, and C_{HCO_3} across the calibration and testing periods

are 0.03, 0.06, 0.02, and 0.07 respectively. The adjusted $(BS)^{1/2}$ shows a relatively poor match of simulated C_{Ca} to observed values, possibly for the following reasons:

1) $CaCO_3$ is present in the soils of the LARV at levels of 0 to 11% by weight and dissolution of $CaCO_3$ is one of the sources of C_{Ca}. The SEC module currently does not fully accommodate the C cycle in a closed system (Tavakoli Kivi et al., 2019). The simple dissolution formula for $CaCO_3$ is used. The C_{Ca} concentrations in the saturated zone can be improved by introducing the full C cycle and the partial pressure of CO_2, which determines the extent of dissolution of $CaCO_3$ as shown below:

$$CO_2 + H_2O + CaCO_3 \longleftrightarrow Ca^{2+} + 2HCO_3^- \qquad \text{EQ.17}$$

2) The mass transfer of solutes in up flux from the shallow water table into the unsaturated zone is not simulated in the current version of the model. A better match between the observed and the simulated data can be achieved by including the solute up flux from the shallow groundwater.

3) Major salt ions when they are immersed in the river water, enter into different chemical reactions in the presence of other active substances and producing different chemical compounds. Transformation also can occur due to exposure to different bacteria and other living organisms. The effect of such transformations is in the change of the original pollutant concentration in the river and eventually in groundwater as the river water used for irrigation seeps through the soil root zone to the groundwater.

SO_4^{2-} varies in concentrations in all natural waters. In the current study, SO_4^{2-} enters the river water from the groundwater where it originates primarily from $CaSO_4$. In the presence of oxygen, some bacteria convert reduced forms of sulfur to the oxidized form in SO_4^{2-}. The bacteria can also reduce SO_4^{2-} to H_2S. The overall reaction is:

$$SO_4^{2-} + 2\{CH_2O\} + 2H^+ \rightarrow H_2S + 2CO_2 + 2H_2O \quad \text{EQ.18}$$

The chemical reaction module of the *S* species within the stream system is not included in the current study. Therefore, the redox reactions of *S* species in the streams are not included. In order to calibrate $C_{So_4\text{-}S}$ in the stream water in the present study, the concentration of the salt minerals in the groundwater cells adjacent to the streams were set higher than average values reported in the USDA soil survey (NRCS data base). This served to increase simulated $C_{So_4\text{-}S}$ in the stream system but also increased simulated C_{Ca} in the groundwater. Inclusion of solute mass transported in irrigation runoff to streams, inadvertently omitted in the current version of the model, also might serve to increase simulated $C_{SO_4\text{-}S}$ in the stream system.

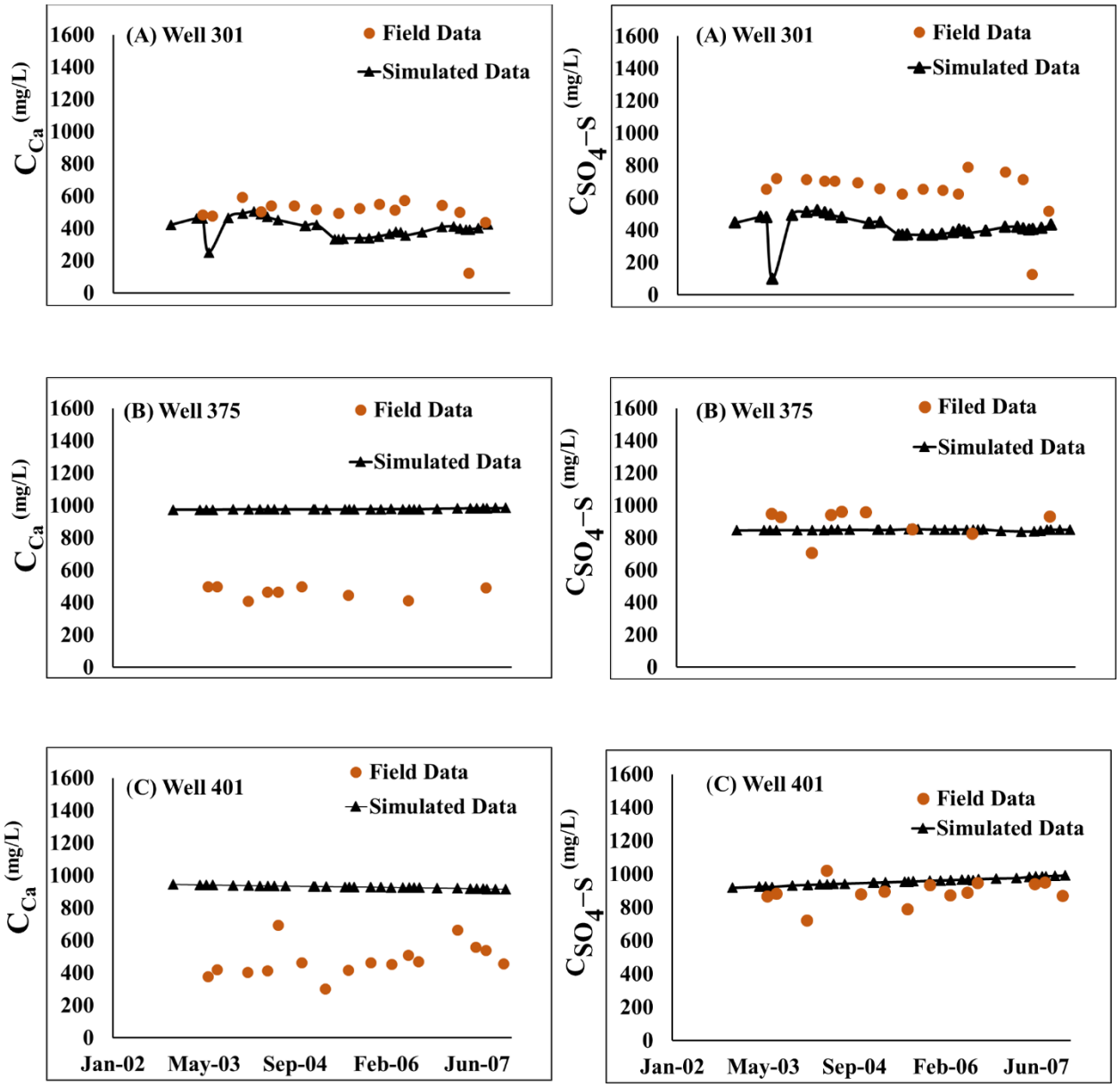

Figure 4. 8. Time series plots of simulated and observed values of C_{Ca} and $C_{So_4\text{-}S}$ for three monitoring wells in the DSR. Simulated values are for the computational grid cell containing the monitoring well location.

Time series plots of observed values of C_{Ca} and $C_{SO_4\text{-}S}$ (mg/L) in three monitoring wells along with simulated values in the respective grid cells containing the well locations are shown in Figure 4.8. The plots show a fairly good match for wells 375 and 401 for $C_{SO_4\text{-}S}$ and at well 301 for C_{Ca}; however, a poor match is seen for well 301 for $C_{SO_4\text{-}S}$ and for wells 375 and 401

for C_{Ca}. This poor match is due in part to the large discrepancy between the model grid scale and the observation scale. To obtain better matches, cell-by-cell chemical parameters would need to be calibrated, which would require extra computational effort and arguably would violate the principal of parsimony.

4.2.2 Water Content and Salt Reactive Transport Results in Root Zone

The water content in the unsaturated zone is of critical interest because of its direct influence on plant growth and crop production. Soil water is also a medium through which contaminants move and potentially harm the crop yield and the water quality of the connected stream-aquifer system. The water content in the soil root zone is particularly variable mainly due to variation in applied irrigation water, upflux from shallow groundwater, and daily climatic conditions. The water content in the soil root zone is calculated in the current model using the Unsaturated Zone Flow package (UZF1) module in MODFLOW.

Salts are present in the soils as remains of weathered rocks, and as solutes in applied irrigation water and in upflux from shallow saline groundwater. Salts are leached to the underlying groundwater in deep percolating rainfall and irrigation water that exceeds the soil storage capacity. The Variably Saturated Transport (VST) package for RT3D/SEC-OTIS is used in the present model to simulate the downward reactive transport of salts in the unsaturated zone. An empirical relationship is used in UZF1 to simulate upflux from the water table into the root zone when the calculated soil water content drops below the residual water content level. An accompanying model subroutine calculates the transport of dissolved salts in this upflux and simulates their deposit within the root zone; but, unfortunately, it was discovered late in this research that this subroutine had been commented out and was not functioning during model calibration and application. Hence, the results presented here do not include the effect of salt

upflux and will need to be amended later by activating this subroutine, adjusting model calibration, and re-running the simulations.

The cell-by-cell variation of the water content and C_{TDS} in the soil root zone for three cells located at three different locations in the study region is shown in Figure 4.9 (A-D). The duration of the model is from the year 2003 to the year 2007. For cell-by-cell water content and C_{TDS} comparison, the year 2005 is chosen as it is considered as a normal year with respect to average mean monthly flow rates. Generally, as the predicted water content in the soil root zone increases, C_{TDS} decreases because more water is available for dilution of salts. Contrarily, as the water content in the soil root zone decreases, C_{TDS} in the soil root zone increases. This relationship is not linear, however the model accounts for equilibrium chemical reactions that are affected by water content and individual ion concentrations.

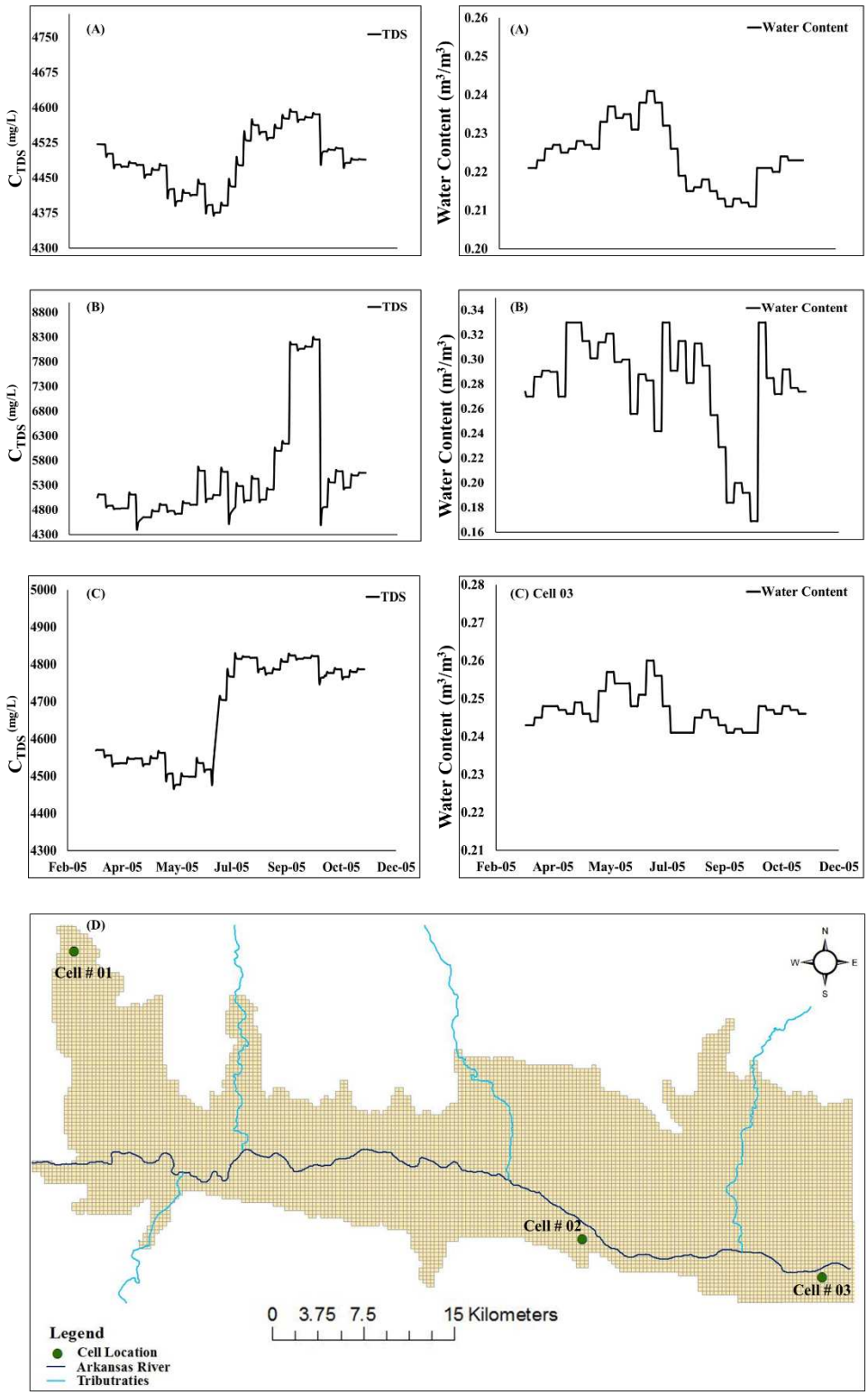

Figure 4. 9. Cell-by-cell time series plots of simulated C_{TDS} water content in the crop root zone for irrigation season of the year 2005 at three different cells (A = cell 01, B = Cell 02, C = Cell 03) located at three different locations in DSR (D).

The simulated cell-by-cell values of C_{TDS} in the root zone, averaged over the simulation period, are shown in Figure 4.10 (A). High values observed in subregions 6, 8, 12, 13, 15, and in areas near the Arkansas River. The average values of C_{TDS} in the observed and simulated data are 5136 mg/L and 5145 mg/L, respectively, which are substantially higher than the average values of C_{TDS} 4034 mg/L in USR, as reported by Tavakoli Kivi et al., (2019). The average C_{TDS} values both in the USR and the DSR are higher than the permissible limits of about 3300 mg/l for corn and 3500 mg/l for alfalfa in gypsiferous soils (Morway and Gates 2012; Gates et al, 2016), suggesting a considerable area suffering from crop yield reduction due to salinity. The difference between the simulated USR and DSR average C_{TDS} values is likely due to higher irrigation water salinity, different mineral salts, and varying chemical reactions in the DSR compared to the USR. Assuming an average crop yield threshold of about 3400 mg/L for the crops in the DSR, there is approximately 51 percent of the irrigated fields in DSR, which are simulated to exceed this threshold. The results of the current study are comparable with the results presented in Morway and Gates (2012) for the same region.

Figure 4.10 (B) shows the relative frequency histograms of simulated and observed C_{TDS} values for near-saturated soil conditions (cells in which water content is greater than 95%) in the DSR. Simulated conditions near saturation allow comparison to observed data where electrical conductivity of soil saturated extract (EC_e) were estimated. The value of Adjusted Brier Score $(BS)^{1/2}$ for comparison of the simulated and observed histograms is 0.01, indicating a reasonably good match between the simulated and observed values for the given conditions of calibration.

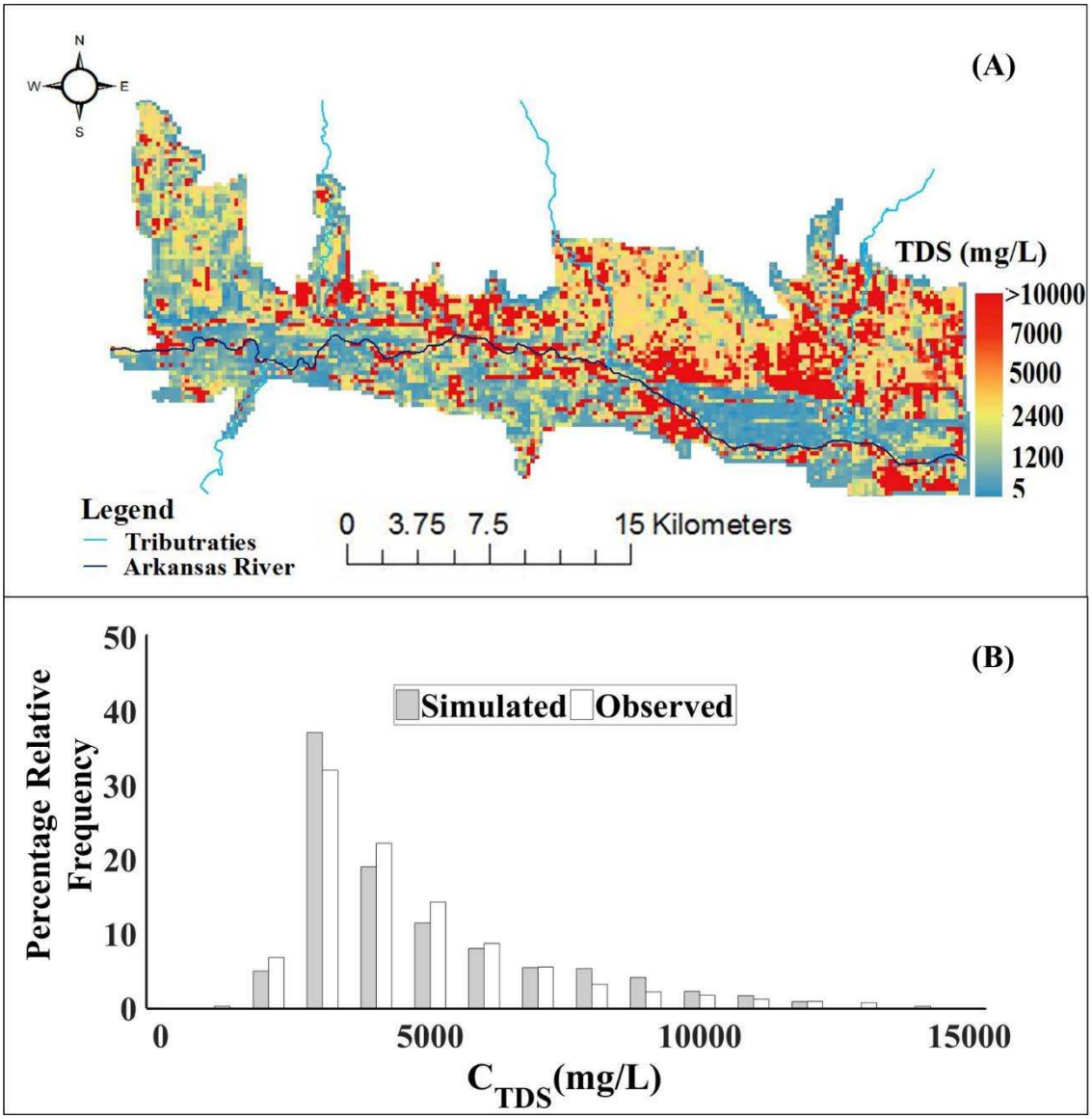

Figure 4. 10. (A) Raster plot of simulated C_{TDS} in the root zone, (B) Comparison of percentage relative frequency histogram of simulated and observed C_{TDS} in the soil root zone for near-saturated cells.

To meet water quality standards in streams and aquifers, management of nonpoint-source (NPS) mass loading from agricultural lands is required. The current model estimates NPS salt loading using the product of simulated flow and salt ion concentrations, providing support for management decisions and investments.

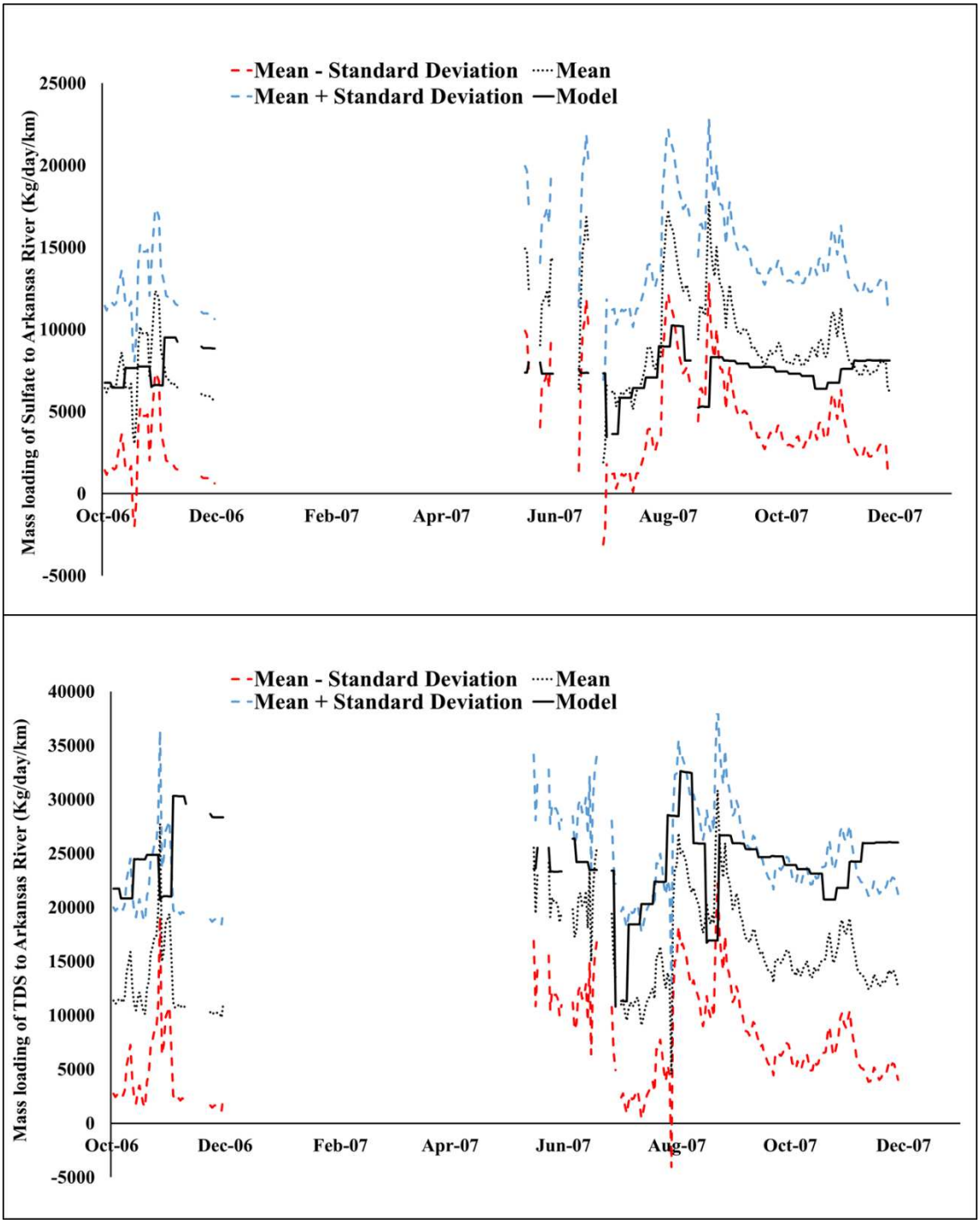

Figure 4. 11. (A) Model-simulated groundwater mass loadings of SO_4 to Arkansas River compared to statistics of total unaccounted-for return loads of SO_4 (groundwater return loads plus ungauged surface water return loads) from a stochastic river mass balance, (B) Model-simulated groundwater mass loadings of TDS to Arkansas River compared to statistics of total unaccounted-for return loads of TDS from a stochastic river mass balance.

Average simulated groundwater mass loadings (kg/day/km) of SO_4 and TDS to the Arkansas River over the simulated period are shown in Figure 4.11. The simulated mass loadings to the Arkansas River are compared to statistics of total unaccounted-for return flows (groundwater return loads plus ungauged surface water return loads) from stochastic river mass balance estimates (Gates et al 2018) for a period spanning 2006-2007. The simulated groundwater mass loadings are mostly within mean ± one standard deviation of the distribution of mass loadings predicted by stochastic mass balance results. The high trends seen in the simulated TDS mass loadings may be due in part to excessively high simulated values of C_{Ca} in the saturated zone.

4.2.3 Reactive Transport Results in Arkansas River and its Tributaries

Reactive transport of major salt ions and TDS was simulated along the Arkansas River and within its tributaries. The Arkansas River was divided into six stream segments and four main tributaries as shown in Figure 3.8. The process of the calibration was completed for two periods, i.e. a calibration period and a testing period. The calibration period extends from 2003 to 2005 and the testing period from 2006 to 2007. Figure 4.12 (A-F) and Figure 4.14 (K-P) shows the time series plots of model-simulated and observed $C_{SO_4\text{-}S}$, C_{Ca}, and C_{TDS}, at six locations along the Arkansas River and at four locations within the tributaries (Figure 4.13 G-J and Figure 4.14 Q-T). Results for both calibration and testing period shows that the model provides an acceptable match between the observed and the simulated data regarding the magnitude and spatiotemporal variability of stream concentrations.

Moreover, for many locations model is accurately predicting the major trends that appear in the measured data but the model is not predicting good results in Big Sandy Creek and Buffalo Creek. The model is not predicting accurate results in these streams in part because they were shortened in the flow model, with flows originating outside of the irrigated valley not accounted

for. Another reason for model under-prediction of tributary concentrations in the presence of shale layers under tributaries, which may release SO_4 via autotrophic reduction of O_2 and NO_3 and are not directly accounted for in the present version of the model. In addition, excess flows from the farmer's irrigation ditches are discharged into the Big Sandy Creek which are not adequately accounted for in the flow model. The same model deficiency was observed for Big Sandy Creek and Buffalo Creek in relation to the reactive transport model of *Se* and NO_3 developed by Qurban (2018). All four modeled tributaries discharge into the Arkansas River, which affects the simulated results in river segments 1, 5, and 6. The in-stream reactive transport results could perhaps be improved by including the complete carbon cycle in the SEC module and by accounting for additional chemical reactions that may be occurring in the streams. Also, the current version of the model does not simulate the solute mass loadings from overland flow, which affects the in-stream reactive transport results and perhaps would contribute to an increase in simulated in-stream solute concentrations.

There are four locations in DSR where observed flow data are available from USGS flow monitoring gauges. At these four locations, in-stream TDS mass loadings are calculated and compared with the estimated TDS mass loading calculated from the river mass balance which are summarized in Table 4.1. The difference between the estimated and simulated TDS mass loadings are high in the tributaries as compared to the Arkansas River, perhaps due to the shortening of the tributaries in the flow model, the absence of complete carbon cycle and instream redox chemical reactions, and the neglect of solute mass loading from the overland flows.

Table 4. 1. Estimated and simulated mass loadings to the Arkansas River and its Tributaries

Stream No.	Estimated C_{TDS} Mass Loadings (kg/Day)	Simulated C_{TDS} Mass Loadings (kg/Day)
Arkansas River Stream Segment 1	2,227,978	2,263,325
Arkansas River Stream Segment 3	2,458,013	1,836,588
Big Sandy Creek	191,083	168,221
Wild Horse Creek	86,949	108,488

Quantitative performance measure of the model in the river and tributaries is evaluated by calculating the Nash and Sutcliffe (NCSH) (Nash and Sutcliffe., 1970) and the absolute difference between the observed and the simulated concentration of TDS as presented in Table 4.2. The NCSH value in certain stream segments and in tributaries are less than zero for both the calibration and testing period. These negative values may be due to the absence of complete carbon cycle, instream redox chemical reactions, shortening of the tributaries in the flow model, and the neglect of solute mass loading from the overland flows.

Table 4. 2. In Stream Uncertainty Evaluation Using NCSH for TDS.

In Stream TDS Concentration	Calibration Period (2003-2005)			Testing Period (2006-2007)		
Stream No.	**Absolute Difference (Model - Observed)**	**NSCH**	**NSCH Over the Whole Study Region**	**Absolute Difference (Model - Observed)**	**NSCH**	**NSCH Over the Whole Study Region**
Stream Segment 1	155.30	0.85	-0.34	181.29	0.70	-3.38
Stream Segment 2	153.06	0.72		218.05	-0.57	
Stream Segment 3	597.58	-0.37		573.47	-2.27	
Stream Segment 4	583.79	-0.32		1117.16	-6.58	
Stream Segment 5	348.72	0.61		586.70	-1.56	
Stream Segment 6	443.26	0.44		671.32	-4.69	
Clay Creek	434.23	-0.47		285.53	-4.14	
Big Sandy Creek	644.08	-5.58		483.67	-0.67	
Buffalo Creek	201.14	0.33		342.59	-11.74	
Wild Horse Creek	359.74	0.35		897.79	-2.30	

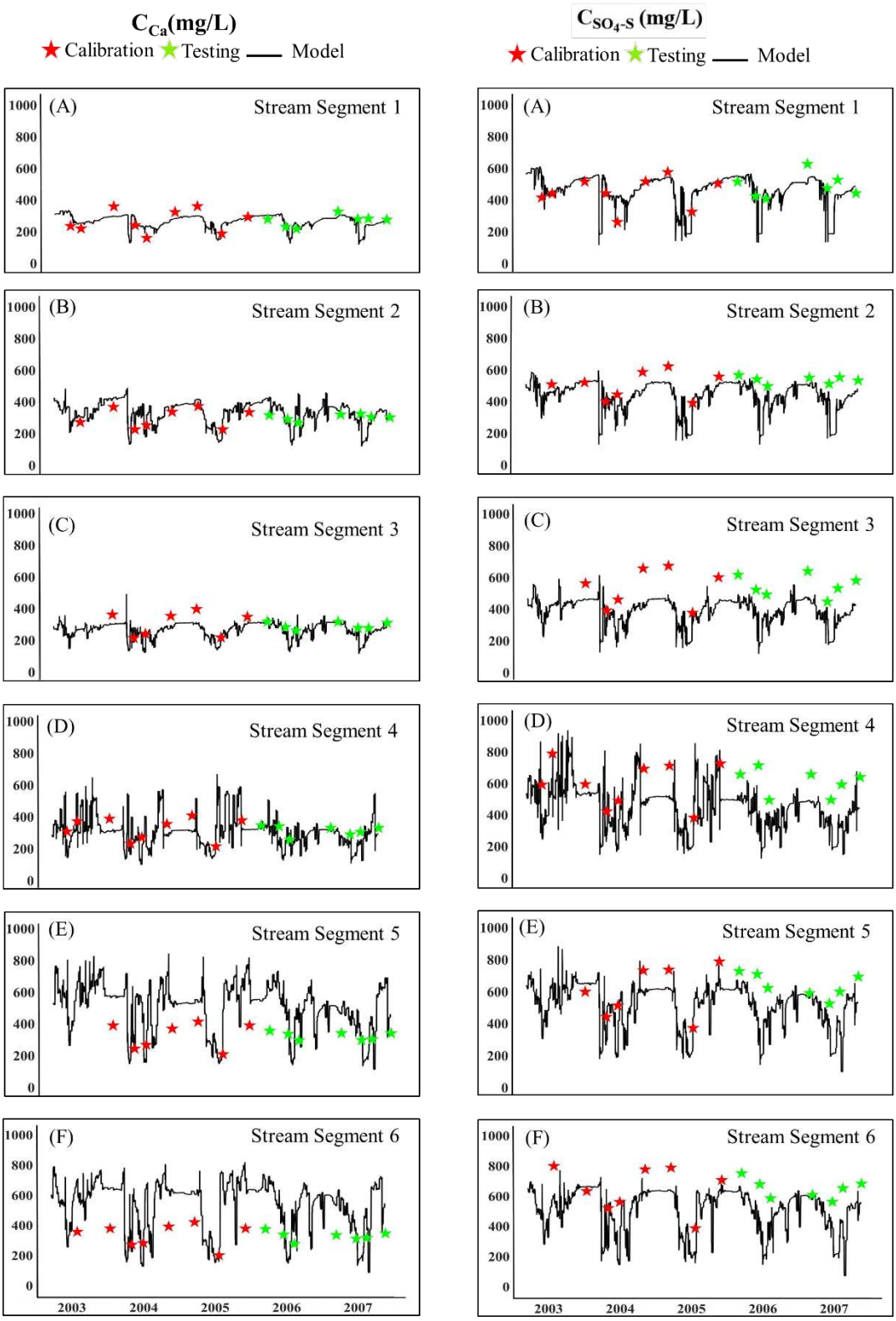

Figure 4. 12. Observed and simulated surface water concentrations for C_{Ca} and $C_{SO_4\text{-}S}$ for stream segments 1-6 (A-F) along the Arkansas River.

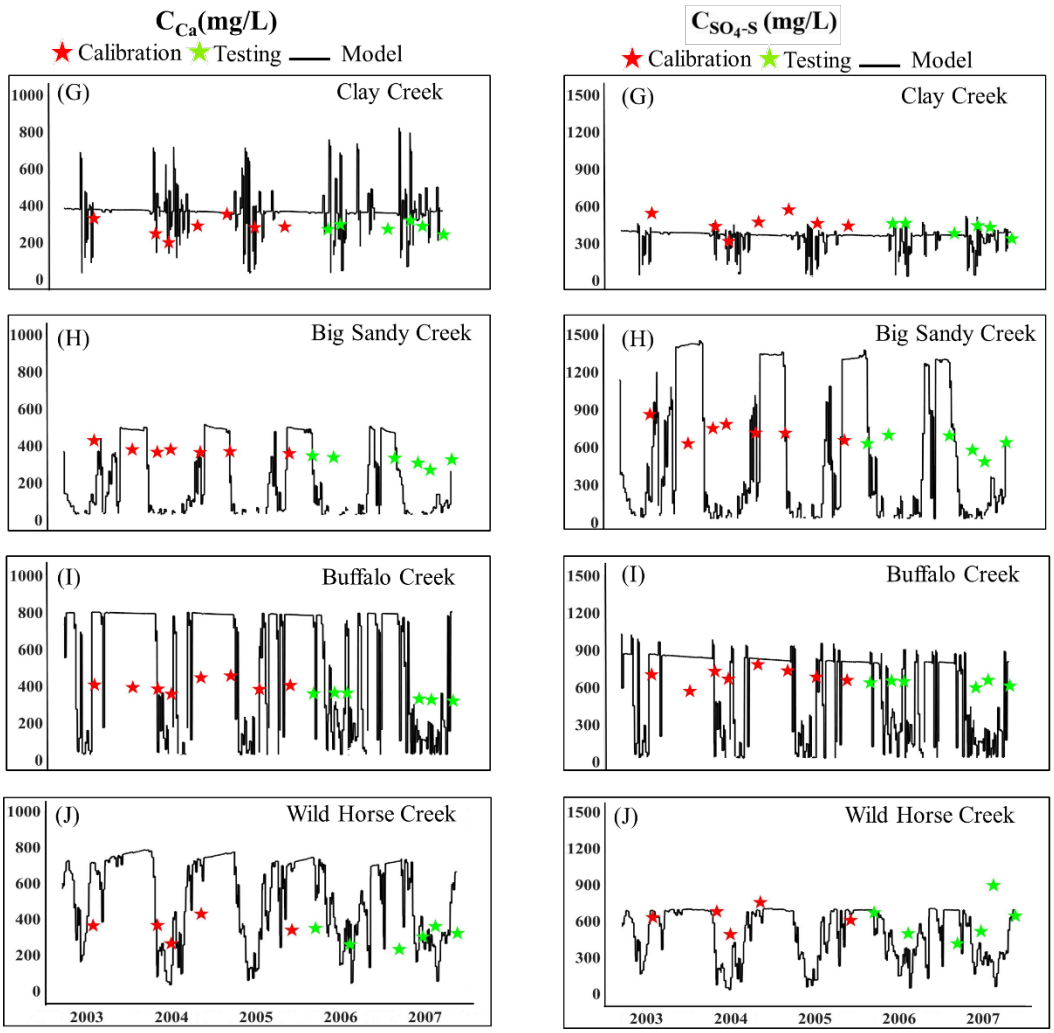

Figure 4. 13. Observed and simulated surface water concentrations for C_{Ca} (G-J) and $C_{SO_4\text{-}S}$ (G-J) in the tributaries (Clay Creek, Big Sandy Creek, Buffalo Creek, and Wild Horse Creek).

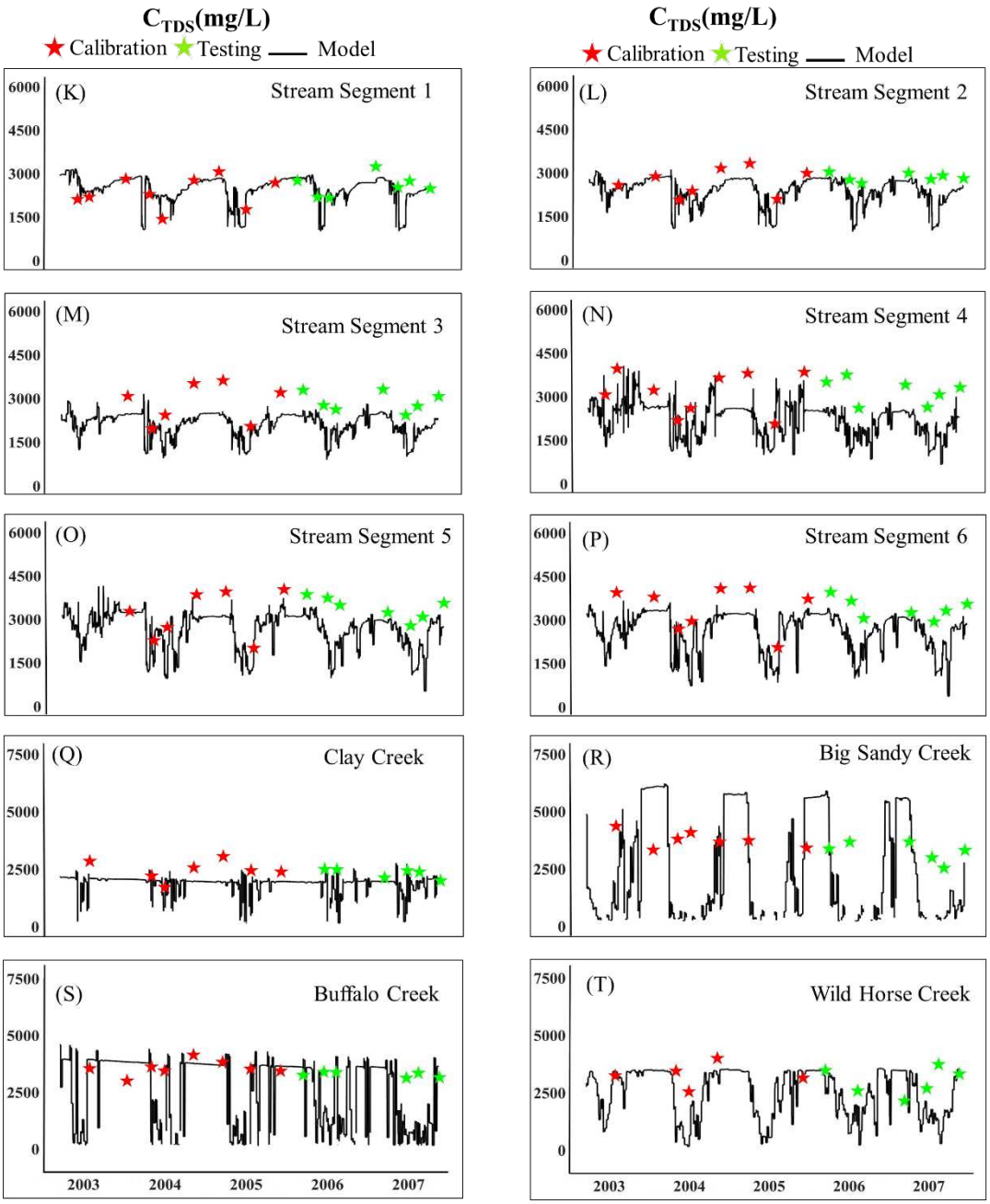

Figure 4. 14. Observed and simulated surface water concentrations for C_{TDS} in the Arkansas River and the tributaries (Clay Creek, Big Sandy Creek, Buffalo Creek, and Wild Horse Creek).

4.3 Groundwater and In-stream Water Quality Comparison with Water Quality Standards and Guidelines

Model results are used to study aquifer and stream zones wherein the concentrations of *TDS* and other salt ions are high then the regulatory water quality standards or guidelines. The value of C_{TDS} in water may affect portability. Water quality criteria for irrigation purposes are crop specific. Crops differ in their tolerance to *TDS* and to specific ions and respond differently to the quality of water with which they are irrigated. The major crops cultivated in the LARV have moderate salt tolerance, though some, like onions and melons, are sensitive.

The secondary maximum contamination level (SMCL) for C_{TDS} established by USEPA for drinking water is 500 mg/L. The threshold value of C_{TDS} for saturated soil water is about 3400 mg/L for the major crops, corn and alfalfa, in the gypsiferous soils of the DSR (Morway and Gates 2012, Gates et al 2016). Figure 4.15 (A) shows subregions wherein groundwater C_{TDS} is greater than this threshold. C_{TDS} in the soil will often be substantially higher than these values. Figure 4.15 (B) compares the simulated in-stream C_{TDS} with the drinking water quality standard and the USEPA irrigation water quality guideline of 1500 mg/L along the Arkansas River within the DSR. Results show a high degree of violation of water quality standards and guidelines along the river reach. An increasing trend in C_{TDS} is observed in the downstream direction towards the Colorado- Kansas state line in part because of the evaporative concentration and cycling of irrigation water along the reach and accumulation of groundwater return flows to the river. Relatively abrupt changes in C_{TDS} in the stream water may be due in part to the effects of tributary inflows to the Arkansas River or too high volume canal diversions causing groundwater return flows to make a relatively larger contribution to in stream concentrations. Figure 4.15 (B) also shows the simulated and observed spatial variation of the C_{TDS} along the Arkansas River. The model's underprediction of in-stream concentrations may be due to the following:

1. The absence of a complete carbon cycle in the SEC module and incomplete representation of chemical reactions in the in-stream reaction module.
2. Solute mass loadings from overland flows to tributaries which are not accounted for in the model. A separate subroutine is required to compute the surface runoff mass loading, which will improve the in-stream spatiotemporal TDS concentrations.
3. Unaccounted-for flows and solute loads in the truncated upper extent of the tributaries, which feed directly into the Arkansas River. At times, simulated TDS loading in the tributaries drops very low because the flow becomes very small, with detrimental effects on simulated C_{TDS} in the river.
4. A limited number of available observed data samples. Results likely could be improved by including a greater number of observed data samples, which could empower the statistical analysis.

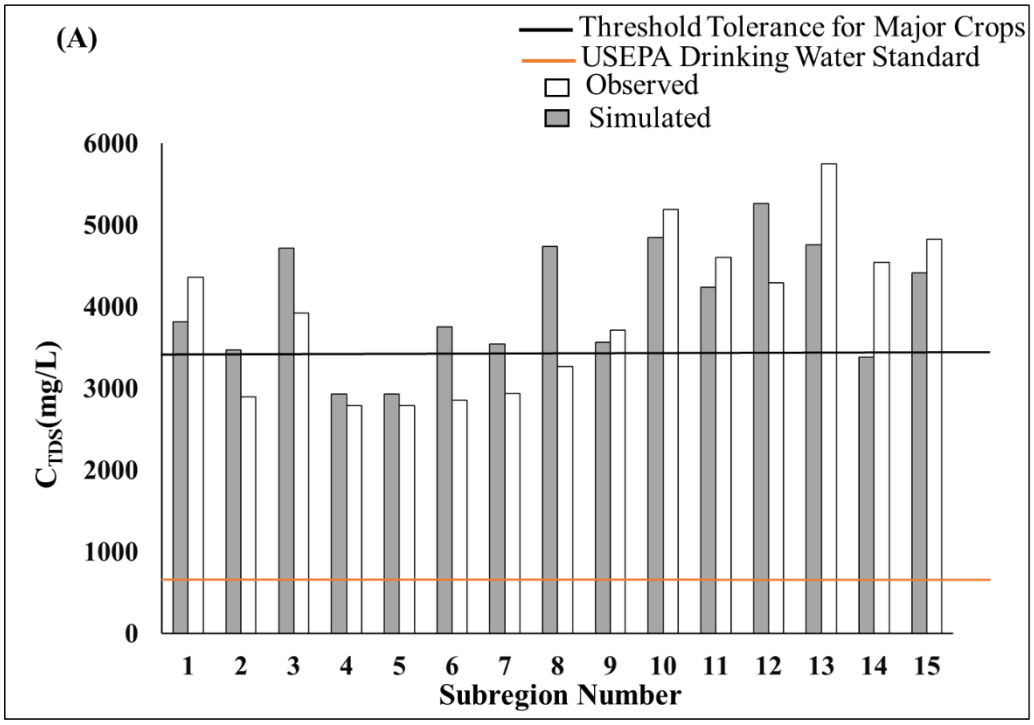

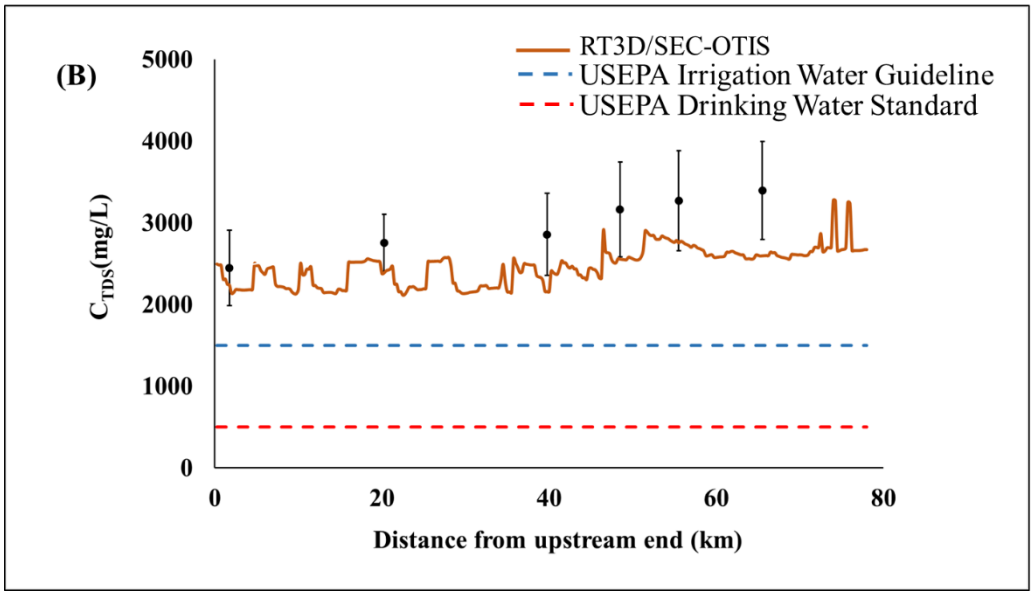

Figure 4. 15. (A) Average simulated and observed groundwater C_{TDS} in the subregions of the DSR, with comparison to the threshold for corn and alfalfa crops and to the USEPA Drinking Water Standard, (B) Average simulated and observed C_{TDS} in in the Arkansas River within the DSR, with comparison to USEPA Irrigation Water Guideline and Drinking Water Standard (black observed data are plotted with error bars of ± one standard deviation).

CHAPTER 5

CONCLUSIONS, AND

RECOMMENDATIONS FOR FUTURE WORK

5.1 Summary Conclusions

Providing food for the growing global population, expected to reach 9.7 billion people by 2050 (Rosegrant et al., 2002), without degrading natural resources is a major challenge for society. Irrigated agriculture will be essential to meeting this challenge; yet, in many areas, the productivity of irrigated lands has diminished due to waterlogging and salinization.

The development of numerical water quantity and quality models is a matter of intensive research currently, with the aim of obtaining reliable tools that are able to closely approximate real-world stream-aquifer systems and are suitable to be applied in exploring management decisions to limit the degradation of irrigated agricultural regions. The research presented herein summarizes efforts towards simulating the fate and transport of major salt ions in an irrigated stream-aquifer systems over regional scales, resulting in the RT3D/SEC-OTIS model.

The RT3D/SEC-OTIS model presented in this thesis is a spatially-distributed, physically-based finite-difference model. This previously developed model involved the coupling of a soil-aquifer reactive transport model and salinity equilibrium chemistry module with a 1D stream transport model. In this study, the model is calibrated and tested in a 552 km^2 agricultural region along the downstream end of Colorado's Lower Arkansas River Valley in southeastern Colorado. The model accounts for *S* cycling in the crop-soil zone (*S* organic matter composition, mineralization/immobilization, root uptake), oxidation-reduction reactions, including release of *S* from marine shale material containing pyrite (FeS_2), precipitation-dissolution, complexation, cation exchange for the major salt ions, and sources and sinks such as canal seepage, infiltrated

water from flood and sprinkler irrigation, groundwater pumping, evapotranspiration from both the unsaturated and shallow saturated zones; addition of salt mass via fertilizer and irrigation water; and chemical kinetics affecting salt ions. RT3D/SEC-OTIS also includes cycling of *C, N,* and *S* in the plant-soil system, with redox reactions and sorption included for dissolved oxygen, ammonium, nitrate and sulfate. All flow rates and sources/sinks are provided by the accompanying flow model (MODFLOW-UZF).

The developed model is applied to simulate baseline conditions in the 552 km^2 study region in the Lower Arkansas River Valley. A five-year historic period from 2003-2007 was repeated eight times for a total of about 40 years of simulation to predict the concentrations of major salt ions in the stream-aquifer system. The model also simulates the salt ion concentrations in the soil root zone, which determines the impacts on crop yield, along with groundwater and surface water salt ion concentrations. The model also calculates the groundwater mass loading to the river network, which affects salt concentrations in the streams and in flows diverted to the downstream-irrigated areas.

Model results show that the concentration of TDS and major salt ions in the Arkansas River increase in the downstream direction from the city of Lamar to the Colorado-Kansas State line. The average simulated concentration of TDS in the river near Lamar is about 2400 mg/L and near the Colorado Kansas State line is approximately 3400 mg/L. The simulated concentration of TDS and major salt ions also increases in the alluvial aquifer from the upstream to the downstream end of the study region, due partly to the repeated cycling of irrigation water that dissolves and mobilizes more and more salts and concentrates salts due to evapotranspiration. The average simulated concentration of TDS in the soil root zone is found to markedly exceed the permissible limits for corn and alfalfa. Approximately 51% of the irrigated area in the DSR

exceeds the average crop yield threshold for salinity. Groundwater mass loadings of sulfate and TDS to the river are generally within ± one standard deviation of the mean of the distribution of mass loadings predicted by stochastic mass balance results except during periods when simulated mass loadings of TDS are higher due to excessively high simulated concentrations of calcium in the groundwater.

5.2 Avenues for Future Research

Major limitations in the development, testing, calibration, and application of RT3D/SEC-OTIS were described in Chapters 3 and 4. Recommendations for future work, associated with some of these limitations, are presented here. Possible areas of future research fall into six categories:

- **Refine the model representation of condition near the tributaries**

  The boundaries of flow and reactive transport model should be extended to include areas that are outside the domain of the study region to better investigate the effects of geological formations outside the study region which impact the concentration of the salt ions in the groundwater. Refining the modeling of the tributaries, to better represent inflows from outside the irrigated valley, should improve both the flow and reactive transport results.

- **Include the full carbon (C) cycle**

  $CaCO_3$ is present in the soils of the LARV by 0 to 11% and dissolution of $CaCO_3$ is one of the sources of C_{Ca}. The SEC module currently does not fully accommodate the C cycle in a closed system (Tavakoli Kivi et al., 2019); instead, the simple dissolution formula for $CaCO_3$ is used. The simulated C_{Ca} concentrations in the saturated and unsaturated zone

can be improved by including the full *C* cycle and the partial pressure of CO_2, which determines the extent of dissolution of $CaCO_3$.

- **Include the redox chemical reactions in streams**

  The developed reactive transport model simulates conservative salt transport with advection and dispersion only in the streams. Redox reactions, chemical precipitation, and dissolution are not simulated in the in-stream module of RT3D/SEC-OTIS. The inclusion of redox reactions, chemical precipitation, and dissolution in the simulation likely will alleviate some of the misfits in the results both for groundwater and surface water.

- **Include surface water mass loadings from overland flow**

  Water mass loading of salt ions due to surface runoff from irrigation and precipitation are not accounted in the current version of the model. A separate subroutine is required to compute the surface water mass loading, which should improve the in-stream spatiotemporal TDS concentrations.

- **Add solute mass transfer in upflux from the shallow water table**

  The mass transfer of solutes in upflux from the shallow water table into the unsaturated zone is not simulated in the current version of the model. This addition should significantly alter the representation of salt concentrations in the unsaturated zone.

- **Implementation for evaluation of alternative best management practices**

  After refinement and re-calibration, the model should be employed to forecast relative comparisons of conditions under alternative land and water management interventions for salinity mitigation with baseline conditions to guide decision makers based on the results.

REFERENCES

Acquaah, G., 2005. Principles of crop production: theory, techniques, and technology. Pearson Prentice Hall, Upper Saddle River, N.J.

Allison, J., Kevin, J., 1991, MINTEQA2: A geochemical assessment model for environmental systems: Version 3.0 User's manual, Technical Report, 600/3-91/021.

Appelo, C.A.J., Postma, D. and Geochemistry, G., 2005, Geochemsitry, Groundwater and Pollution. Taylor & Ykolirancis Group.

Arnold J.G., Williams J.R., Srinivasan R., King K.W., Griggs R.H.,1996. "SWAT — Soil and Water Assessment Tool (User manual)". Temple, TX: U.S. Department of Agriculture, Agricultural Research Service, Grassland Soil and Water Research Laboratory.

Bailey, R.T., Hunter, W.J., and Gates, T.K. (2012), The influence of nitrate on selenium in irrigated agricultural groundwater systems. Journal of Environmental Quality, 41, 783-792.

Bailey, R.T., Gates, T.K., Halvorson, A.D., 2013a, Simulating variably-saturated reactive transport of selenium and nitrogen in agricultural groundwater systems, J. Contam. Hydrology, 149, 27-45.

Bailey, R.T., Morway, E.D., Niswonger, R., and Gates, T.K., 2013b, Modeling variably saturated multispecies reactive groundwater solute transport with MODFLOW-UZF and RT3D. Groundwater, 51(5), 752-761.

Bailey, R. T., Gates, T. K., & Ahmadi, M. (2014). Simulating reactive transport of selenium coupled with nitrogen in a regional-scale irrigated groundwater system. Journal of Hydrology, 515, 29-46. doi:10.1016/j.jhydrol.2014.04.039

Barry D.A, Bajracharya K, Crapper M, Prommer H, Cunningham CJ., 2000, Comparison of split-operator methods for solving coupled chemical non-equilibrium reaction/groundwater transport models. Math Comput Simul , 53(1–2):113–27.

Barta, R., Ward, R., Wasksom, R. M., Smith, Dan., 2004 Stretching urban water supplies in Colorado: strategies for landscape water conservation. Colorado Water Institute.

Bencala, K.E., 1983. Simulation of solute transport in a mountain pool-and-riffle stream with a kinetic mass transfer model for sorption. Water Resour. Res. 19 (3), 732–738.

Bethke, C.M., 1996, Geochemical reaction modeling-Concepts and applications. Oxford Univ. Press, New York, NY.

Bethke, C.M., 1994, The Geochemist's Workbench. Version 2.0, A Users Guide to Rxn, Act2, Tact, React, and Gtplot, Hydrogeology Program, University of Illinois.

Boonstra, J., and N.A. de Ridder., 1990. Numerical Modeling of Groundwater Basins. Publication no. 29, Wageningen, The Netherlands: International Institute for Land Reclamation and Improvement (ILRI).

Brendle, D.L., 2002. Evaluation of possible alternatives to lower the high water table of St. Charles Mesa, Pueblo County, Colorado, U.S. Geological Survey. Water-Resources Investigations Report 01-4190. Denver, Colo.

Bresler, E. 1967. A model for tracking salt distribution in the soil profile and estimating the efficient combination of water quality and quantity under varying field conditions. Soil Science 104:227.-233

Birka Wicke , Edward Smeets , Veronika Dornburg , Boris Vashev , Thomas Gaiser , Wim Turkenburg and André Faaij. 2011. "The global technical and economic potential of bioenergy from salt-affected soils" Energy Environ. Sci., 2011, 4, 2669-2681

Brown, L.C. and Barnwell, T.O. ,1987. "The enhanced stream water quality models QUAL2E and QUAL2E-UNCAS: documentation and user manual." EPA/600/3-87/007. U.S. Environmental Protection Agency, Environmental Research Laboratory, Athens, GA. 127(5), 295-305.

Burkhalter, J.P., Gates, T.K., 2005. Agroecological impacts from salinization and waterlogging in an irrigated river valley. Journal of Irrigation and Drainage Engineering, 131(2): 197 209.

Calabrese, E.J., Tuthill.W.R. "The influence of elevated levels of sodium in drinking water on elementary and high school students in Massachusetts". Journal of Environmental Pathology and Toxicology, 4 (1980), pp. 151-165.

Carrayrou J, Mose R, Behra P., 2008, Operator-splitting procedures for reactive transport and comparison of mass balance errors. J Contam. Hydrol., 68(3–4):239–68.

Chen, W., Hou, Z., Wu, L., Liang, Y., and Wei, C. 2010. "Evaluating salinity distribution in soil irrigated with saline water in arid regions of northwest China. Agric. Water Mgmt., 97(12), 2001 – Wang, Y., Deng, C., Liu, Y., Niu, Z., and Li, Y. 2018. "Identifying

change in spatial accumulation of soil salinity in an inland river watershed." Sci. Total Environ., 621, 177 – 185.2008.

Clement, T.P., 1997, RT3D-A modular computer code for simulating reactive multi-species transport in 3-dimensional groundwater aquifer. Draft report. PNNL-SA-28967. Pacific Northwest National Laboratory, Richland, Washington.

Clement, T.P., Peyton, B.M., Skeen, R.S., Jennings, D.A., and J.N. Petersen (1997), Microbial growth and transport in porous media under denitrification conditions: experiments and simulations. J. Contam. Hydrol., 24, 269-285.

Clement, T.P., Sun, Y., Hooker, B.S., and J.N. Peterson (1998), Modeling multispecies reactive transport in groundwater. Groundwater Mon. & Rem., 18, 79-92.

Cocchetto DM, Levy G.,1981. Absorption of orally administered sodium sulfate in humans. Journal of Pharmaceutical Sciences, 70:331–333.

Cooper, C.A., 2006, Salt chemistry effects on salinity assessment and soil solution modeling in the Arkansas River Basin, Colorado, Submitted in Department of Soil and Crop Sciences

Corrales, J., Naja., G.M., Dziuba, C., Rivero, R.G., Orem, W., 2011, Sulfate threshold target to control methylmercury levels is wetland ecosystems, Science of the Total Environment, 409,2156-2162.

Cole, S.E., Sharma, D., Schreiider, W.A., 1994. A modern, refined application of a ground water flow model to the Arkansas River Basin. In: Warner, J.W., Van Der Heijde, P. (Eds.), Proceeding of the 1994 Groundwater Modeling Conference. Colorado School of Mines, Fort Collins, CO.

Darton, N.H., 1906. Geology and underground waters of the Arkansas Valley in eastern Colorado. U.S. Geological Survey, Professional Paper 52, 90 p.

Dai, T., Labadie, J.W., 2001. "RIVER BASIN NETWORK MODEL FOR INTEGRATED WATER QUANTITY/QUALITY MANAGEMENT". J. Water Resour. Plann. Manage.

Doherty, J., 2002. Manual for PEST, 5th edition, Brisbane, Australia: Watermark Numerical Computing. Downloadable from www.sspa.com/pest.

Elhaddad, A., Garcia, L., 2008. Surface energy balance-based model for estimating evapotranspiration taking into account spatial variability in weather. Journal of Irrigation and Drainage Engineering, 134: 681.

Faust, C.R., Sims, P.N., Spalding, C.P., Andersen, P.F., Lester, B.H., Shupe, M.G., Harrover, A.,1993. FTWORK: groundwater flow and solte transport in three dimensions Documentation Version 2.8. Geo-Trans, Sterling, VA.

Felmy, A.R., 1995. GMIN: A computerized chemical equilibrium model using a constrained minimization of the Gibbs free energy.

Felmy, A.R., 1995. GMIN, A computerized chemical equilibrium program using a constrained minimization of the Gibbs free energy: summary report. In: Loeppert, R.H. (Ed.), Chemical Equilibrium and Reaction Models. American Statistical Association and SSSA, Madison, WI, pp. 377±407.

Foster 2000. In "Reducing Cancer Mortality: A Geographical Perspective" Available online: (http://www.elements.nb.ca/theme/transportation/salt/salt.htm).

Frasier, W.M., Waskom, R.M., Hoag, D.L., and T.A. Bauder, 1999, Irrigation Management in Colorado: Survey Data and Findings. Technical Report TR99-5 Agricultural Experiment Station, Colorado State University. Fort Collins, CO.

Frind, E.O., Duynisveld, W.H.M., Strebel, O., Boettcher, J., 1990, Modeling of multicomponent transport with microbial transformation in groundwater: The Fuhrberg case, Water Resources Research, Vol. 26, NO. 8, 1707-1719.

Fullen, M.A., Catt, J.A., 2004. Soil management: problems and solutions. Arnold London, UK.

Gates, T.K., Burkhalter, J.P., Labadie, J.W., Valliant, J.C., Broner, I., 2002, Monitoring and modeling flow and salt transport in a salinity-threatened irrigated valley, Journal of Irrigation and Drainage Engineering, Vol. 128, No. 2, 88-99

Gates, T. K., Cody, B. M.* , Herting, A. W.* , Donnelly, J. P.* , Bailey, R. T.* , and Mueller Price,J.* 2009. "Assessing selenium contamination in the irrigated streamaquifer system of the Arkansas River, Colorado". Journal of Environmental Quality, 38(6): 2344 – 2356.

Gates, T.K., Garcia, L.A., Labadie, J.W., 2006. Toward optimal water management in Colorado's Lower Arkansas River Valley: monitoring and modeling to enhance agriculture and environment. Colorado Water Resources Research Institute Completion Report (205).

Gates, T. K., Garcia, L. A., Hemphill, R. A., Morway, E. D., and Elhaddad, A. (2012). "Irrigation practices, water consumption, & return flows in Colorado's Lower Arkansas River Valley: Field and model investigations." Colorado Water Institute

Completion Report No. 221, Colorado Agricultural Experiment Station No. TR-12, Colorado State University, Fort Collins, CO.

Gates, T.K, Steed, G.H., Niemann, J.D., Labadie, J.W., 2016, Data for Improved Water Management in Colorado's Arkansas River Basin, Hydrological and Water Quality Studies, Colorado State University.

Gates, T. K., Cox, J. T., & Morse, K. H. (2018). Uncertainty in mass-balance estimates of regional irrigation-induced return flows and pollutant loads to a river. Journal of Hydrology: Regional Studies, 19, 193-210. doi:10.1016/j.ejrh.2018.09.004.

Glas, T.K., Klute., A and McWhorter, D.B., 1979, Dissolution and Transport of Gypsum in Soils: II. Experimental.

Goff, K., Lewis, M.E., Person, M.A., Konikow, L.F.,1998. "Simulated Effects of Irrigation on Salinity in the Arkansas River Valley in Colorado." Ground Water. 36(1), 76-86.

Ghassemi, F., Jakeman, A., and Nix, H., 1995, Salinization of land and water resources: Human causes, extent, management, and case studies in salinity-affected regions, University of New South Wales Press, Sydney, Australia.

Gorban, G.R., and S. Miyamoto.,1985. Dissolution rate of gypsum in aqueous salt solutions. Soil Science 140:89-93.

Grieve, C. M., Grattan, S. R., and Maas, E. V. 2012. Plant salt tolerance. Chap. 13 in Wallender, W. W., and Tanji, K. K., Agricultural salinity assessment and management, 2nd ed. Manuals and Reports on Engineering Practice No. 71, Amer. Soc. Civil Engineers, Reston, VA

Harrington, N., Cook, P., 2014, Groundwater in Australia, National Centre for Groundwater Research and Training, Australia.

Harbaugh, A.W., 2005. MODFLOW-2005, The U.S. Geological Survey modular ground-water model--the Ground-Water Flow Process, U.S. Geological Survey Techniques and Methods 6-A16.

Haynes, W.M., 2016, Handbook of Chemistry and Physics, CRC Press, Boca Raton, FL.

Herczeg, A.L., Dogramaci, S.S., Leanet, F.W.J., 2001, Origin of dissolved salts in a large, semi-arid groundwater system: Murray Basin, Australia, Marine Freshwater Research, 52, 41-52.

Hillel, D., 2000. Salinity management for sustainable irrigation - integrating science, environment, and economics. Environmentally and socially sustainable development rural development, Washington, DC: The World Bank Ground Water. 51(5), 752 61.

Houk, E., Frasier, M., Schuck, E., 2006. The agricultural impacts of irrigation induced waterlogging and soil salinity in the Arkansas Basin. Agricultural Water Management, 85(1-2): 175-183.

Hsieh, P.A., Barber, M.E., Contor, B.A., Hossain, A., Johnson, G.S., Jones, J.L., Wylie, A.H., 2007. Ground-water flow model for the Spokane Valley-Rathdrum Prairie Aquifer, Spokane County, Washington, and Bonner and Kootenai Counties, Idaho. US Geological Survey, Scientific Investigations Report 07-5044.

Hukkinen, J., 1993. Institutional distortion of drainage modeling in Arkansas River Basin. Journalof Irrigation and Drainage Engineering, 119: 743.

Hutmacher, R.B., Ayars, J.E., Vail, S.S., Bravo, A.D., Dettinger, D, Schoneman, R.A., 1996, Uptake of shallow groundwater by cotton: growth stage, groundwater salinity effects in in column lysimeters, 31, pp. 205-223.

Jennings, D.H ., 1976, The effects of sodium chloride on higher plants.

Kemper, W.D., J. Olsen , and C.J DeMooy., 1975. Dissolution rate of gypsum in flowing water. Soil Sci Soc Amer Proc 39:458-463

Kipp, K.L., 1987, HST3D—A computer code for simulation of heat and solute transport in three dimensional ground-water flow systems: U.S. Geological Survey Water-Resources Investigations Report 86-4095, 517 p.

Kitanidis, P., Vomvoris, E., 1983. A geostatistical approach to inverse modeling in groundwater modeling and one-dimensional simulations. Water Resources Research, 19(3): 677–690.

Knoll, D.A., and Keyes, D.E., 2004, Jacobian-free Newton– Krylov methods: a survey of approaches and applications: Journal of Computational Physics, 193, issue 2, p. 357-397.

Konikow, L.F., Bredehoeft, J.D., 1974. “Modeling flow and chemical quality changes in an irrigated stream-aquifer system”. Water Resour. Res. 10(3), 546-561.

Latif, M., Ahmad, M.Z., 2009, Groundwater and soil salinity variation in a canal command area in Pakistan, Irrigation and Drainage, 58: 456-468.

Lin, Y.W., Garcia, L., 2008, Development of a Hydro-Salinity Simulation Model for Colorado’s Arkansas Valley, Journal of Irrigation and Drainage Engineering, Vol. 134, 757-767.

Lindsay, W.L., 1979. Chemical Equilibrium in Soils. Wiley, New York. 449p.

Longenbaugh, R.A., 1967. Mathematical simulation of a stream-aquifer system, Proc. 3rd Annual American Water Resources Conference, pp. 74-83.

Matheron, G., 1963. Principles of geostatistics. Economic Geology, 58(8), 1246-1266.

Mahmood, K., Morris, J., Collopy, J. and Slavich, P., 2001. Groundwater uptake and sustainability of farm plantations on saline sites in Punjab province, Pakistan. Agricultural Water Management, 48(1), pp.1-20.

Mayer, K.U., Frind, E.O., and D.W. Blowes.,2002, Multicomponent reactive transport modeling in variably saturated porous media using a generalized formulation for kinetically controlled reactions, Water Resour. Res., 38(9), 1174-1194.

Mcdonald, M., & Harbaugh, A. (1984). A modular three-dimensional finite-difference ground water flow model. Open-File Report. doi:10.3133/ofr83875

McDonald, M.G., Harbaugh, A.W., 1988. "A modular three-dimensional finite-difference ground-water flow model". Washington, USA.

Moore, J., Wood, L., 1967. Data requirements and preliminary results of an analog-model evaluation—Arkansas River valley in eastern Colorado. Ground Water, 5(1): 20-23.

Morris ME, Levy G.,1983 Absorption of sulfate from orally administered magnesium sulfate in man. Journal of Toxicology — Clinical Toxicology, 20:107–114.

Morway, E.D., Gates, T.K., 2012, Regional assessment of soil water salinity across an intensively irrigated river valley, Journal of Irrigation and Drainage Engineering, Vol. 138, No.5,393405.

Morway, E. D., Gates, T. K., & Niswonger, R. G., 2013. Appraising options to reduce shallow groundwater tables and enhance flow conditions over regional scales in an irrigated alluvial aquifer system. Journal of Hydrology, 495, 216–237. https://doi.org/1. Journal of Hydrology, 495, 216 237.https://doi.org/10.1016/j.jhydrol.2013.04.047

Miles, D.L., 1977. Salinity in the Arkansas Valley of Colorado. Cooperative Extension Service, Colorado State Univ., Fort Collins, Colo.

Nash, J., & Sutcliffe, J. (1970). River flow forecasting through conceptual models part I — A discussion of principles. Journal of Hydrology, 10(3), 282–290.

Narula, K., Gosain, A., 2013. "Modeling hydrology, groundwater recharge and non-point nitrate loadings in the Himalayan Upper Yamuna basin". Science of the Total Environment. 468 469, S102–S116.

Niemann, J.D., Lehman, B.M., Gates, T.K., Hallberg, N.U., Elhaddad, A., 2011. Impact of shallow groundwater on evapotranspiration losses from uncultivated land in an irrigated river valley. Journal of Irrigation and Drainage Engineering, 137(8): 501-512.

Niswonger, R.G., Prudic, D.E., 2004. Modeling variably saturated flow using kinematic waves in MODFLOW, in Hogan, J. F., Phillips, F. M., Scanlon, B. R., eds., Groundwater Recharge in a Desert Environment: The Southwestern United States: American Geophysical Union, Washington, D.C., Water Science and Application Series, v. 9, p. 101-112, 101-112 pp.

Niswonger, R., Prudic, D., Regan, R., 2006. Documentation of the unsaturated-zone flow (UZF1) package for modeling unsaturated flow between the land surface and the water

table with MODFLOW-2005. US Department of the Interior, US Geological Survey Techniques and Methods 6-A19 62 p; Reston, VA.

Odell, J.W., Coffin, D.L., Langford, R.H., 1964. Mineral and water resources of Colorado, Report for use of U.S. Senate Committee on Interior and Insular Affairs, 88th Congress, 2nd Session, p. 249.

Osborn, B., Orlando, A. S., Hoag, D. L., Gates, T. K., and Valliant, J. C. 2017. The economics of irrigation in Colorado's Lower Arkansas River Valley. Colorado Water Institute Special Report No. 32, Colorado State Univ., Fort Collins, Colo.

Olsen, S.R and F.S. Watanabe., 1959. Solubility of calcium carbonate in calcareous soils. Soil Science 88:123-129.

Oster, J. D., and Rhoades, J. D.,1975. "Calculated drainage water compositions and salt burdens resulting from irrigation with river waters in the western United States." J. Environ. Qual., 41, 73–79

Oosterbaan R.J.,1989. SALTMOD. In:Annual Report(pp 1–49). ILRI, Wageningen, TheNetherlands, December.

Parkhust D., Appelo, 1999, User's guide to PHREEQC (Version-2)-a computer program for speciation, batch-reaction, one-dimensional transport, and inverse geochemical calculations, USGS, Report 99(4259), 326.

Parkhurst, D.L., Kipp, K.L., Engesgaard, P., and S.R. Charlton (2004), PHAST – A program for simulating ground-water flow, solute transport, and multicomponent geochemical reactions.U.S. Geological Survey, Denver, Colorado.

Parkhurst D.L., Kipp K.L., Engesgaard P., Charlton S.R. (2010), PHAST Version 2 - A program for simulating groundwater flow, solute transport, and multicomponent geochemical reactions, U. S. Geological Survey Techniques and Methods 6-A35, 235 pg.

Pauwels, H., W. Kloppmann, J.-C. Foucher, A. Martelat, and V. Fritsche, 1998, Field tracer test for denitrification in a pyrite-bearing schist aquifer. Applied Geochemistry. 13:767-778.

Pereira, L. S., Goncalves, J. M., Dong, B., Mao, Z. and Fang, S. X. 2007. "Assessing basin irrigation and scheduling strategies for saving irrigation water and controlling salinity in the upper Yellow River Basin, China." Agric. Water Mgmt., 93(3), 109 – 122.

Postel, S., 1999. Pillar of sand: Can the irrigation miracle last? Norton, New York.

Postma, D., Boesen, C., Kristiansen, H., and F. Larsen, 1991, Nitrate reduction in an unconfined sandy aquifer: water chemistry, reduction processes, and geochemical modeling. Water Resources Research 27(8), 2027-2045.

Poeter, E., Hill, M., Banta, E., Mehl, S., Christensen, S., 2005. UCODE_2005 and six other computer codes for universal sensitivity analysis, calibration, and uncertainty evaluation. USGS Techniques and Methods Report TM 6-A11.

Prince, R., 2016. Water salinity and plant irrigation. Department of Primary Industries and Regional Development. Government of Western Autralia.

Prommer, H., Barry, D.A., and C. Zheng (2003), MODFLOW/MT3DMS-based reactive multicomponent transport modeling. Ground Water, 41(2), 247-257.

Qurban, I.A., 2018. Finding water management practices to reduce selenium and nitrate concentrations in the irrigated stream-aquifer system along the lower reach of

Colorado's Arkansas River Valley, Submitted in Department of Civil and Environmental Engineering.

Qureshi, A.S., McCornick, P.G., Qadir, M. and Aslam, Z., 2008. Managing salinity and waterlogging in the Indus Basin of Pakistan. Agricultural Water Management, 95(1), pp.1-10.

Robbins, C.W., Jurinak, J.J. and Wagenet, R.J., 1980, Calculating Cation Exchange in a Salt Transport Model 1. Soil Science Society of America Journal, 44(6), pp.1195-1200.

Rosegrant, M. W., Cai, X., & Cline, S. (2002). World Water and Food to 2025: Dealing with Scarcity. Food Policy. https://doi.org/10.1098/rstb.2005.1744

Rubin, J. (1983), Transport of reacting solutes in porous media: Relation between mathematical nature of problem formulation and chemical nature of reactions. Water Resour. Res., 19(5),1231-1252.

Runkel, R.L.,1998. "One-dimensional transport with inflow and storage (OTIS): a solute transport model for streams and rivers." U.S. Geological Survey Water-Resources Investigation Report 98-4018, Denver, Colo.

Saurez, D.L., 2005. Chemistry of salt affected soil,p. 689-705, In M.A. Tabatabai and D. L. Sparks, eds. Chemical processes in soils, Number 8 in soil science society of America book series. Soil Science Society of America, Inc., Madison, WI.

Scanlon, B.R., Jolly, I., Sophocleous, M., and Zhang, L. (2007) "Global impacts of conversions from natural to agricultural ecosystems on water resources: Quantity versus quality". WATER RESOURCES RESEARCH. 43, W03437.

Schoups, G., Hopmans, J.W., Young, C.A., Vrugt, J.A., Wallender, W.W., Tanji, K.K., and S.Panday., 2005. Sustainability of irrigated agriculture in the San Joaquin Valley, California. Proceedings of the National Academy of Sciences of the United States of America, 102(43), 15352-15356.

Sharp, M., Hoag, D., Bailey, R. T., Romero, E. C. , and Gates, T. K., 2016. "Institutional constraints on cost-effective water management: Selenium contamination in Colorado's Lower Arkansas River Valley." J. Amer. Water Resour. Assoc., 52(6), 1420 – 1432.

Shultz, C. D., Bailey, R. T., Gates, T. K., Heesemann, B. E., & Morway, E. D., 2018. Simulating Selenium and Nitrogen Fate and Transport in Coupled Stream-Aquifer Systems of Irrigated Regions. Journal of Hydrology. https://doi.org/10.1016/j.jhydrol.2018.02.027

Sherow, J.E., 1990. Watering the valley: Development along the High Plains Arkansas River, 1870-1950. University Press of Kansas.

Silva, C., Martínez, V., Carvajal, M., 2008. Osmotic versus toxic effects of NaCl on pepper plants. Biologia Plantarum, 52(1): 72-79.

Singh, A., Panda, S.N., 2012, Integrated salt and water balance modeling for the management of waterlogging and salinization; I: Validation of SAHYSMOD, Journal of Irrigation and Drainage Engineering, Vol. 138, 955-963.

Šimůnek, J., and D. L. Suarez., 1994, Two-dimensional transport model for variably saturated porous media with major ion chemistry, Water Resources Research, 30(4), 1115-1133.

Šimůnek, J., and D. L. Suarez., 1997, Unsaturated water and solute transport model with equilibrium and kinetic chemistry, Soil Science Society of America Journal, 61(6), 1633.

Šimunek, J., Šejna, M ., Van Genuchten, MT., 2005. HYDRUS-1D, version 4.14, code for simulating the one-dimensional movement of water, heat, and multiple solutes in variably saturated porous media, Tech. rep., University of California Riverside.

Šimůnek, J., M. Šejna, and M. Th. van Genuchten., 2012, The UNSATCHEM Module for HYDRUS (2D/3D) Simulating Two-Dimensional Movement of and Reactions Between Major Ions in Soils, Version 1.0, PC Progress, Prague, Czech Republic, 54 pp.

Skarie,R.L., J.L. Arndt,and J.L. Richardson.,1987a. Sulfate and gypsum determination in saline soils. Soil Sci Soc Am J 51:1372-1377.

Skarie,R.L., J.L. Arndt,and J.L. Richardson, G.J. McCarthy, and A.Maianu.,1987b. Evaporative mineralogy and groundwater chemistry associated with saline soils

Smith, R.E., 1983, Approximate sediment water movement by kinematic characteristics: Soil Science Society of America Journal, v. 47, p. 3-8.

Smith, R.E., and Hebbert, R.H.B., 1983, Mathematical simulation of interdependent surface and subsurface hydrologic processes: Water Resources Research, v. 19, no. 4, p. 987-1001. in eastern North Dakota. Soil Sci Soc Am J 51:1372-1377.

Soil salinity: A serious environmental issue and plant growth promoting bacteria as one of the tools for its alleviation Pooja Shrivastava∗ and Rajesh Kumar

Sparks, D.L., 2003. Environmental soil chemistry, Academic press, Second Edition. 17

Tafteh, A. and Sepaskhah, A.R., 2012. Application of HYDRUS-1D model for simulating water and nitrate leaching from continuous and alternate furrow irrigated rapeseed and maize fields. Agricultural Water Management, 113, pp.19-29.

Sweet, A. T., & Inman, W. (1930). Soil survey of the Arkansas Valley area, Colorado. Washington, D.C.: U.S. Dept. of Agriculture, Bureau of Chemistry and Soils.

Tanji, K.K., Kielen, N.C., 2002. Agricultural drainage water management in arid and semi-arid areas. Irrigation and Drainage Paper 61, Food and Agriculture Organization United Nations, Rome. FAO.

Tavakoli Kivi, S., & Bailey, R. T., 2017. Modeling sulfur cycling and sulfate reactive transport in an agricultural groundwater system. Agricultural Water Management, 185, 78-92.

Tavakoli-Kivi, S., Bailey, R. T., & Gates, T. K. 2019. A salinity reactive transport and equilibrium chemistry model for regional-scale agricultural groundwater systems. Journal of Hydrology, 572, 274-293. doi:10.1016/j.jhydrol.2019.02.040

Tilman, D., Cassman, K., Matson, P., Naylor, R., Polasky, S., 2002. Agricultural sustainability and intensive production practices. Nature, 418(6898): 671-677.

Trescott, P., & Larson, S. (1976). Solution of three-dimensional groundwater flow equations using the strongly implicit procedure. Journal of Hydrology, 35(1-2), 49-60.

Truesdell, A.H., Jones, B.F., 1974, WATEQ-a computer program for calculating chemical equilibrium for natural waters, US Geological Survey.

Tuteja, N.K., Beale, G., Dawes, W., Vaze, J., Murphy, B., Barnett, P., Rancic, A., Evans, R., Geeves, G., Rassam, D., Miller, M., 2003, Predicting the effects of landuse change on water and salt balance—a case study of a catchment affected by dryland salinity in NSW, Australia, Journal of Hydrology, 283, 67-90.

Tweed, S.O., Leblanc, M., Webb, J.A. and Lubczynski, M.W., 2007. Remote sensing and GIS for mapping groundwater recharge and discharge areas in salinity prone catchments.

Water Quality Standards Handbook. (1994). Washington, DC: U.S. Environmental Protection Agency, Office of Science and Technology, Water Quality Standards Branch.

Van Genuchten, M. Th. (1981). Analytical solutions for chemical transport with simultaneous adsorption, zero-order production and first-order decay. J. Hydrol. 49, 213-233.

Vaze, J., Beale, G.T.H., Barnett, P. and Tuteja, N.K., 2003, Predicting the spatial and temporal effects of landuse change using the CATSALT modelling framework. MODSIM 2003.

Wallender, W.W., Tanji, K.K., 2012. Agricultural salinity assessment and management. 2nd Ed., ASCE, Reston, VA.

Wagenet, R.J., and J.L. Hutson., 1987. LEACHM-Leaching estimation and chemistry model. Center Environ. Res., Cornell Univ., Ithaca, NY.

Wichelns, D., Qadir, M., Achieving sustainable irrigation requires effective management of salts, soil salinity, and shallow groundwater., 2015, Agricultural Water Management, 157, 31 38.

Wicke, B., Smeets, E., Dornburg, V., Vashev, B., Gaiser, T., Turkenburg,W., Faaij, A., 2011. The global technical and economic potential of bioenergy from salt-affected soils. Energy & Environmental Science, 4, 2669-2681.

Wild A., 2003. Soils, land and food: managing the land during the twenty-first century. Cambridge, UK: Cambridge University Press.

Frasier, W.M., Waskom, R.M., Hoag, D.L., and T.A. Bauder, 1999, Irrigation Management in Colorado: Survey Data and Findings. Technical Report TR99-5 Agricultural Experiment Station, Colorado State University. Fort Collins, CO.

Yasin, M., R. Zada., B.H. Niazi., 1998. Effectiveness of chemical and biotic methods for reclamation of saline-sodic soil. Pak. J. Soil Sci., 15: 179-182.

Yeh, G.T., and V.S. Tripathi (1989), A critical evaluation of recent developments in hydrogeochemical transport models of reactive multichemical components. Water Resour. Res., 25(1), 93-108.

Zheng, C.,1990. “A modular three-dimensional transport model for simulation of advection, dispersion and chemical reactions of contaminants in groundwater systems”. U.S.E.P.A Report.

Zheng, C., Wang, P., 1999a. MT3DMS: A modular three-dimensional multispecies transport model for simulation of advection, dispersion, and chemical reactions of contaminants in groundwater systems; Documentation and user's guide, Contract Report SERDP-99-1.